

Wenjia Guo

**Roles of autism-related genes
neurexin and *neurobeachin*
in synaptic function**

2014

Biologie

Roles of autism-related genes *neurexin* and
neurobeachin in synaptic function

Inaugural-Dissertation
zur Erlangung des Doktorgrades
der Naturwissenschaften im Fachbereich Biologie
der Mathematisch-Naturwissenschaftlichen Fakultät
der Westfälischen Wilhelms-Universität Münster

vorgelegt von
Wenjia Guo
aus Gansu, China
-2014-

Dekan: Prof. Dr. Michael Weber
Erster Gutachter: Prof. Dr. Markus Missler
Zweiter Gutachter: Prof. Dr. Andreas Püschel
Tag der mündlichen Prüfung(en): 26.11.2014
Tag der Promotion: 12.12.2014

Contents

Contents	i
Abbreviations	iii
1. Introduction	1
1.1 Autism spectrum disorders (ASD)	2
1.1.1 ASD is a global disease	2
1.1.2 Genetic basis of ASD	2
1.1.3 Molecular diversity of ASD	3
1.2 Neurons and synapses	4
1.2.1 Synaptic signal transmission	5
1.2.2 Excitatory and inhibitory synapses	6
1.2.3 Synaptic plasticity	8
1.2.4 Synaptic cell adhesion molecules (SynCAMs)	9
1.3 Nrnx	9
1.3.1 Nrnxns are brain specific proteins	9
1.3.2 Functional studies of Nrnxns	11
1.3.3 Binding partners of Nrnxns	13
1.4 Nbea	15
1.4.1 Nbea is located near the Golgi in neurons	15
1.4.2 Protein structure of Nbea	15
1.4.3 Functional investigations of Nbea	17
1.5 Aims and objectives	19
2. Materials and methods	21
2.1 Materials	21
2.1.1 General chemicals	21
2.1.2 General apparatus and consumables	21
2.1.3 Materials for electrophysiology	21
2.1.4 Materials for molecular biology	25
2.1.5 Software	28
2.2 Methods	29
2.2.1 Electrophysiological recordings	29
2.2.2 Molecular biology	37

i

CONTENTS

3. Results	43
3.1 Neurotransmission in β Nrnx knockouts	43
3.1.1 Basal properties of β Nrnx KO variants	44
3.1.2 Spontaneous excitatory neurotransmission	47
3.1.3 Evoked excitatory neurotransmission	50
3.1.4 Short-term plasticity of excitatory synapses	52
3.1.5 Basal synaptic transmission at inhibitory synapse	57
3.1.6 Short-term plasticity at inhibitory synapse	59
3.1.7 Expression of α Nrnx and Nlgn in the β Nrnx TKO	62
3.2 Cloning of Full-length Nbea and domains	65
3.2.1 FL-Nbea cloning	65
3.2.2 Cloning of Nbea domains	69
4. Discussion	86
4.1 Comparison of β Nrnx KO and α Nrnx KO	86
4.2 Underlying explanations for the β Nrnx mutant phenotypes	90
4.3 Roles of Nbea at synapse	94
4.4 Potential functions of Nbea domains	96
5. Summary	99
References	100
Acknowledgement	111
Curriculum Vita	113

ii

Abbreviations

1/3DKO	Double Knockout of Nrnx β 1 and 3
2SKO	Single Knockout of Nrnx β 2
ACSF	Artificial Cerebrospinal Fluid
AKAP	A-Kinase Anchoring Protein
APV	D-(-)-2-Amino-5-phosphonopentanoic acid
ARM	Armadillo domain in Nbea
ASD	Autism Spectrum Disease
BDCP	BEACH domain containing protein
BEACH	<i>beige</i> and <i>Chediak-Higashi</i>
BNE	pBlueScript-Nbea-EcoRI
CaM	Calmodulin
CaS	Calcium sensor
CASK	Calcium/calmodulin-dependent serine protein kinnase
Cbln	Cerebellin
CMV	Cytomegalovirus
CNQX	1,1,1-trifluoro-ethane-6-Cyano-7-nitroquinoxaline-2, 3- dione disodium salt hydrate
CNV	Copy Number Variant
ddH ₂ O	disdilled water
DAG	Dystroglyan
DUF1088	Domain of Unknown Fuction 1088
eEPSC	evoked excitatory postsynaptic current
EGF	Epidermal growth factor
EGFP	enhanced Green Fluorescent Protein
eIPSC	evoked inhibitory postsynaptic current
ePSC	evoked postsynaptic current
EYFP	enhanced Yellow Fluorescent Protein
FL	Full-length
HKG	House keeping gene
IV relationship	Current-voltage relationship
LNS	Laminin-Nrxn-Sex hormone binding globulin
LB medium	<i>Luria Bertani</i> medium
LRRTM	leucine-rich repeat molecules
LYST	Lysosomal trafficking regulator protein
mEPSC	miniature excitatory postsynaptic current
mIPSC	miniature inhibitory postsynaptic current
mPSC	miniature Postsynaptic current
Nxph	Neurexophilin
Nbea	Neurobeachin
P	Postnatal day
PAGE	Polyacrylamide gel electrophoresis
PH	Pleckstrin homology
PKA	Protein kinase A
PPR	Paired pulse ratio

iii

PS	Penicillin-Streptomycin
PSC	Postsynaptic current
PSD	Postsynaptic density
S1	primary somatosensory cortex
SAP102	Synapse associated protein 201
SN Δ E	pSyn5-eGFP-Nbea Δ EcoRI
SCAM	Synaptic cell adhesion molecule
Syn	Synapsin 1 promoter
TAE buffer	Tris/Acetate/EDTA buffer
TE buffer	Tris/EDTA buffer
TKO	Triple Knockout of Nrnx 1, 2 and 3 β
WT	Wild Type

iv

1. Introduction

The brain mediates the complexities of our personalities, memories and emotions. Despite that the brain has been investigated for centuries, we still lack a lot in comprehensive understanding of details about brain function. During the past century, neurodevelopmental disorder and learning disability has been broadly used to label a variety of cognitive impairments. Autism is one of the mental impairments and is especially interesting because it affects the highly sophisticated brain function of social awareness and communication. Although autism is clearly a disorder that affects the brain, the biological causes are yet not clear. It is under discovering how genetic mutations can be responsible for the behavioral and cognitive problems found in those patients. Most of the mutations identified in autistic people generally affect synapses. A significant proportion of patients are believed to carry mutants in key neurodevelopmental genes (Abraham and Geschwind, 2008). *β -neurexin* (*β nrxn*) and *neurobeachin* (*nbea*) are two autistic candidate genes and both play a role in neurodevelopment. β Nrxn has been shown as an essential trans-synaptic adhesion molecule that is involved in inducing synaptic differentiation (Dean et al., 2003; Graf et al., 2004). Surprisingly, mice lacking β Nrxn are vital and fertilizable. So far, studies of β Nrxn deficient mutants are missing. In contrast, mice lacking Nbea have been investigated and presented lethal phenotypes and impaired neural transmission (Su et al., 2004; Niesmann et al., 2011). While the underlying determinants of this large multi-domain protein is not clear. In this study, I used animal models to probe these genes. With the electrophysiological techniques, I studied for the first time the synaptic transmission in neurons lacking β Nrxn. Clones of Nbea were made as tools for studying links between these two proteins, as well as their relation with autism.

1

INTRODUCTION

1.1 Autism spectrum disorders (ASD)

1.1.1 ASD is a global disease

ASD is one of the most common neurodevelopmental disorders. It consists of a range of complex symptoms. The major symptoms of ASD include: impaired social interactions, communication difficulties, and restricted, repetitive and stereotyped behavior (Lord et al., 2000). Besides autism, which is the most severe form of ASD, there is also milder forms known as Asperger syndrome, and pervasive developmental disorder not otherwise specified (PDD-NOS) (Lord et al., 2000; Abrahams and Geschwind, 2008). Symptoms of ASD are typically apparent before age three and probably last for lifelong (Abrahams and Geschwind, 2008). Boys are four times more likely to be diagnosed as ASD than girls (Carter et al., 2007; Giarelli et al., 2010; Werling et al., 2013).

ASD is a major public health concern that occurs in all ethnic and socioeconomic. The global ASD prevalence shows that one out of 68 (1.5%) children among the age of eight is diagnosed as ASD patient (Centers for Disease Control and Prevention: Morbidity and Mortality Weekly Report, March 28, 2014). This prevalence has strikingly increased about thirtyfold from 0.5% since the first statistics in 1960s (Lotter, 1966; Wing et al., 1976). One prevailing argument for the apparent rising ASD prevalence is the increased awareness, and improved criteria in ASD diagnosis (Posserud et al., 2010).

1.1.2 Genetic basis of ASD

The cause of ASD is yet not certain, but both genetics and environment probably play a role. Twin and family studies strongly suggest that in many cases of ASD, they have a genetic predisposition (Grice and Buxbaum, 2006; Shastry, 2003). Both monozygotic and dizygotic twins studies show greater concordance of ASD

2

INTRODUCTION

than normal prevalence (Grice and Buxbaum, 2006). Studies of monozygotic twins show that when one twin is affected, there is 70-90% possibility the other twin will be affected (Ronald and Hoekstra, 2011; Hallmayer et al., 2011). Dizygotic twins, on the other hand, show about 30% concordance of ASD (Rosenberg et al., 2009; Ronald and Hoekstra, 2011). In addition, in families with one ASD child, the risk of having a second child with ASD is 5%, which is also greater than in the general population (1.5%) (Hughes et al., 1999; Lauritsen et al., 2005). Higher diseases co-occurrence in monozygotic twins than non-twin siblings, as well as the greater concordance of ASD appearance in the same family provides strong evidence that ASD has genetic origins.

1.1.3 Molecular diversity of ASD

Over the past decade, several dozen ASD susceptibility genes have been identified (Geschwind, 2011; Moy et al., 2006; Grice and Buxbaum, 2006). Until now, single mutations, genomic syndromes, and *de novo* copy number variants (CNVs) account for 10-20% of ASD cases (Geschwind, 2011; Abrahams and Geschwind, 2008). However, the cause of autism seems not determined by a single gene, since none of these genes or CNVs account for more than 1% of the ASD cases (Geschwind, 2011). This should not be surprising, since ASD is not defined by the causes of disease, but by observations of abnormal cognition and behaviors.

Candidate genes that are reported to account for ASD represent a diversity of molecular mechanisms in the neuron (Geschwind, 2011). Some of them encode cell adhesion molecules, such as the presynaptic *Nrxn* and postsynaptic Neuroligin (*Nlgn*), which connect the pre- and postsynaptic membranes. These proteins play a role in maturation and balance of excitatory and inhibitory synapses (Bang and Owczarek, 2013; Giannone et al., 2013). Other candidates like *Shank* and *Nbea* are multi-domain scaffold proteins. *Shank* exists at the postsynaptic density and connects neurotransmitter receptors and ion channels

3

INTRODUCTION

to the cytoskeleton and is part of the G-protein coupled signaling pathway (Sheng and Kim, 2000). *Nbea* locates near the trans-Golgi network, and is important for dendritic spine formation, as well as synaptic transmission (Medrihan et al., 2009; Niessman et al., 2011). Notably, there are also ASD candidate genes encoding postsynaptic GABA_A receptor $\beta 3$ subunit, extracellular signal-regulated kinase MAPK3 (Shinoda et al., 2013).

In recent years, various types of genetically modified animal models have been established to study the effects of mutants corresponding to ASD associated genes or loci in humans. Other animal models may involve mutations in pathways that altered in autism (Moy et al., 2006). These animal models provide substantially applicable advances to investigate several facets of ASD, such as changes in neuronal physiology, animal behavior, and hereditary (Moy et al., 2006). The most common strategy for genetic modification is to generate a null allele that prevents the production of functional protein. The advance of this strategy is that only the selected gene is deleted. Other genes, in this case, will not be affected like in knockin animal models (Moy et al., 2006). The mouse models used in this study, *Nrxn* knockout (KO) mice and *Nbea* KO mice, are based on targeted-disruption approach.

1.2 Neurons and synapses

In this study, I focused on the two ASD candidates, *Nrxn* and *Nbea*. These two proteins locate at different regions of the neuron, *Nrxn* at the presynaptic membrane, and *Nbea* near the trans-Golgi network. Therefore, it is quite interesting to ask how these proteins function in neurons, and relate to ASD.

Neurons are among the most morphologically and functionally diverse cells in the human body. Nevertheless, all neurons have common features that distinguish them from cells in other tissues. First of all, neurons are highly polarized cells. The chief functional compartments of neurons, including

4

INTRODUCTION

dendrites, cell body, axons and terminals, are in specific arrangement and usually separated by considerable distance. Secondly, neurons process electrical signals. They are excitable by signals from upstream neurons or outside stimulus, and are able to integrate these signals into an all-or-none response. The sophisticatedly developed polarity and electrical excitability enable neurons to receive, compute and conduct signals over long distance (Kandel et al., 2012).

1.2.1 Synaptic signal transmission

Signals between different neurons are transmitted at a specialized compartment named synapse. Most synapses use a chemical transmitter (Kandel et al., 2012). The chemical synapse is an asymmetric compartment consisting of mainly three parts: presynaptic terminal of axon, synaptic cleft, and postsynaptic terminal of dendrite.

At resting potential of about -65mV , presynaptic vesicles containing neurotransmitter are positioned near the active zone, which is a membrane region specialized for releasing transmitters (Fig. 1.1 A; Südhof and Rothman, 2009; Südhof, 2013). When an action potential depolarizes the presynaptic terminal, voltage-gated Ca^{2+} channels at the active zone open and Ca^{2+} flow into the presynaptic terminal (Fig. 1.1 B). The increased Ca^{2+} concentration triggers fusion of vesicles with presynaptic membrane by stimulating synaptotagmin binding to a core fusion machinery composed of SNARE and Sec1/Munc18-like proteins (Südhof, 2013). The membrane fusion in turn releases neurotransmitters (Fig. 1.1 C).

The transmitters diffuse across the synaptic cleft and bind to their receptors at the postsynaptic membrane. That binding results in the activation of postsynaptic receptors, which are in most cases ion-gated channels. The influx or outflow of ions from receptors in turn depolarizes or hyperpolarizes the

5

INTRODUCTION

postsynaptic terminal (Fig. 1.1 D; Purves et al., 2001; Lisman et al., 2007). In this way, information is transmitted from one neuron to another.

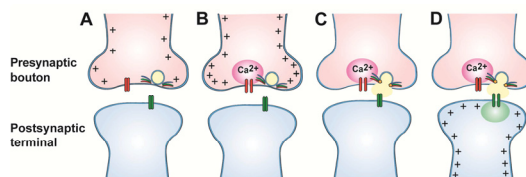


Figure 1.1 Steps in the process of chemical synaptic transmission. These steps occur at the synapses of central nervous system and neuromuscular junction. **A)** Presynaptic action potential is generated by opening of Na^+ channels. **B)** Depolarization of presynaptic terminal opens Ca^{2+} channels (red). Therefore, concentration of Ca^{2+} elevates in microdomain at active zone. **C)** Ca^{2+} binds to synaptotagmin, as well as SNARE and Sec1/Munc18-like proteins complex, which causing opening of fusion pore and neurotransmitter release. **D)** Neurotransmitters diffuse across the synaptic cleft and bind to the postsynaptic receptors (green). Activation of receptors generates postsynaptic signal (Figure modified from Lisman et al., 2007).

1.2.2 Excitatory and inhibitory synapses

The chemical synapses are divided into two classes depending on their postsynaptic responses: excitatory and inhibitory synapse. Activation of excitatory synapses lead to postsynaptic depolarization, and may fire an action potential. Activation of inhibitory synapses, on the other hand, hyperpolarizes the postsynaptic membrane and prevents action potential (Kandel et al., 2012).

Excitatory and inhibitory synapses also differ in locations and molecular contents (Fig. 1.2). Excitatory synapse is majorly located at synaptic spines, while inhibitory synapse locates at dendritic shafts and the cell body (Kandel et al., 2012). Excitatory synapse uses glutamate containing vesicles at presynaptic and AMPA and NMDA receptors at postsynaptic site. Postsynaptic density (PSD)-95 largely functions as a scaffold at excitatory postsynaptic terminals. Inhibitory

6

INTRODUCTION

synapses, on the other hand, are specialized to use GABA as neurotransmitter in presynaptic vesicles, while GABA receptors and scaffolding protein gephyrin characterize the postsynaptic site (De Camilli et al., 2001; Fig. 1.2).

Morphological studies on central nervous system synapses revealed different ultrastructural features of excitatory and inhibitory synapses. The type I synapse that is primarily glutamatergic is characterized with spherical vesicles, larger synaptic cleft, and thicker submembranous postsynaptic scaffolds. Whereas type II synapse is primarily GABAergic, recognized by ovoid/flattened vesicles, smaller synaptic cleft, and thinner postsynaptic scaffolds (De Camilli et al., 2001). The compositional differences are believed to underlie this structural dichotomy.

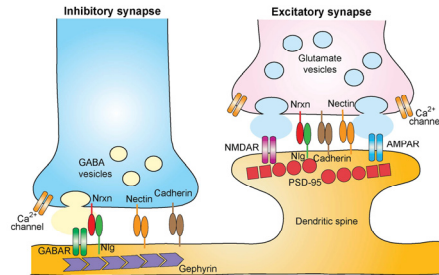


Figure 1.2 Molecular architecture of inhibitory and excitatory synapses. Inhibitory synapse (blue) is present at the dendritic shaft, and excitatory synapse (pink) targets on mature mushroom-shaped spine. These two types of synapses are equipped with distinct subsets of neurotransmitter vesicles, receptors and scaffold proteins. Inhibitory synapse contains GABA vesicles at the presynaptic site, and GABA receptor and Gephyrin scaffold protein at the postsynaptic site. Excitatory synapse contains glutamate vesicles at presynaptic site, AMPA and NMDA receptors are at the postsynaptic membrane. PSD-95 is the specific postsynaptic scaffold protein of the excitatory synapse. The pre- and postsynapses are bridged by several groups of cell adhesion molecules, including Nectin, Cadherin, and pairs of Nrxn and Nign.

7

INTRODUCTION

1.2.3 Synaptic plasticity

Synaptic plasticity is a change of synaptic transmission strength depending on use and experience. It can be either enhanced or depressed (Ho et al., 2011). This change may last from milliseconds to hours, or even longer. Depending on the persistence, the synaptic plasticity is classified into short-term plasticity that last for milliseconds to minutes, and long-term plasticity that last for hours or longer (Sippy et al., 2003). The short-term plasticity is thought to be important for neurons to perform computational tasks, response appropriately to acute changes in activity, and initiate changes necessary for long-term plasticity (Sippy et al., 2003). Short-term effects are such as summation of residual Ca²⁺, altering number of vesicles available for release, and change of post-synaptic receptor activity (Ho et al., 2011). A common method to measure short-term plasticity is an electrophysiological paired-pulse experiment, in which a pair or a series of electrical stimulation is applied to evoke postsynaptic responses. When the ratio of the later response to the first is larger than one, it is defined as synaptic facilitation. If the ratio is smaller than one, it is synaptic depression (Zucker and Regehr, 2002). Long-term plasticity lasts from hours to a whole lifetime. It is believed that the long-term plasticity is induced at appropriate synapses during memory formation, and is both necessary and sufficient for the information storage underlying the type of memory mediated by the brain area in which that plasticity is observed (Martin et al., 2000). The experimental models of long-term plasticity include long-term potential (LTP) and long-term depression (LTD) (Martin et al., 2000; Malenka and Bear, 2004). The most prominent forms of LTP and LTD are induced following the activation of NMDA receptor (Martin et al., 2000). Other physiological changes that lead to long-term plasticity include mobilization or stabilization of post-synaptic receptors, synthesis of new RNA and proteins (Ho et al., 2011). In addition, structural modifications, such as synapse formation or regression, are also involved in long-term plasticity (Feldman, 2009).

8

1.2.4 Synaptic cell adhesion molecules

Synaptic cell adhesion molecules bridge pre- and postsynaptic membranes (Fig. 1.2). In fact, these molecules are not only "glue", but also important in multiple processes in the life of synapses (Missler et al., 2012). The spatially and temporarily coordinated assembly of pre- and postsynaptic specializations ensures the signaling processes, also synaptic establishment, specification and plasticity (Missler et al., 2012). Several molecules are involved, such as cadherins, Ig-domain proteins, presynaptic Nrnx and postsynaptic Nlgn (Fig. 1.2; Missler et al., 2012). Loss-of-function animal models of these proteins revealed that they fulfill several roles in synaptic formation and function. KO studies of Nrnx or Nlgn revealed the essential roles of them in vesicle release and postsynaptic NMDA/AMPA ratio (Zhang et al., 2005; Missler et al., 2003; Varoqueaux et al., 2006). The total number of synapses, however, is not changed (Missler et al., 2003; Varoqueaux et al., 2006; Dodanova et al., 2007). Cadherins are reported to influence early synapse development through catenin signaling (Elia et al., 2006) and synaptic plasticity (Jüngling et al., 2006). Loss of Ig-domain proteins, such as Nectin, may reduce the excitatory synaptic number (Lyckman et al., 2008).

1.3 Nrnx

1.3.1 Nrnxns are brain specific proteins

In mammals, there are three Nrnx genes, namely *nrnx 1-3*. In ASD and other neurodevelopmental disorders, copy number variants and/or *de novo* mutants have been detected in the loci of all three *nrnxns*. Among them, mutations within *nrnx1* exons are one of the most consistently observed finding in ASD (Szatmar et al., 2007). Truncating mutations in Nrnx2 and deletion of Nrnx3 were also reported in ASD and schizophrenia patients (Gauthier et al., 2011; Vaags et al., 2012). Cognitive impairment, behavioral changes and synaptic electrophysiology abnormality that observed in Nrnx1 KO and Nrnx2 KO mouse models further

proved strong evidence for the involvement of Nrnxns in ASD (Eherton et al., 2009; Born et al., 2014).

Each *nrnx* gene has two independent promoters generating a longer α isoform and a shorter β isoform (Fig. 1.3). *In situ* hybridization revealed that in the central nervous system, mRNAs of α - and β Nrnx are distributed only in partially differential patterns (Püschel and Betz, 1995; Ullrich et al., 1995). In particular, the three β isoforms distribute in unique patterns in mouse and rat brains: Nrnx1 β is restricted to cortical layers 2 and 3, thalamus and parts of the hippocampus; Nrnx2 β distributes evenly within the cortex, and slightly enhances in layer 2 and in the septal nuclei; Nrnx3 β is evenly expressed in most brain structures and only slightly more pronounced in the anterior and medial thalamic nuclei (Püschel and Betz, 1995; Ullrich et al., 1995; Aoto et al., 2013). Subcellularly, the endogenous Nrnxns distribute in a dispersed pattern, and highly enriched in synaptic regions (Dean et al., 2003; Zeng et al., 2007).

Both α - and β Nrnxns are presynaptic type I membrane proteins (Fig. 1.3). They share the same C-terminal region, which contains an extracellular laminin-Nrnx-sex hormone binding globulin (LNS)-domain, a transmembrane part, and a short cytoplasmic PDZ-binding domain. The differences between α - and β Nrnxns are at the extracellular N-terminal part, where α Nrnxns additionally contain five LNS domains and three interspersed epidermal growth factor (EGF)-like domains, while the unique N-terminus of β Nrnxn is made of 37 histidine-rich amino acids (Fig. 1.3; Missler et al., 1998).

INTRODUCTION

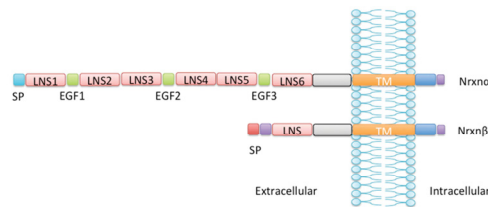


Figure 1.3 Domain organizations of Neurexins (Nrxns). In α Nrxn, there are three LNS (pink)-EGF (green)-LNS repeats, whereas in β Nrxn, there is only one extracellular LNS domain. The C-terminal parts of these two isoforms are identical, except for unique 37-residues (violet) in β Nrxn. LNS: Laminin-neurexin-sex hormone binding globulin domain; EGF: epidermal growth factor-like domain; TM: trans-membrane; SP: signal peptide.

1.3.2 Functional studies of Nrxns

Previous studies of α Nrxns show that they are essential molecules for synaptic transmission (Missler et al., 2003; Kattenstroth et al., 2004; Zhang et al., 2005; Sons et al., 2006; Dodanova et al., 2006). A triple KO of all α Nrxns is lethal to mice (Zhang et al., 2005; Dodanova et al., 2006). Also, most of double KO mice perished within the first week after birth because of abnormal breath (Missler et al., 2003). In addition, even single KOs of α Nrxns lead to a reduced survival probability (Missler et al., 2003). Further studies show that phenotypes of α Nrxn KO variants are related to Ca^{2+} channels and NMDA receptors. In the brainstem and neocortex of α Nrxn KO mice, Ca^{2+} triggered neurotransmitter release was severely impaired in excitatory and inhibitory synapses (Missler et al., 2003; Dudanova et al., 2006). N- and P/Q- type Ca^{2+} channels are selectively affected in the α Nrxn KO mice (Zhang et al., 2005). In addition, activity of NMDA receptor is decreased in the α Nrxn-deficient synapses, while AMPA-receptor-dependent components are unaffected (Kattenstroth et al., 2004). Transmission defects observed in α Nrxn KO mice could not be rescued by β Nrxns (Zhang et al., 2005).

11

INTRODUCTION

Homologous of Nrxn1 α , but not β isoforms, was found in *D. melanogaster* (Zeng et al., 2007). Flies of Nrxn1 null mutant are viable and fertile, but have shortened lifespan and deficient associative learning (Zeng et al., 2007). Further investigations show that null mutant of Nrxn1 in *Drosophila* causes reduced proliferation of synaptic buttons at glutamatergic neuromuscular junctions, while overexpression leads to synaptic overgrowth (Zeng et al., 2007; Chen et al., 2010; Banovic et al., 2010).

Functional investigations of β Nrxn were mainly from exogenous expression in neurons or mouse model, while β Nrxn KO studies are quite limited. A recent study from Born et al. (2014) shows that deletion of both Nrxn2 α and 2 β decreases the frequency of spontaneous synaptic transmission. Exogenous β Nrxn introduced into cultured neurons revealed that β Nrxn is able to induce the formation of new synapses (Dean et al., 2003; Graf et al., 2004; Mondin et al., 2011). Clustering of Nrxn1 β alone may trigger recruitment of markers of presynaptic active zone, like synapsin and synaptobrevin (Dean et al., 2003). On the other hand, β Nrxn may also influence the balance between excitatory and inhibitory synapses together with Nlgn (Mondin et al., 2011; Giannone et al., 2013). The ectopically expressed Nrxn1 β on the surface of COS cells induces accumulation of both glutamate and GABA associated postsynaptic scaffold proteins, PSD-95 and Gephyrin respectively (Graf et al., 2004). In addition, soluble Nrxn1 β could capture postsynaptic membrane-diffusing AMPA receptor via complexes of Nlgn and PSD-95 (Mondin et al., 2011). Other investigations suggest that Nrxn1 β recruits PSD-95 or Gephyrin in dependence of phosphorylation of tyrosine 782 of Nlgn (Giannone et al., 2013). Recent studies of transgenic knockin Nrxn3 β in neuronal cultures and transgenic brain slides reveal that Nrxn3 β plays a role in AMPA receptor endocytosis, and by that influences excitatory synaptic transmission and plasticity (Aoto et al., 2013). These studies suggest that the overexpression of β Nrxn may function in synaptic establishment and specialization. They also imply that β Nrxn KO mouse models will have a more dramatic effect than that have shown in α Nrxn KO.

12

1.3.3 Binding partners of Nrnxns

Nlgns are the most intensively investigated trans-synaptic binding partner of Nrnxn. In human, there are four major isoforms of Nlgn, namely Nlgn 1-4. In mouse, there are only isoforms of Nlgn 1-3. Investigations of mouse models show that all Nlgns are found at the excitatory synapse, while only Nlgn2 is additionally located at inhibitory synapse (Reissner et al., 2013). Studies prove that all of these four Nlgns are able to bind β Nrnxns via the extracellular LNS domain (Ichtchenko et al., 1995; Zhang et al., 2005; Reissner et al., 2008;). Binding between Nlgn and α Nrnxn is regulated with the splice sites in these proteins (splice site B in Nlgn and splice site 4 in Nrnxn) (Missler and Südhof, 1998; Tabuchi and Südhof, 2002; Boucard et al., 2005). Only Nlgn with splice site B would bind with α Nrnxn, while binding with β Nrnxn is largely unaffected (Boucard et al., 2005; Reissner et al., 2008). In addition, these bindings are Ca^{2+} -dependent (Nguyen and Südhof, 1997; Reissner et al., 2008).

Besides Nlgn, there are several other proteins found to interact with Nrnxns (Fig. 1.4). The leucine-rich repeat molecules (LRRRTMs) and $GABA_A$ receptor interact with both α - and β Nrnxns lacking an insert at splice site 4 (de Wit et al., 2009; Zhang et al., 2010), while the Cerebellin (Cbln) bridges postsynaptic GluR δ 2 to Nrnxns containing splice site 4 (Uemura et al., 2010; Joo et al., 2011). Neurexophilin (Nxph), on the other hand, binds to the second LNS domain in α Nrnxn (Fig. 1.4; Missler et al., 1998). Furthermore, Dystroglycan (DAG), a transmembrane protein linking extracellular matrix and cytoskeleton, is reported to interact with both the second and the sixth LNS domains of α Nrnxn (Fig. 1.4; Reissner et al., 2013). The G-protein-coupled receptor C1RL/latrophilin-1 (CL1), another α -latrotoxin receptor, is reported to form stable intercellular adhesion complex with Nrnxn (Boucard et al., 2012). A recent research from Pettem et al. (2013) identified another α Nrnxn-specific interacting partner Calsyntenin-3. These interacting partners are not only physically bind with Nrnxns, but also essential for proper glutamatergic and GABAergic synapse development.

13

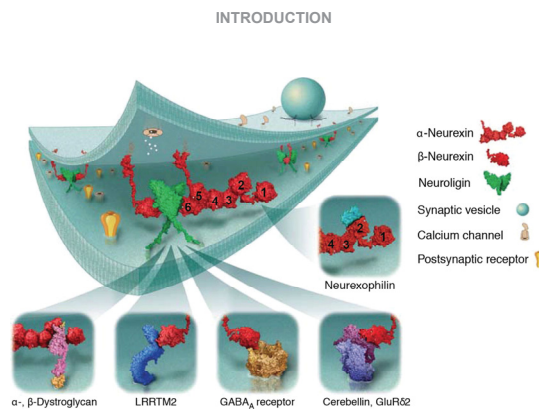


Figure 1.4 Extracellular binding partners of Neurexins (Nrnxns). Schematic diagram shows binding partners of α - and β Nrnxns. The presynaptic Nrnxn is colored in red. The extracellular LNS domains of α Nrnxn are labeled with Arabic numbers. The postsynaptic proteins Nlgns (green), LRRRTM2 (dark blue), $GABA_A$ receptor (yellow), and Cerebellin (violet)-GluR δ 2 (light blue) complex interact with β Nrnxn LNS domain. Dystroglycan (magenta) may interact with second and sixth LNS domain in α Nrnxn. The intercellular Neurexophilin only interacts with the second LNS domain in α Nrnxn. (Figure modified from Missler et al., 2012).

Intracellularly, the PDZ-binding domain is known to interact with calcium/calmodulin-dependent serine protein kinase (CASK), and thereby associates with a tripartite complex comprising CASK, Veli and Mint1 (Mukherjee et al., 2008). This complex might involve in recruitment of synaptic vesicles via Mint1 and Munk18. In addition, Mint1 and CASK also associate with Ca^{2+} channels, which may relate to the Ca^{2+} channel dysfunctions observed in the α Nrnxn KO variants (Zhang et al., 2005; Dodanova et al., 2006). Thus, the trans-synaptic interaction between Nrnxn and its interacting proteins may bridge the synaptic cleft, and align the presynaptic neurotransmitter release machinery with postsynaptic receptors and densities.

14

1.4 Nbea

1.4.1 Nbea is located near the Golgi in neurons

The gene of *nbea* is on human chromosome 13 at a low-frequency common fragile site (FRA13) linked to ASD (Savelyeva et al, 2006). Mutations of *nbea* were also identified in several independent ASD patients. For example, one patient had a breakpoint in intron 2 of *nbea*, which results in an *nbea* haploinsufficient status (Castermans et al., 2003). In addition, monoallelic deletion of *nbea* was reported in four unrelated ASD patients (Smith et al., 2002). Copy number variants were also detected within the Nbea gene in three other patients with ASD (reviewed from Nuytens et al., 2013). These studies suggest a risk of Nbea mutation in ASD.

Nbea is a brain-enriched multi-domain protein with a size of 2946 amino acids and a calculated MW of 328kDa. Western blots of mouse Nbea show that this protein is detectable in brain stem, forebrain and cerebellum (Wang et al., 2000). Immunocytochemical staining of rat brain indicates that Nbea is largely accumulated inside cytoplasm and proximal dendrites of neurons, while the nuclei are spared (Wang et al., 2000). Co-labelling of Nbea with Golgi marker protein GM130 further suggests that Nbea is present in tubulovesicular organelles adjacent to the Golgi apparatus (Niesmann et al., 2011). Its membrane association is stimulated by GTP and dispersed by brefeldin A, an inhibitor of protein transport from the ER to the Golgi apparatus (Wang et al., 2000). The localization and patterns of membrane association suggests a functional link to the post-Golgi sorting or targeting of membrane proteins (Medrihan et al., 2009).

1.4.2 Protein structure of Nbea

Nbea contains a highly conserved BEACH domain. This domain has been identified across different kingdoms (data from NCBI

15

<http://www.ncbi.nlm.nih.gov/protein/?term=BEACH+domain>). The name of BEACH is extracted from Beige and Chediak-Higashi Syndrome that is diagnosed in mice and human, respectively (Kaplan et al., 2008). The BEACH domain in human was firstly identified in the lysosomal trafficking regulator (LYST) protein. Besides Nbea and LYST, there are another seven similar BEACH domain containing proteins (BDCPs) in human, namely neurobeachin-like 1 (NBEAL1), neurobeachin-like 2 (NBEAL2), WD repeat domain 81 (WDR81), lipopolysaccharide-responsive, beige-like anchor protein (LRBA), WD and FYVE zinc finger domain containing proteins (WDFY3, WDFY4), and neutral sphingomyelinase activation-associated factor (NSMAF) (Fig. 1.5 A; Cullinane et al., 2013). The members of BDCP family are large cytosolic proteins (mostly 3,000-4,000 amino acids), and are proposed to be involved in the subcellular targeting of membrane proteins (Medrihan et al., 2009).

BDCPs share a common domain architecture that the BEACH domain is preceded by an atypical pleckstrin homology (PH) domain and followed by C-terminal WD40 repeats (Fig. 1.5 A; Cullinane et al., 2013; De Lozanne, 2003). In Nbea, there are five WD repeats domains, four of which locate at the C-terminal, and the other one is in the middle of the sequence. Computational structure analyses opens the possibility that the WD repeats in the middle is assembled together with the other four WD repeats domains via protein folding (Fig. 1.5 B). Another computational study suggests, six of the nine BDCPs contain an N-terminal lectin-like domain, which may be involved in carbohydrates binding (Burgess et al., 2009). It is further proposed that the lectin-like domain in BDCPs associate with protein traffic and sorting along the secretory pathway (Cullinane et al., 2013). Interestingly, a domain of unknown function 1088 (DUF1088) is shared in both Nbea and LRBA (Cullinane et al., 2013). This domain may indicate a specific function of these two proteins.

Furthermore, an A-kinase anchoring protein (AKAP) motif is identified in Nbea (Wang et al., 2000). This AKAP motif is found only in Nbea, but not its putative

INTRODUCTION

isoform LRBA or other BDCPs (Wang et al., 2000). The AKAP motif is 19 amino acids long, and has high affinity (K_d , 10nM) to type II regulatory subunit of protein kinase A (PKA RII) (Wang et al., 2000). AKAP site is suggested to concentrate inactive PKA holoenzyme to Nbea (Wong and Scott, 2004). Rise of local cAMP causes the release and activation of catalytic subunits of PKA that later phosphorylate substrate proteins in their vicinity (Wong and Scott, 2004).

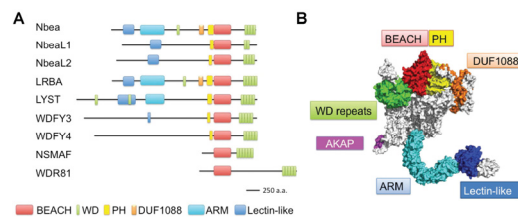


Figure 1.5 Schematic diagram of human BEACH domain containing protein (BDCP) and Nbea computational structure **A** All nine human BDCP are aligned at the BEACH domain (red). The WD repeats domain (green) follows the BEACH domain in all BDCPs. The PH domain (yellow) precedes the BEACH domain in seven out of nine proteins. Other recognized domains include domain of unknown function (DUF) 1088 (orange) in Nbea and LRBA, Armadillo (ARM, cyan), and Lectin-like (blue) domains. Scale bar represents length of 250 amino acids. (Figure A is modified from Cullinane et al., 2013). **B** Computational predicted Nbea protein structure. Domains are highlighted with same colors as in A.

1.4.3 Functional investigations of Nbea

Nbea has been identified in both invertebrates and vertebrates. The homolog in *Drosophila*, *Rugose* (Rg), shares an identical domain arrangement with mouse Nbea, and over 60% sequence conservation within the defined domains (Volders et al., 2012). *Drosophila rg* null mutants present altered associative odor learning, brain morphology, and neuromuscular junction architecture and function. Interestingly, a mouse Nbea transgene could partially rescue the Rg KO phenotypes (Volders et al., 2012). This indicates that Rg and Nbea are, at least partially, functionally redundant.

17

INTRODUCTION

In newborn mice, homozygous KO of Nbea results in lethal paralysis (Su et al., 2004; Medrihan et al. 2009). The newborn mice of Nbea KO are cyanotic, lack spontaneous and stimulated motor activity, and usually have an umbilical hernia and hump. They die within minutes after birth (Su et al., 2004; Medrihan et al. 2009). While the WT littermates are active, responsive and have a pink complexion (Su et al., 2004). The lethal paralysis of Nbea-deficient mice may be due to the abolishment of evoked presynaptic vesicle release at neuromuscular junctions (Su et al., 2004). Besides, neurotransmission at excitatory and inhibitory synapses in the brain stem and cultured hippocampus neurons are also severely impaired (Medrihan et al., 2009; Niesmann et al., 2011). Both of these defects may lead to asphyxia and death.

Besides neurotransmission, altered neuronal protein expression was detected in Nbea KO mice. Several vesicle-related synaptic proteins, including synaptophysin, synapsin, SV2 and Mint-1, were down regulated by 25-40%. Other proteins including active zone proteins, scaffold proteins and receptors were not changed (Medrihan et al., 2009). This indicates that Nbea affects specific vesicle-related proteins at presynaptic site, and may have an effect on the number of synaptic terminals or vesicles in the central nervous system (Medrihan et al., 2009).

Further studies confirmed the hypothesis that the number of dendritic spine is reduced in both cultured Nbea KO neuron and cortical tissue from heterozygous mice (Niesmann et al., 2011). The underlying cause of the reduced spine number might be altered organization of synaptic contacts in absence of Nbea. For example, the most obvious change is an accumulation of cytoskeletal F-actin inside soma and processes in Nbea KO neurons (Niesmann et al., 2011). While in WT neurons, F-actin is mostly evenly distributed and slightly concentrated at the synapses. Besides cytoskeletal proteins, some synaptic proteins, like synaptopodin and PSD-95, are also ectopically recruited (Niesmann et al., 2011). Synaptopodin, a spine associated protein with actin-bundling activity, is abnormally accumulated near the Golgi (Niesmann et al., 2011). The postsynaptic scaffold protein PSD-95 of excitatory synapses, in addition, is more

18

INTRODUCTION

likely to cluster at the synaptic shaft, rather than the spinous synapses (Niesmann et al., 2011). These observations are quite interesting as previous investigations of protein expression profile from immunoblotting shows that the amount of synaptopodin and PSD-95 are not changed in Nbea KO mice (Medrihan et al., 2009). It implies a role of Nbea in transporting important proteins to proper positions in the neuron.

Proves of that Nbea is involved in synaptic protein trafficking keep emerging. Some recent studies show that Nbea could interact with several post-synaptic proteins. For example, an anchoring protein for glutamate receptors named Synapse associated protein 102 (SAP102) could binds with Nbea (Lauks et al., 2012). Neurotransmitter receptor GlyR could also interact with Nbea (de Pino et al., 2011). Interactions between Nbea and these two proteins require the C-terminal part of Nbea, which contains at least the DUF1088, PH-BEACH, and WD40 repeats domains (Lauks et al., 2012; de Pino et al., 2011). Receptors including AMPA, NMDA, kainate and GABA_A fail to reach the synapse in the neurons without Nbea (Nair et al., 2013). Preliminary investigation from C. Neupert (unpublished data) reveals altered trafficking speed of α - and β Nrxns in the axons of Nbea KO neurons. These findings together suggest that Nbea might be involved in trafficking important cargo to synaptic compartments, thus influence the formation and transmission of synapses.

1.5 Aims and objectives

In summary, both *nrxn* and *nbea* are ASD-related genes. Among them, Nrxns have been shown as essential trans-synaptic proteins. Most of α Nrxns KO mice perished within one week after birth (Missler et al., 2003; Zhang et al., 2005; Dodanova et al., 2006). Overexpression of the other isoform, β Nrxn, could induce postsynaptic differentiation and interact with several postsynaptic cell adhesion molecules and receptors (Dean et al., 2003; Graf et al., 2004; Uemura et al., 2010; Giannone et al., 2013). However, mice lacking β Nrxn are surprisingly vital and

19

INTRODUCTION

fertilizable. Therefore, it is questioned: 1) would the deletion of β Nrxn influence the synaptic function? 2) Whether the β Nrxn is functionally redundant with the α Nrxn? Furthermore, the brain-enriched multi-domain protein Nbea is likely to involve in the trafficking of Nrxns. Mice lacking Nbea showed a more rapid death within hours after birth (Su et al., 2004; Madrihan et al., 2009). These facts raised the question of whether Nbea is an upstream regulator in the pathway of Nrxn function.

In this project, I firstly characterized the neurotransmission and synaptic plasticity of β Nrxn KO variants with whole-cell patch clamp. Additionally, expressions of *anrxns* and *nlgn*s were studied via RT-qPCR to probe possible changes in the genes closely related with *βnrxns*. At last, plasmids of Nbea and Nbea domain related constructs were made for further investigations.

20

2. Materials and methods

2.1 Materials

2.1.1 General chemicals

Substance	Company
Ethanol	AppliChem, Germany
Sodium chloride (NaCl)	Carl Roth, Germany
Potassium hydroxide (KOH)	AppliChem, Germany
Potassium chloride (KCl)	Carl Roth, Germany
Chloroform	Roth, Germany

2.1.2 General apparatus and consumables

Apparatus/consumables	Company
Centrifuges	Eppendorf, Germany; Beckman, USA
Water bath	Julabo, Germany
Filter papers	Whatman, GE Healthcare, UK
Magnetic stirring plates	IKA, Germany
pH-meter	WTW, Germany
Pipettes	Gilson, France
Vortex machine	IKA, Germany

2.1.3 Materials for electrophysiology

2.1.3.1 Chemicals for electrophysiology

Substance	Company
(2S)-3-[[[(1S)-1-(3,4-Dichlorophenyl)-ethyl] amino-2-hydroxypropyl] (phenylmethyl) phosphinic acid hydrochloride (CGP55845)]	Tocris, UK
1,1,1-trifluoro-ethane-6-Cyano-7-nitroquinoxaline-2, 3- dione disodium salt hydrate (CNQX)	Sigma-Aldrich, USA
1(S), 9(R)-(-)-Bicuculline methiodide (Bicuculline)	Sigma-Aldrich, USA
Agar	AppliChem, Germany
Calcium chloride (CaCl ₂)	Carl Roth, Germany
Cesium hydroxide (CsOH)	Alfa Aesar, Germany
Cesium methanesulfonate (CsMeS)	Sigma-Aldrich, USA
D -(-)-2-Amino-5-phosphonopentanoic acid (APV)	Tocris, UK

21

MATERIALS AND METHODS

Substance	Company
Ethylene glycol tetraacetic acid (EGTA)	Carl Roth, Germany
Glucose	Roth, Germany
Isoflurane	Abbott, USA
Lidocaine N-ethyl chloride (QX-314)	Sigma-Aldrich, USA
Magnesium chloride (MgCl ₂)	Carl Roth, Germany
Magnesium sulphate (MgSO ₄)	Carl Roth, Germany
Monosodium phosphate (NaH ₂ PO ₄)	Carl Roth, Germany
Na ₂ -ATP	Carl Roth, Germany
Na ₂ -GTP	Carl Roth, Germany
Potassium chloride (KCl)	Carl Roth, Germany
Potassium gluconate (K-gluconate)	Sigma-Aldrich, USA
Potassium hydroxide (KOH)	AppliChem, Germany
Sodium bicarbonate (NaHCO ₃)	Carl Roth, Germany
Sucrose	Carl Roth, Germany
Tetraethylammonium chloride (TEA-Cl)	Sigma-Aldrich, USA
Tetrodotoxin (TTX)	Alomone Labs, Israel

2.1.3.2 Consumables for electrophysiology

Consumables	Company
Capillary glass	Harvard Apparatus, USA
Concentric bipolar electrode, SNEX-100/1	Science Products, Germany
Filter papers	Whatman, GE Healthcare, UK
Reference electrode	Luigs & Neumann, Germany
Slice anchor	Harvard Apparatus, USA
Stainless steel blades	LUTZ Blades, Germany
Syringe Filter	SUN Sri, USA
Syringe needle	World Precision Instruments, USA
Tissue adhesive	Aesculap - B. Braun, Germany

2.1.3.3 Apparatus for electrophysiology

Apparatus	Company
Bath chamber	Mechanical Workshop, Institute of Physiology, Münster, Germany
Cryoscopic osmometer, Osmomat 030	Gonotec, Germany
Fixed-stage microscope, Axio Examiner	Carl Zeiss, Germany
Manipulator controller, Keypad SM-5	Luigs & Neumann, Germany
Manipulator units, Mini25 3Axes	Luigs & Neumann, Germany
Microscope objectives EC Plan-neofluar 5x/0.16 Achroplan IR 40x/0.80 W	Carl Zeiss, Germany
Noise eliminator, HumBug	Quest Scientific, Canada

22

MATERIALS AND METHODS

Apparatus	Company
Patch-Clamp amplifier, EPC 10 USB Double	HEKA Elektronik, Germany
Peristaltic pump	IDEX Health & Science, Switzerland
Pipette puller, PIP 6	HEKA Elektronik, Germany
Pulse stimulator, 2100	A-M Systems, USA
Slice mini chamber I	Luigs & Neumann, Germany
Temperature controller, Badcontroller V	Luigs & Neumann, Germany
Video camera, infrared video camera	TILL Photonics, Germany

2.1.3.4 Solutions for electrophysiology

Artificial cerebrospinal fluid (ACSF)

ACSF was used to provide an appropriate physiological environment for brain slices during and after brain slice preparation. It was always freshly prepared from stock solutions A, B and C. Stock solutions were kept at 4°C in a fridge for no longer than 10 days. During experiments, ACSF solution was continuously gassed with 5% CO₂ and 95% O₂ to maintain the pH at 7.3. The final osmolarity of the ACSF solution was around 300-310 mOsmol/kg.

Stock solution A (20x concentrations):	
NaCl (MW 58.4)	2.36 M
KCl (MW 74.56)	60 mM
NaH ₂ PO ₄ •H ₂ O (MW 137.99)	20 mM
D-Glucose (MW 180.2)	400 mM
MgCl ₂ •6H ₂ O (MW 203.3)	20 mM
Stock solution B:	
CaCl ₂ •2H ₂ O (MW 147.02)	1 M
Stock solution C:	
NaHCO ₃ (MW 84.01)	500 mM

ACSF was prepared from stock solutions and distilled water. The final concentrations of ACSF solution were:

NaCl	118 mM
KCl	3 mM
NaH ₂ PO ₄	1 mM
D-Glucose	20 mM
MgCl ₂	1 mM
CaCl ₂	1.5 mM
NaHCO ₃	25 mM

23

MATERIALS AND METHODS

Intracellular pipette solution

Different pipette solutions were prepared according to the purpose of the experiments. For recordings of miniature excitatory postsynaptic currents (mEPSCs), evoked excitatory postsynaptic currents (eEPSCs) and evoked inhibitory postsynaptic currents (eIPSCs), a K-gluconate based solution was used. For the miniature inhibitory postsynaptic currents (mIPSCs) recordings, a K-chloride based solution was applied. QX-314 was added in the intracellular solution to ensure the blockage of Na⁺ channels (McCleskey, 2007). The final osmolarity of the intracellular pipette solution was adjusted with K-gluconate (For gluconate based solution) or K-Chloride (chloride based solution) and water. The final osmolarity was around 300-310 mOsmol/kg.

K-gluconate based pipette solution (pH 7.3):

K-gluconate	140 mM
CaCl ₂	1 mM
HEPES	10 mM
MgCl ₂	2 mM
Na ₂ -ATP	4 mM
Na ₂ -GTP	0.5 mM
EGTA	10 mM
QX-314	5 mM

K-chloride based pipette solution (pH 7.3):

KCl	140 mM
CaCl ₂	1 mM
HEPES	10 mM
MgCl ₂	2 mM
Na ₂ -ATP	4 mM
Na ₂ -GTP	0.5 mM
EGTA	10 mM
QX-314	5 mM

24

MATERIALS AND METHODS

2.1.3.5 Animals

Mice for the electrophysiological studies were held at the animal facility of the Institute of Anatomy and Molecular Neurobiology of University Hospital Münster in accordance with local institutional and governmental regulations for animal welfare. Mice used for electrophysiological recordings are Wild-Type (WT), *Nrxn2* β single knockout (2SKO), *Nrxn1* β /*3* β double knockout (1/3DKO) and *Nrxn1* β /*2* β /*3* β triple knockout (TKO). These mouse lines were kindly provided from Prof. Thomas C. Südhof's lab (Stanford University). The first exons of all three β *Nrxn* genes were flanked by LoxP (floxed). The homologous triple floxed mice were used as WT. One or more β *Nrxn* genes were knocked out by a recombination of LoxP sites when the floxed mouse lines were crossed with *Elle-Cre* transgenic mice. Postnatal 13-21 (P13-21) days old mice were used for electrophysiological experiments. The genotypes of animals were characterized by PCR before each experiment and remained unknown until analysis was finished.

2.1.4 Materials for molecular biology

2.1.4.1 Chemicals for molecular biology

Substance	Company
Agarose	Invitrogen, Netherland
DNA ladder and loading buffer	Thermo Scientific, Germany
dNTP	Invitrogen, Netherland
EDTA	Amersham Pharmacia Biotech, Germany
Ethidium Bromide	Roche, Germany
Isopropanol	Roth, Germany
LB-agar	Invitrogen, Netherland
<i>Luria Bertani</i> (LB) powder	Carl Roth, Germany
Dephosphatase	Roche, Germany
Lysozyme	Roche, Germany
Restriction endonucleases, buffers	New England Biolabs, USA
Tris	Amersham Pharmacia Biotech, Germany

25

MATERIALS AND METHODS

2.1.4.2 Apparatus/consumables for molecular biology

Apparatus/consumables	Company
Biospectrometer	Eppendorf, Germany
Centrifuge (for Maxi prep)	Beckman, USA
Centrifuge 5424	Eppendorf, Germany
Conical 15 ml tubes	BD Falcon, USA
Electrophoresis power supply	Biometra, Germany
Electroporators	BioRAD, Germany
Heat block	Eppendorf, Germany
Incubator shaker, for bacterial culture	Eppendorf, Germany
Ligation chamber	Techne, Cambridge, UK
PCR machines	Eppendorf, Germany
Petri dish	Sarstedt, Germany

2.1.4.3 Solutions and Media

Tris/EDTA (TE) buffer (pH 8.0):

TE buffer was prepared with distilled water (ddH₂O) and was applied to dissolve purified DNA from mini prep or maxi prep.

Tris	10mM
EDTA	1mM

Tris/Acetate/EDTA (TAE) buffer (pH 8.5):

TAE buffer was the running buffer in gel electrophoresis, and the buffer in making agarose gel. It was prepared from a 50x stock solution. The stock solution was prepared with ddH₂O as:

Tris	242.28g/L
EDTA-Na	18.61g/L
Acetic acid	40ml/L

Luria Bertani (LB) medium:

LB Broth	20 g/L
----------	--------

The powder of LB Broth was dissolved in ddH₂O. The mixture was sterilized at 121 °C for 15 min, and cooled down. Proper antibiotic was added before use.

26

MATERIALS AND METHODS

LB agar plates:

LB agar 32 g/L

The powder was mixed with ddH₂O. Then it was dissolved and sterilized at 121°C for 15min. Proper antibiotic was added when the LB agar was cooled down to about 50 °C. Then the mixture of LB agar and antibiotics was poured to petri dishes and solidified. These dishes were stored in 4 °C, and briefly warmed up at 37 °C before spreading *E.coli* on it.

NZY⁺ medium:

MgCl₂ · 6H₂O 1M
MgSO₄ · 6H₂O 1M
Glucose 2M

They were dissolved in LB medium. The prepared NZY⁺ medium was stored at -20 °C and melted shortly before use.

2.1.4.4 Kits for molecular biology

DNA ligation	Fermentas Rapid Ligation kit	Thermo Scientific, Germany
PCR	iProof High Fidelity	BioRAD, Germany
Quikchange	QuikChange Lightning Site-Directed Mutagenesis Kit	Agilent Technologies, Germany
DNA extraction from agarose gel	QIAEXII Gel Extraction Kit	QIAGEN, Germany
Mini prep	NucleoSpin Plasmid	Macherey Nagel, Germany
Maxi prep	NucleoBond [®] PC500	Macherey Nagel, Germany

2.1.4.5 Bacterial strains

E.coli XL1-Blue	Stratagene, USA
E.coli XL10-Gold	Stratagene, USA

27

MATERIALS AND METHODS

2.1.4.6 DNA materials

Vectors

pEYFP-C1-Nbea	Imagenes, UK
pBlueScript	Stratagene, USA
pSyn-EGFP	Lab storage

Primers for DNA cloning

Name	Description	Sequence
MM11-131	Mlul-Syn-EGFP-Nott f	TTATTAACGGCTAGACTCGACAGGGCCCTCGGTATGAGT
MM11-132	Mlul-Syn-EGFP-Nott r	GATGATCGCGCCCGACTGTACAGCTCGTCCATGCCGAGATG
MM12-45	Nbea ΔAKAP +Spel f	GGTGAGAGAAATGGTGCCTAGTGAATGATGGAAGTGTGG
MM12-46	Nbea ΔAKAP +Spel r	CAAACACTTCCATGTACATCTCACTAGTGCACATCTCTCCACC
MM12-47	ARM f	GCCTGCAGGTCGACCTTTTGGCCAAATGGATAATAGGAGCTCAATG
MM12-48	ARMA r	ATCCTCTAGATTCCTCTGTTGGGATTTTATCAAGAGAAATG
MM12-68	Lectin-like f	GCCTGCAGGTCGACACTTTTTCAATTCCTCGTGTAGCGC
MM12-69	Lectin-like r	GGATCCTTAGAGAAAGTACTCTATATCCAGGTCTAACTGATGAATTCG
MM12-70	PH-BEACH f	GCCTGCAGGTCGACGCCAGTGTCTCAGCACCCCTG
MM12-71	PH-BEACH r	GGATCCTTAGAGAAAGGCGGATGGTCTCAATAAGCAACTG
MM12-84	DUF f	CTGCAGGTCGACGAAGGAGTACTGCTGATGCTATGAAG
MM12-85	DUF r	GATCCTCTAGAGTCTCTCCAGCATAAGTCTGTCTC
MM13-18	WD long f	CTGCAGGTCGACACTACAATGTTTCTGATTCCTGAGTTAAATGG
MM13-01	WD 2-5 f	CTGCAGGTCGACGCCATGGGATGGTCACTTG
MM13-02	WD 2-5 r	GATCCTCTAGACTCATAATGCCACCGATTAATCTATATAAAGC
MM13-05	QC ΔDUF Clal1 f	GCAGGACTTGCTATTGAGCTCATGATAAATGAAGGAGTACTGTGCCATG
MM13-06	QC ΔDUF Clal1 r	CATGGCACAGTAATCTCTCATTATCGATGAGCTCAATAAATGCAAGTCCTGC
MM13-07	QC ΔDUF Clal2 f	CAGAATCTATGCTGGAAGGAGACGATATCGATGAGTCTGCTACAGGAG
MM13-08	QC ΔDUF Clal1 r	CTCCTGTAGCAGACTGACTGCATGATCTGCTCTTCCAGCATAAGTTCTG

2.1.5 Software

Software	Vision	Company
ABF File Utility	V2.1.76	Synaptspft
Adobe Illustrator CS3	13.0.2	Adobe
Clampfit	10.0.0.61	Molecular Device
FitMaster	V2x73	HEKA Elektronik
Microsoft Excel	14.3.1 (130117)	Microsoft
MiniAnalysis	6.0.7	Synaptosoft
Parallels Desktop	6.0.12106	Parallels
Patch clamp amplifier	EPC-10	HEKA Elektronik
PatchMaster	V2x35	HEKA Elektronik
PrimerSelect	8.0.2 (13) Intel	DNASTAR
Prism	4.0c	GraphPad Software
SeqBuilder	8.0.3 (1) Intel	DNASTAR
SeqMan	8.0.2 (16) Intel	DNASTAR

28

2.2 Methods

2.2.1 Electrophysiological recordings

All electrophysiological recordings were performed in mouse layer V pyramidal neurons of the primary somatosensory (S1) cortex (Fig. 2.1). This is a region responding for collecting and processing mouse whisker movement (Fig. 2.1 A; Aronoff and Petersen, 2008). Four aspects were mainly recorded and analyzed: 1) Basic cell properties of the recorded cells, such as the cell membrane resistance and cell capacity; 2) Spontaneous synaptic transmission (mEPSCs and mIPSCs); 3) Action potential dependent synaptic transmission, which is also named as evoked synaptic transmission; 4) Short-term synaptic plasticity. All recordings were performed with the whole-cell voltage-clamp technique, which means to hold the cell membrane at certain voltages (holding potentials) and record the current changes during experiments. The recording region on the brain slice is shown in figure 2.1 B. The recording pipette serves two responsibilities: current injector to maintain the neuron at holding potential, and current detector to test the current changes during recording. For the spontaneous synaptic transmission experiments, only the recording pipette is required, while in the evoked ones, a stimulus electrode is placed literally 100 μm from the recording position (Fig. 2.1 B). A Patch clamp amplifier (HEKA Elektronik) and software Patchmaster (HEKA Elektronik), Fitmaster (HEKA Elektronik) were used in electrophysiological recording and evaluation.

29

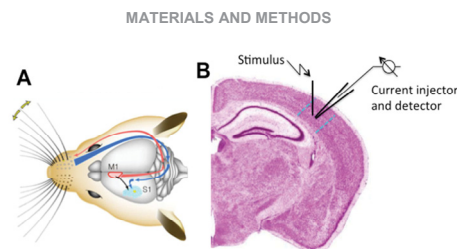


Figure 2.1 Mouse brain primary somatosensory cortex (S1) and electrical recording setup. **A)** This figure shows an impressive position of rodent S1 (blue). The whiskers send sensory information to S1 via the brainstem and the thalamus. Signals are further transduced to motor cortex (M1, red), which in turn regulates whisker movements. Figure A was modified from Aronoff and Petersen, 2008. **B)** Blue dashed lines mark the S1 region. Pyramidal neurons from layer V in the S1 region were recorded. A stimulating electrode was placed approximately 100 μm aside to the recorded neurons according to the experimental protocol. Figure B was modified from High Resolution Mouse Brain Atlas (Sidman et al., 1996 <http://www.hms.harvard.edu/research/brain/atlas.html>).

2.2.1.1 Acute brain slice preparation

Mice at postnatal days (P) 13 to 21 were used for slice preparation and recordings. Before decapitation, the body weight of each mouse was documented to detect a possible phenotype. Afterwards, mice were deeply anesthetized by an isoflurane inhalation and quickly decapitated. The brain was removed immediately from the skull and cooled down in ice-cold ACSF that was gassed with 5% CO_2 and 95% O_2 .

The olfactory bulb, parts of the frontal cortex and the cerebellum were removed with a pre-chilled scalpel in a petri dish containing frozen ACSF. The remaining brain was then fixed vertically onto a small cube of 4% agar by tissue adhesive and cut with a vibrating microtome (Campden Instruments) into slices of 300 or 360 μm thickness. Those slices containing the S1 region were transferred into a slice bath chamber filled with ACSF at room temperature and equilibrated with 5% CO_2 and 95% O_2 . Slices were incubated for at least one-hour in the ACSF before recordings.

30

2.2.1.2 Patch-clamp setup

The components for patch-clamp setup mainly include a microscope, buffer circulation, an amplifier, a computer, a recording pipette and a stimulus electrode (Fig. 2.2). The microscope, recording pipette and stimulus electrode were placed on a vibration-isolated platform. Recordings were established under infrared contrast microscopy and the slice was submerged with pre-warmed floating ACSF (29°C, flow rate 2 - 4 ml/min). An infrared video camera assisted 40x water immersion objective guarantees the visual control of the experimental setup (Fig. 2.2). The pipettes were prepared from glass capillary (Harvard apparatus limited) shortly before experiments. They were pulled in two steps with a vertical electrical pipette puller (HEKA Elektronik) into two pipettes. Then, one of the pipettes was filled with proper pipette solution with a capillary syringe needle and installed in the recording setup. The fine-tip pipette had a resistance of 2-4 M Ω when merging into the bath solution. The pipette was then navigated with a manipulator controller to achieve the whole-cell configuration.

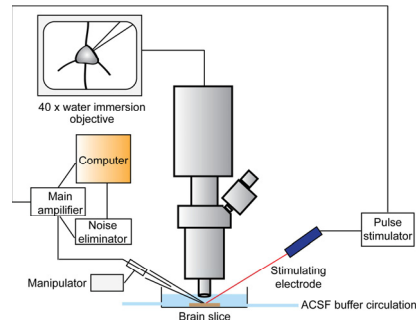


Figure 2.2 Schematic diagram of the patch-clamp setup. A conventional fixed-stage upright microscope was equipped with an infrared light through the bath chamber. The recording pipette, noise eliminator and stimulating electrode were connected with the main amplifier that was controlled by the computer. The movement of recording pipette was achieved through the manipulator controller. The stimulating electrode was placed closely to the recording pipette in the evoked stimulation experiments. ACSF buffer floats through of the bath chamber during the recordings.

2.2.1.3 Whole-cell configuration

Whole-cell configuration is to patch the neuron at cell body and connect cytoplasm with the pipette solution and further the recording system. Recording electrode was navigated to the target cell with help of a manipulator (Fig 2.2). The recording pipette was applied with a positive pressure to blow away tissues covering the target cell at the beginning of the whole cell configuration procedure (Fig. 2.3 A and B). When the recording pipette reached the cell surface, a concave on the cell surface was observed and the on-cell status was achieved (Fig. 2.3 C-I). Then the positive pressure of the pipette was gently removed and the cell surface was attached to the pipette (Fig. 2.3C-II). A constant giga-ohm seal (gigaseal, resistance $\geq 1\text{G}\Omega$) was formed by gentle suctions (Fig 2.3C-II). During the gigaseal formation, the holding potential of the pipette was changed from 0 mV to -60 mV. After achieving a constant gigaseal, stronger suction was applied to rupture the cell membrane that was attached to the pipette tip. The breaking of the cell membrane connects the pipette solution with the cytoplasm, and produces a large transient current. The pipette solution was then intermixed with the cytoplasm (Fig 2.3 C-III). Cell capacitance and input resistance should be compensated at this stage. The whole-cell configuration was thus established.

MATERIALS AND METHODS

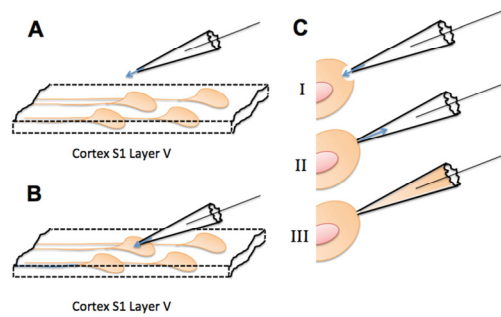


Figure 2.3 Achieving the whole-cell configuration **A)** Before approaching the brain slice, positive pressure was applied to the pipette. **B)** The positive pressure blows away tissues surrounding the target cell soma. **C)** After achieving the on-cell status (I), the positive pressure was gently reduced, so that the pipette is attached with the cell membrane. A gigaseal was achieved by gently providing suction to the cell (II). The suction ruptures the attached cell membrane. Thus the cell and the pipette were connected for measurements (III).

2.2.1.4 Basal cell property assessment

Immediately after achieving the whole-cell configuration, the current-voltage (IV) relationship was measured to assess the basal cell property. This measurement uses steady-state voltage steps of 200 ms duration. The patched cell was held at -60 mV. Then the holding potential rises in 10 steps to constant voltages from -100 mV to -10 mV, with difference of 10 mV between each step. Between each clamp step there was a one second interval. For analysis, the current values were plotted against the corresponding voltage value, and linear regression curves were built. The slope of the linear curve represents the conductance of the cell, and the x-axis intercept value resembles the calculated resting membrane potential. Input membrane resistance was calculated as the inversion of the conductance. Only cells with an input resistance between 80-400M Ω and membrane potential between -55 to -75 mV were considered as a good-property recording and included for further analysis.

33

MATERIALS AND METHODS

2.2.1.5 Spontaneous neural transmission

Spontaneous neuronal transmission, which is termed as miniature post-synaptic currents (mPSCs), refers to the vesicle releases at resting potential in presence of TTX (500 nM). Under this condition, Na⁺ channels are blocked, so that no action potential will be produced and transduced to the synaptic terminals. The synapses were kept at holding potential of -70 mV, which was close to the resting potential in a living animal. The remaining synaptic currents is produced from the spontaneous vesicle release and opening of postsynaptic neurotransmitter receptors, which are mostly ion channels (Kandel et al., 2012)

The mPSCs of excitatory (mEPSCs) and inhibitory synapses (mIPSCs) were measured separately via applying different receptor blockers. For mEPSC recordings the K-gluconate based pipette solution was used. This solution is close to the physiological intracellular conditions of neurons. In addition, 10 μ M bicuculline was applied to the bath solution to block GABA_A receptors. The mIPSC, on the other hand, was measured with the K-chloride based pipette solution. This solution provides high concentration of Cl⁻ inside the cell. It is different from the real *in vivo* condition, but can produce clear mIPSC reverse current from efflux of Cl⁻. Furthermore, pure mIPSC signals were measured in presence of 10 μ M CNQX (to block AMPA receptors) and 25 μ M APV (to block NMDA receptors) in the bath solution.

Each spontaneous event recording lasted for at least 3 minutes with a filter of 1 kHz. Every patched neuron was measured at least three times. The one with best quality (e.g. moderate and stable noise background, small holding current) of these three recordings was analyzed by MiniAnalysis program (Synaptosoft). Background noise was digitized and quantified by the program. Only events that were at least fourfold larger than the noise were selected for further analysis. Parameters of amplitude, frequency, rise time and decay time were evaluated for each event and averaged values were calculated for each cell. Data from at least 22 cells were averaged for each genotype.

34

MATERIALS AND METHODS

2.2.2.6 Activity dependent neurotransmission

Electrically evoked postsynaptic currents (ePSCs) were measured to study the activity dependent basal synaptic transmission. Extracellular field stimulation was applied in the same layer (layer V) of cortex as the recorded neuron (Fig. 2.1). The distance between the stimulating electrode and the patched cell was approximately 100 μm .

Evoked excitatory postsynaptic currents (eEPSCs) were recorded at -70 mV in presence of 2 μM bicuculline. Evoked inhibitory postsynaptic currents (eIPSCs) were recorded at -20 mV. Pharmacology of 20 μM CNQX and 25 μM APV were additionally applied to block AMPA and NMDA receptors. The K-gluconate based pipette solution was used for both, eEPSC and eIPSC recordings. Single 70 μs stimulation shocks were given with 0.02 - 0.20 mA stepwise increasing strengths. The difference between each stimulation step was 0.02 mA. Stimulations were given with a 5 s interval time. The responding membrane currents were digitized and recorded for further analysis.

At least three response sweeps were calculated under each stimulus. Maximal amplitudes, and amplitudes at half-maximum stimulation intensities were calculated with the FitMaster software. The time constants such as decay times were analyzed with the Clampfit software (Molecular Device) as a monoexponential fit. Input/output relationships between the stimulus strengths and the evoked amplitudes were diagrammed with GraphPad Prism software.

2.2.1.7 Short-term plasticity

Short-term plasticity acts on a time scale from milliseconds to a few minutes (Zucker and Regehr, 2002). The short-term plasticity was measured via two protocols: one pair pulses experiment and 20-Hz stimulus train experiment.

35

MATERIALS AND METHODS

The paired-pulse experiment uses two successive electrical pulses with different inter-stimulus intervals varying from 30 ms to 200 ms. Paired stimuli were applied 10 times with 20 s breaks. The paired-pulse ratio (PPR) was calculated as the averaged ratio of second to first amplitude of two consecutive ePSCs from the same inter-stimulus intervals. In particular, the failures of evoked events were excluded in analyzing the PPR. The 20 Hz stimulus train consists 10 sequential pulses with an inter-stimulus interval of 50 ms. Five sweeps with an interval of 20 s were recorded. The traces with best quality were used for analysis. The ratio was defined as the 2nd to the 1st (A_2/A_1), the 5th to the 1st (A_5/A_1), and the 10th to the 1st (A_{10}/A_1) amplitude.

The eEPSC PPR was recorded at -70mV in presence of 2 μM bicuculline. The eIPSC PPR was recorded at -20mV with 20 μM CNQX and 25 μM APV. The K-gluconate based pipette solution was used for both eEPSC and eIPSC recordings. For the eEPSC PPR, rather weak stimulus strengths were individually adjusted to ensure clear monosynaptic responses to avoid summation effects. The eIPSC PPR recordings, on the other hand, used half-maximum stimulus strength.

36

MATERIALS AND METHODS

2.2.2 Molecular biology

2.2.2.1 Polymerase chain reaction (PCR) for cloning

PCR was performed to amplify DNA fragments for full length Nbea and domains cloning with iProof High Fidelity (BioRAD) kit according to the manufacturer's protocol.

Reaction mixture (Set up on ice)

Template DNA	1 pg-10 ng
25mM dNTP	1 µl
Primer1 (10µM)	2.5 µl
Primer2 (10µM)	2.5 µl
5* buffer	10 µl
DMSO (optional)	x µl (final concentration 3%)
Polymerase	1 µl
H ₂ O	Fill up to 50 µl

Thermal cycling

Initial denaturation	98°C	1 min	×1
Denaturation	98°C	20 s	
Annealing	(T _m +3)°C	45 s	×35
Extension	72°C	1 min/kb	
Final extension	72°C	10 min	×1

2.2.2.2 Quikchange mutagenesis PCR

Nucleotide base pair substitutions were performed by sit-directed mutagenesis using the QuikChange[™] lightning (Agilent Technologies) kit according to the manufacturer's protocol.

MATERIALS AND METHODS

Reaction mixture (Set up on ice)

	Sample	Control
10* reaction buffer	5 µl	5 µl
Template/control DNA	10 ng	25 ng
Primer 1	125 ng	125 ng
Primer 2	125 ng	125 ng
dNTP mix	1 µl	1 µl
QuickSolution	1.5 µl	1.5 µl
H ₂ O	To 50 µl	To 50 µl
QuickChange Lighting Enzyme	1 µl	1 µl

Thermal cycling

95°C	2 min	×1
95°C	20 sec	
60°C	10 sec	×18
68°C	1 min/kb	
68°C	5 min	×18

2.2.2.3 Restriction enzyme digestion and dephosphorylation of DNA

It requires a restriction digestion before ligating the PCR amplified Nbea domain sequences into a desired vector.

The restriction sites Sall and XbaI were used as sticky ends for Nbea domains ligation. Different combinations of enzymes were used for full-length Nbea cloning as described in "Results".

Vector digestion (NEB)

DNA	5 µg
Endonuclease	0.5 µl each
10* Buffer	5 µl
10* BSA (optional)	5 µl
H ₂ O	Add to 50 µl

MATERIALS AND METHODS

PCR product (inserts) digestion (NEB)

DNA (purified)	20 µl
Endonuclease	0.5 µl each
10* Buffer	5 µl
10* BSA (optional)	5 µl
H ₂ O	Add to 50 µl

Digestions take 3 h to overnight at proper temperature. Directly after digestion, vectors were dephosphorylated (Roche), 6 µl 10X buffer, 2 µl Alk. dephosphatase and 2 µl ddH₂O were added into the digestion mixture to reach a final volume of 60 µl. Then it was incubated at 37°C for 30 min.

2.2.2.4 Polyacrylamide gel electrophoresis (PAGE)

After digestion and/or dephosphorylation, DNA fragments were separated with electrophoresis in 0.8 % agarose gel. Agarose was mixed with TAE buffer and boiled until it was completely dissolved. Before gel was solidified, ethidium bromide (1:10,000) was added to visualize DNA fragments under ultraviolet light.

Electrophoresis was at 80 V – 120 V for 60 – 90 min, depending on sizes of DNA fragments and gel. GeneRuler 1 kb Plus DNA Ladder (Thermo Scientific) was used as a standard to estimate the DNA size.

2.2.2.5 DNA extraction from agarose gel

DNA fragments were extracted after electrophoresis with QIAEX™II Gel Extraction Kit (QIAGEN) according to the manufacturer's protocol.

39

MATERIALS AND METHODS

2.2.2.6 DNA ligation

Ligation was with Fermentas Rapid Ligation kit (Thermo Scientific). The 20 µl ligation mixture includes 50ng vector DNA, x ng insert DNA (molar ration of vector to insert was 1:3-1:10), 2 µl 10X T4 buffer, proper volume of ddH₂O, and 1 µl T4 DNA ligase. The mixture was incubated overnight at 11°C.

2.2.2.7 Electrotransformation and plating

Electroporation was used to amplify circular plasmids. Before transformation, cuvette was cooled on ice. Then 1µl diluted ligation mixture (dilute with TE buffer 1:4) or miniprep/maxiprep purified plasmid (dilute with TE buffer 1:300) was mixed with 50 µl competent *E.coli*. The mixture was incubated on ice for 45 s, and then transferred into the ice-cooled cuvette. 2.5 kV pulse was applied. Cells were re-suspended with 1ml room temperature LB medium in a round-bottom 15 ml falcon tube and incubated at 37°C for 1h with 250 rpm shaking. After incubation, the tube was briefly centrifuged at 4000 rmp for 1 min. Afterwards, 800 µl supernatant was discarded, and cells were re-suspended with the rest 200 µl medium and spread on LB-Agar plate containing proper antibiotic. Plate was incubated at 37°C overnight.

2.2.2.8 Miniprep

5 ml LB medium with proper antibiotic were inoculated with a single *E.coli* colony and incubated at 37°C, 250 rpm, overnight. In purpose of screening correct ligation, express miniprep was applied. For other purposes like sequencing or transformation, plasmid was purified with Nucleo Spin Plasmid kit according to the manufacturer's protocol.

Express miniprep was performed with 1.5 out of 5 ml overnight culture that was centrifuged at 13,000 g for 1min. The pellet was briefly dried and re-suspended

40

MATERIALS AND METHODS

in STET buffer and lysed with 25 μ l freshly prepared lysozyme (10 mg/ml in TE buffer) at 100°C, 45 s. Afterwards, 10min centrifuge at 13,000 g was applied to separate the cellular debris and lysate that contains DNA. The DNA was precipitated with 100 μ l 3.3 M sodium acetate and 500 μ l 100% ethanol. After centrifuging at 13,000 g for 15 min, the DNA pellet was washed with 500 μ l cold 70% ethanol and air dried at room temperature. Finally, DNA was dissolved in 50 μ l TE or ddH₂O. Minipreps were analyzed by restriction enzymes and stored at 4°C.

2.2.1.9 Maxiprep

In order to collect high concentration and purity plasmid, maxiprep was used after confirming the correct sequence of the plasmid. A single colony was inoculated in 5ml LB medium containing proper antibiotic. After a day culture of 8h, the 5ml culture was added into a 500ml LB medium containing proper antibiotic, and incubated at 37°C, 250rpm overnight. Plasmid was purified with NucleoBond[®] PC500 kit according to the manufacturer's protocol. The DNA was dissolved in TE buffer and stored at 4°C.

MATERIALS AND METHODS

3. Results

3.1 Neurotransmission in β Nrxn knockouts

To investigate the cellular function of β Nrxn in neurons, I used three β Nrxn KO variants: Nrxn2 β single KO (2SKO), Nrxn1 β /3 β double KO (1/3DKO) and Nrxn1 β /2 β /3 β triple KO (TKO). In order to test the function of β Nrxn in synaptic transmission, I performed electrophysiological recordings on pyramidal neuron in the primary somatosensory cortex in wild type (WT) and β Nrxn deficient mice. Reasons for choosing this region for the present study is firstly, all three β Nrxns are expressed in the cortex (Puschel et al., 1995; Ullrich et al., 1995; Aoto et al., 2013). In addition, α Nrxn mutants showed several changes on the somatosensory cortex neurons, including reduced spontaneous excitatory transmission, impaired short-term plasticity and reduced NMDA/AMPA ratios (Born et al., 2014). Since β Nrxn is almost identical with C-terminal part of α Nrxn, it is interesting to study the function of β Nrxn in the same area in the cortex.

In this project, I mainly investigated synaptic transmission and short-term plasticity. Synaptic transmission was measured with two methods: spontaneous vesicle release at resting potential with miniature postsynaptic currents (mPSCs), and action potential evoked neural transmission with evoked postsynaptic currents (ePSCs). The short-term plasticity was probed with paired-pulse experiment and 20-Hz stimulus train reaction. In the paired-pulse experiment, two identical electrical pulses were applied with variable intervals. Responses to these pulses were compared. The other approach, 20-Hz stimulus train reaction, was tested with a series of 10 electrical pulses with intervals of 50 ms. Responses to later stimuli were compared with the first one. In each measurement, responses from excitatory and inhibitory synapses were separately via applying proper pharmacology.

43

RESULTS

3.1.1 Basal properties of β Nrxn KO variants

At the beginning, I checked whether the deletion of β Nrxn would result in changes of general properties of mice and neurons. Therefore, I analyzed the body weight of mice used in this study, and several parameters of patched neuron, like membrane resistance and cell capacity.

Postnatal age and body weight of mice were documented prior to each electrophysiological experiment. Statistics of ages showed that these mice were in the same range of ages (Fig. 3.1 A). The average of ages was P16 (WT: 16 ± 0.3 days, $n = 29$ mice; 2SKO: 16 ± 0.6 days, $n = 7$ mice; 1/3DKO: 17 ± 0.3 days, $n = 28$ mice; TKO: 17 ± 0.4 days, $n = 19$ mice; Fig. 3.1 A). Body weights of all genotypes showed no significant difference (WT: 7.3 ± 0.2 g, $n = 29$ mice; 2SKO: 6.6 ± 0.4 g, $n = 7$ mice; 1/3DKO: 7.0 ± 0.2 g, $n = 28$ mice; TKO: 6.6 ± 0.3 , $n = 19$ mice; Fig. 3.1 B). The distributions of ages and weights indicate that there is no obvious shift of these parameters between different genotypes (Fig. 3.1). That means the deletion of β Nrxn does not influence the body weight of the mice.

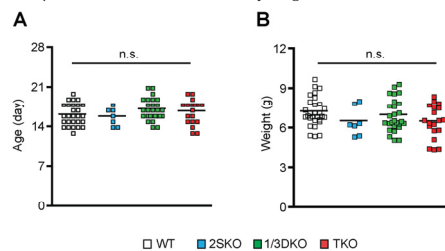


Figure 3.1 Ages and body weights of mice used in electrophysiological analysis. **A)** Mice used in this study are between P 13 and 21. The average of ages is about P 16. **B)** Mice from all genotypes have similar body weights. WT is in white, 2SKO is in blue, 1/3DKO is in green and TKO is in red. Each square represents one mouse. Significance of differences was tested by a Student's t test for unpaired values. "n.s." means not significant.

44

RESULTS

Basal electrophysiological properties of the neurons, including calculated resting potential, membrane resistance, cell capacity and input resistance, were recorded in the voltage-clamp mode (Fig. 3.2). These are essential parameters to estimate properties of neurons and quality of the recording conditions. Resting potential and membrane resistance were calculated from a current-voltage (IV) relationship that recorded immediately after achieving whole-cell configuration (Fig. 3.2 A - C). Cells were firstly held at a holding potential of -60 mV. Then a series of 10 voltage steps ascending from -100 to -10 mV (with 10 mV difference between each step) were applied to the patched neuron (Fig. 3.2 A). The current values injected by the main amplifier were recorded (Fig. 3.2 B). For calculating, amplitude values were collected from the end of the recording traces (Fig. 3.2 B) and plotted against the corresponding voltage values (Fig. 3.2 C). The reverse of the slope represents the membrane resistance, and the x-axis intercept value is the calculated resting potential (Fig. 3.2 C). Cells with membrane resistance below 400 M Ω and resting potential between -50 to -75 mV were included for further data analysis. Resting potentials (Fig. 3.2 D) and membrane resistances (Fig. 3.2 E) of neurons used in this study were calculated and selected in the range of criteria. Cell capacity (Fig. 3.2 F) and input resistance (Fig. 3.2 G), on the other hand, were read out from a test-pulse capacitance current after achieving the whole-cell configuration. Cell capacity is in accordance with the size of the patched cell. Cells with capacity between 80-140 pF were used for further data analysis. In addition, the input resistance represents the resistance between the pipette and the cell. Only the cells with input resistance between 15 to 40 M Ω were taken to further analysis. Statistics shows that basal neuronal properties were not significantly changed in all genotypes (Fig. 3.2).

Thus, the deletions of β Nrxns do not affect the body weights of the mice and the cell properties of pyramidal neurons of the primary somatosensory cortex. This indicates that the data of the following electrophysiological experiments are taken at a comparable background and the differences are not because of the change of general physical or neuronal properties.

45

RESULTS

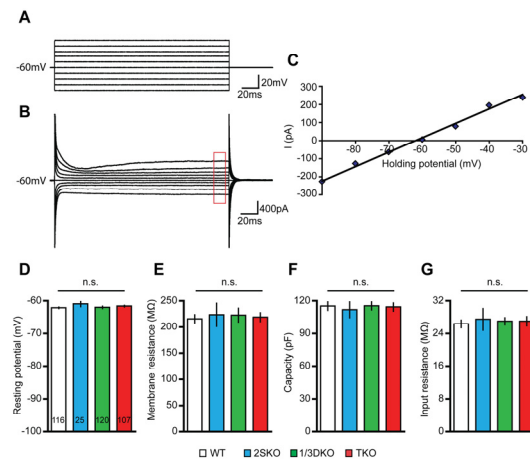


Figure 3.2 Basal cell properties of WT and β Nrxn KO variants. **A)** Stepwise stimulation tests the IV relation. Neurons were clamped at a holding potential of -60 mV. Then stimulation starts from -100mV to -10mV in 10mV steps. Each step lasts for 200 ms. **B)** Representative currents from a patched neuron in response to a stimulation as given in (A). Amplitudes for calculating are taken from the end of currents as marked with the red box. **C)** Representative IV-curve for the calculation of the resting potential and membrane input resistance. **D-G)** Basal neuronal properties including resting potential (D), membrane resistance (E), cell capacity (F) and input resistance (G) are equal in all the genotypes. WT is in white, 2SKO is in blue, 1/3DKO is in green, and TKO is in red. The cell numbers of each genotype were indicated in (D). All data are mean \pm SEM (collected from 25-120 cells from at least seven mice per genotype). Significance of differences was tested by a Student's *t* test for unpaired values. "n.s." is not significant.

46

RESULTS

3.1.2 Spontaneous excitatory neurotransmission

Synaptic transmitters are released in small discrete vesicles called quanta. Each quantum release produces a postsynaptic current of a fixed size (Lisman et al., 2007). The pyramidal cells of the somatosensory cortex spontaneously release transmitters at resting potential and create miniature events termed as minis. The frequency, amplitude, and kinetics of the minis may reflect the synaptic characters like, release probability, amount of neurotransmitter, and postsynaptic receptor number/sensitivity (Kavalali et al., 2011; Lisman et al., 2007).

At the excitatory synapse, mEPSC was measured in presence of TTX in the bath solution to block voltage dependent Na^{2+} channel. Under this condition, there is no vesicle release driven by action potentials, but only spontaneous vesicle release. In addition, bicuculline was applied in the bath solution to block the GABA_A receptor. Therefore, the inhibitory synaptic activity was prevented, and only pure excitatory synaptic events were recorded. The holding potential of mEPSC recording was -70 mV.

Under the given conditions the neurons from WT mice showed an averaged mEPSC frequency of 3.41 ± 0.16 Hz (n = 45 cells/15 mice; Fig. 3.3 A and B). While, averaged frequencies in $\beta\text{Nr}1\text{x}$ variants were decreased about 25% in comparison with WT. (2SKO: 2.50 ± 0.15 Hz, n = 42 cells/7 mice; $P < 0.0001$; 1/3DKO: 2.63 ± 0.30 Hz, n = 22 cells/7 mice; $P = 0.016$; TKO: 2.65 ± 0.18 Hz, n = 23 cells/7 mice; $P=0.005$; Fig. 3.3 A and B). Altered mEPSC frequency always implies a presynaptic change. The decreased frequency in the $\beta\text{Nr}1\text{x}$ mutants suggested a lower probability of spontaneous vesicle release or a reduced number of synapses when one or more $\beta\text{Nr}1\text{x}$ genes are knocked out.

Amplitudes measured from WT and $\beta\text{Nr}1\text{x}$ variants were also different. Comparing with WT, amplitudes in each $\beta\text{Nr}1\text{x}$ KO variants increased about 20%

47

RESULTS

(WT: 13.9 ± 0.5 pA n = 45 cells/15 mice; 2SKO: 15.7 ± 0.6 pA, n = 42 cells/7 mice; $P = 0.007$; 1/3DKO: 16.1 ± 0.8 pA, n = 22 cells; $P = 0.006$; TKO: 15.6 ± 0.9 pA, n = 23 cells; $P = 0.043$; Fig. 3.3 C and D). The amplitude of the mEPSC could be influenced by several factors, mainly the postsynaptic receptor density or the quantal size (Lisman et al., 2007). The increased amplitudes observed in the $\beta\text{Nr}1\text{x}$ KO mutants suggest that there may be more postsynaptic receptors accumulate near the active zone, or a change in the amount of neurotransmitters in the presynaptic vesicles.

Unexpectedly, no dose effect was detected in $\beta\text{Nr}1\text{x}$ variants. The number of deleted $\beta\text{Nr}1\text{x}$ s did not affect the extent of changes observed in frequencies and amplitudes (Fig. 3.3 B-D). This suggests that all three isoforms of $\beta\text{Nr}1\text{x}$ s are required for maintaining a normal excitatory spontaneous neurotransmitter release activity.

The other important parameter of mPSCs is the kinetics. It is reflected by rise time and decay time of a spontaneous neurotransmission. The time constants of rise and decay times of the minis represent the speed of opening and inactivation of postsynaptic receptors. It relies on the composition of postsynaptic receptors, distance between pre- and postsynaptic membrane, as well as the rate of neurotransmitter uptake (Lisman et al., 2007). Quantitative data shows that neither rise times nor decay times were altered when comparing the $\beta\text{Nr}1\text{x}$ KOs with WT neurons (rise time: WT: 1.80 ± 0.05 ms, n = 45 cells/15 mice; 2SKO: 1.70 ± 0.05 ms, n = 42 cells/7 mice; 1/3DKO: 1.61 ± 0.08 ms, n = 22 cells/7 mice; TKO: 1.71 ± 0.12 ms, n = 23 cells/7 mice; Decay time: WT: 5.88 ± 0.15 ms, n = 45 cells/15 mice; 2SKO: 5.60 ± 0.15 ms, n = 42 cells/7 mice; 1/3DKO: 5.21 ± 0.37 ms, n = 22 cells/7 mice; TKO: 5.61 ± 0.41 ms, n = 23 cells/7 mice; Figure 3.3 E and F). Thus, the deletion of $\beta\text{Nr}1\text{x}$ did not affect the kinetics of mEPSC in the somatosensory cortex.

48

RESULTS

Therefore, the observed results from the mEPSC experiment revealed changes in frequency and amplitude of spontaneous neurotransmission. These changes indicated that the deletion of one or more β Nrxns might reduce the probability of spontaneous vesicle release, and increase postsynaptic receptor density or the quantal size. Here raised the question of whether the increased amplitude of β Nrxn variants could also detected form action potential driven synaptic release. In order to test the activity-dependent amplitude, I performed eEPSC experiment within the somatosensory cortex.

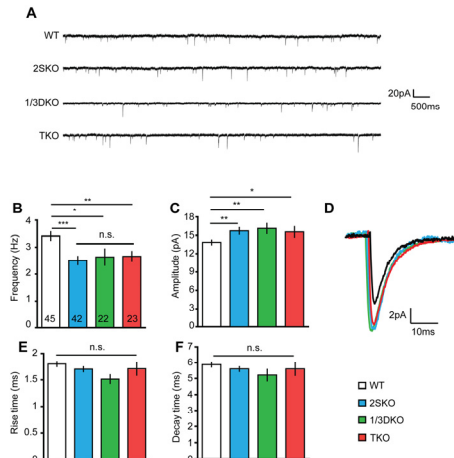


Figure 3.3 The effects of β Nrxn at excitatory synaptic spontaneous neurotransmission
A) Representative mEPSC current traces of WT, 2SKO, 1/3DKO, and TKO. **B)** Frequencies of spontaneous release in 2SKO (blue), 1/3DKO (green) and TKO (red) are decreased when compared with WT (white). Number inside columns represents the number of neurons from each genotype. **C)** Amplitudes of mEPSC in all three β Nrxn KO are increased when compared with WT. **D)** Sample curves averaged from at least 150 single events of a representative neuron of WT (black), 2SKO (blue), 1/3DKO (green) and TKO (red). **E, F)** The calculated kinetics of rise time (E) and decay time (F) in mEPSC are similar in all genotypes. All data are mean \pm SEM (collected from 22-45 cells from at least seven mice per condition/genotype). Significance of differences were tested by Student's *t* test for unpaired values; **P*<0.05, ***P*<0.01, ****P*<0.001 and "n.s." is not significant.

49

RESULTS

3.1.3 Evoked excitatory neurotransmission

In another experimental procedure I used eEPSC to study the activity-dependent neuronal transmission at excitatory synapse. In the eEPSC experiments, bicuculline was applied in the bath solution to inhibit the activity of GABA_A receptor. An electrical stimulation electrode was placed approximately 100 μ m laterally from the recording position. Both the stimulation electrode and recording position were in the region of somatosensory cortex layer V. The patched neuron produces a postsynaptic current change in response to the stimuli-dependent signal. In the eEPSC recordings, stimulus intensity was applied ranging from 0.02 to 0.20 mA. Holding potential was at -70 mV.

The increased amplitude observed in mEPSC was verified by the experimental procedure of eEPSC. Averaged amplitudes of all three β Nrxn variants are larger than that of the WT (Fig. 3.4 A-D). These variants had the same extent of increase comparing with WT (Fig. 3.4 A). In the 2SKO, 20 neurons from three mice were tested for responses to the stimulus strength 0.06 to 0.14 mA. The averaged responses showed higher amplitudes to the corresponding ones in WT (Fig. 3.4 B). In addition, neurons from the other two variants, 1/3DKO and TKO, also presented higher amplitudes than WT after stimulus strengths increased to about 0.1 mA (Fig. 3.4 C and D). The quantified amplitudes at half maximum stimulus strength of all three β Nrxn variants (Fig. 3.4 E) are increased approximately 30% (WT: 628.3 ± 47.9 pA, *n* = 21 cells/6 mice; 2SKO: 830.8 ± 87.51 pA, *n* = 20 cells/3 mice; *P* = 0.04; 1/3DKO: 817.5 ± 85.8 pA, *n* = 22 cells/7 mice; *P* = 0.04; TKO: 815.5 ± 78.1 , *n* = 24 cells/6 mice; *P* = 0.04; Fig. 3.4 E). Decay times of activity-dependent neurotransmission were not significantly altered between different genotypes (WT: 15.67 ± 1.00 ms, *n* = 15 cells/6 mice; 2SKO: 14.71 ± 0.79 ms, *n* = 21 cells/3 mice; *P* = 0.46; 1/3DKO: 14.97 ± 1.22 ms, *n* = 16 cells/7 mice; *P* = 0.68; TKO: 14.01 ± 1.46 ms, *n* = 15 cells/6 mice; *P* = 0.37; Fig. 3.4 F).

50

RESULTS

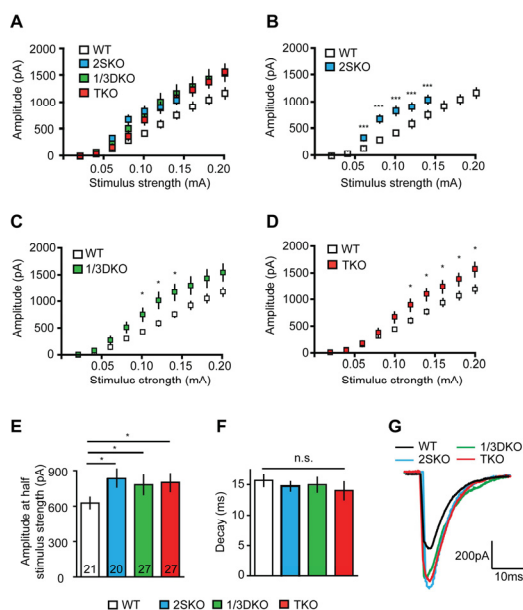


Figure 3.4 eEPSC amplitudes are increased in the β Nrxn deficient neurons. **A)** A combination of amplitudes from all genotypes. Amplitudes are measured at different stimulus strength from 0.02 to 0.20 mA. It shows that amplitudes from β Nrxn mutants (blue, green and red squares) are larger than those from WT (white squares). **B-D)** These figures represent the amplitude comparisons of WT to each β Nrxn KO mutants under different stimulus strength. **E)** Quantification of amplitudes elicited at half maximum stimulus strength indicates that in the β Nrxn KOs (2SKO in blue, 1/3DKO in green and TKO in red), the amplitudes are increased in comparison with WT (white). Numbers in the columns stand for the cell numbers from each genotype. **F)** Time constants of decay times are unaffected in the β Nrxn KO neurons. **G)** Representative curves of amplitudes measured at half stimulus strength. This figure shows higher amplitudes in β Nrxn mutants than in WT. All data are mean \pm SEM (collected from 18-27 cells from at least six mice per condition/genotype). Significance of differences were tested by Student's *t* test for unpaired values; * $P < 0.05$ and "n.s." is not significant.

51

RESULTS

This eEPSC experiment implies that in β Nrxn mutants, the activity-dependent neurotransmission is enhanced. Increased amplitudes were revealed in all three variations of β Nrxn KO neurons. In addition, the increased amplitudes but constant kinetics from the eEPSC were in accordance with results from mEPSC data. In brief, the deletion of β Nrxn resulted in the change of excitatory synaptic transmission with lower frequencies and larger amplitudes in mEPSC, and larger amplitudes in eEPSC. The number of genes deleted did not affect the extent of changes.

3.1.4 Short-term plasticity of excitatory synapses

Changes of synaptic strength are known as synaptic plasticity. There are two major forms of synaptic plasticity: long-term and short-term plasticity. Long-term plasticity lasts for hours to days. It is thought to underlie learning and memory (Sippy et al., 2003). Short-term plasticity occurs in the range of milliseconds to minutes. It is important for neurons to perform computational tasks and initiate the long-term plasticity (Sippy et al., 2003). In this study, I measured short-term plasticity of β Nrxn mutants. It is because changes observed in the mEPSC frequency (Fig 3.3) imply there may be also a change in short-term plasticity due to the involvement of Ca^{2+} channel activity in both cases. In addition, study from Born et al. (2014) showed that deletion of $Nrxn2\alpha$ resulted in decreased short-term plasticity at excitatory synapses in the somatosensory cortex. Therefore, the question arises as whether knockout of β Nrxn would also affect the short-term plasticity at excitatory synapses.

To test the excitatory short-term plasticity, pyramidal neurons in the layer V of the somatosensory cortex were measured in the voltage-clamp mode. Electric stimulations were applied via an electrode that placed approximately 100 μ m laterally from the recording position. This electrode aims to drive action potentials in the neurons close to the patched ones. Bicuculline was added to the bath solution to block the GABA_A receptor activity.

52

RESULTS

In the short-term plasticity measurement, a pair of stimuli was applied successively over a range of inter-stimulus intervals from 30 to 200 ms. Small stimulus strength was applied during recordings. This is to ensure pure monosynaptic responses were recorded and avoid summation of multiple synapses inward currents. The short-term plasticity was measured at a holding potential of -70 mV. At least 15 neurons from each genotype were recorded. At each inter-stimulus interval, the patched neuron was recorded for 10 times. The ratio of two responses was quantified as paired-pulse ratio (PPR) (Fig. 3.5).

The PPR analysis shows that deletion of neurexin 2 β significantly reduces the facilitation that observed in WT neurons (Fig. 3.5 A and B). At the inter-stimulus interval of 50 ms, the facilitation observed in WT excitatory synapses is almost absent in the 2SKO (Fig. 3.5 A). Quantified PPRs at inter-stimulus interval between 30 to 200 ms indicated that the facilitation at intervals of 50 to 125 ms is notably diminished in 2SKO when compared with WT (Fig. 3.5 B). However, Nrnx 1 β and 3 β null neurons kept the same facilitation pattern as WT neurons (Fig. 3.5 C and D). This suggests that neurexin 1 β and 3 β may not severely affect the excitatory synaptic plasticity. In TKO, facilitation was diminished in comparison with WT (Fig. 3.5 E and F). The impaired synaptic facilitation in the TKO was similar as that observed in the 2SKO. Taking together, the PPR experiments revealed a diminished facilitation in 2SKO and TKO, but change in 1/3DKO was not obvious. This implied an important role of Nrnx 2 β in maintaining the short-term plasticity at excitatory synapses. In order to further probe the importance of β Nrxns in the short-term plasticity, I performed a 20-Hz train experiment, in which 10 identical stimuli were applied at the frequency of 20-Hz.

53

RESULTS

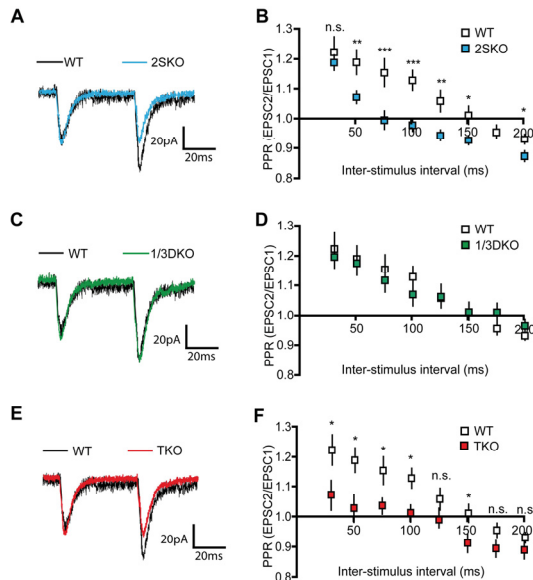


Figure 3.5 Paired-pulse ratios (PPRs) of WT and β Nrxn mutants. **A)** Exemplary current traces of PPR experiments at an inter-stimulus interval of 50 ms. Facilitation seen in WT (black) is abolished in the β Nrxn 2SKO (blue). **B)** Quantified PPR of WT (white) and 2SKO (blue) at different inter-stimulus intervals indicates reduced PPR in the 2SKO when compared with WT. **C)** Paired-pulse facilitation is shown in both WT (black) and Nrnx1/3DKO (green) at an inter-stimulus interval of 50 ms. **D)** Quantified PPR of WT (white) and 1/3DKO (green) at different inter-stimulus intervals. Comparisons indicate these two genotypes have similar PPR values. **E)** Exemplary current traces of PPR experiments at an inter-stimulus interval of 50 ms. Facilitation seen in WT (black) is abolished in the β Nrxn TKO (red). **F)** Quantified PPR of WT (white) and TKO (red) at different inter-stimulus intervals indicates reduced PPR in the TKO when compared with WT. All data are mean \pm SEM (collected from 15-18 cells from at least five mice per condition/genotype). Significance of differences were tested by Student's *t* test for unpaired values; **P*<0.05 and "n.s." is not significant.

54

RESULTS

As a further verification, I tested the short-term plasticity with a second experimental protocol: a 20-Hz stimulation pulse train. In this experiment, stimuli were applied 10 times with an inter-stimulus interval of 50 ms (Fig. 3.6 A). At least 15 cells from each genotype were measured. Recordings of each patched neuron repeated for five times. Finally, data from the same genotype were averaged. Traces of responses showed that the sequential stimulation yielded obvious facilitation in WT neurons. However, β Nrxn mutants failed to facilitate in response to the series of stimuli (Fig. 3.6 A). In the 2SKO, there was only slight facilitation in the second response. Those later responses in 2SKO changed to depression (Fig. 3.6 A). In the 1/3DKO, only the second response facilitated, while the following ones depressed (Fig. 3.6 A). The TKO showed similar pattern as the 2SKO that slight facilitation was observed at the second response, but the following responses depressed stronger than the 1/3DKO (Fig. 3.6 A).

Figure 3.6 B represented the quantified ratios of the second (A2), fifth (A5) and tenth (A10) responses to the first (A1) one. At the beginning (A2/A1), 2SKO and TKO only slightly facilitated, while the 1/3DKO and WT showed similar facilitation extents (WT: 1.21 ± 0.05 , $n = 15$ cells/6 mice; 2SKO: 1.07 ± 0.03 , $n = 20$ cells/3 mice; $P = 0.03$; 1/3DKO: 1.21 ± 0.03 , $n = 17$ cells/7 mice; $P = 0.13$; TKO: 1.10 ± 0.03 , $n = 18$ cells/6 mice; $P = 0.01$; Fig. 3.6 B). As the stimulus series continued (A5/A1 and A10/A1 in Fig. 3.6 B), the facilitation disappeared in the WT. In the 2SKO, 1/3DKO and TKO, the ratio even turned into a depression (PPR of A5/A1: WT: 1.04 ± 0.04 , $n = 15$ cells/6 mice; 2SKO: 0.70 ± 0.02 , $n = 20$ cells/3 mice; $P < 0.0001$; 1/3DKO: 0.88 ± 0.02 , $n = 17$ cells/7 mice; $P = 0.004$; TKO: 0.79 ± 0.05 , $n = 18$ cells/6 mice; $P < 0.0001$; PPR of A10/A1: WT: 0.97 ± 0.08 , $n = 17$ cells/6 mice; 2SKO: 0.48 ± 0.04 , $n = 20$ cells/3 mice; $P < 0.0001$; 1/3DKO: 0.53 ± 0.06 , $n = 17$ cells/7 mice; $P < 0.0001$; TKO: 0.43 ± 0.04 , $n = 18$ cells/6 mice; $P < 0.0001$; Fig. 3.6 B).

These experiments provided further evidence to a role of β Nrxn in synaptic short-term plasticity. Different with WT, synapses lacking β Nrxn had a tendency

55

RESULTS

to depress, rather than to facilitate. In particular, 2SKO and TKO show similar depression patterns, which was more severe than that in 1/3DKO. Together with the PPR results from one pair stimuli (Fig. 3.5), these results indicated that Nrxn2 β was the key component among all three β Nrxns in maintaining the excitatory short-term plasticity. In addition, the other two β Nrxns, neurexin 1 β and 3 β , also played a role when multiple stimulations were applied.

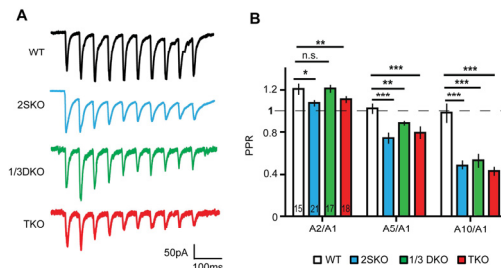


Figure 3.6 Short-term plasticity in pyramidal cells of the somatosensory cortex evoked by a 20-Hz stimulation train **A**) Sample traces from WT, β Nrxn 2SKO, 1/3DKO and TKO reveal synaptic facilitation in the WT but depression in the β Nrxn KO variants. **B**) Quantified ratios of the second (A2), fifth (A5) and tenth (A10) amplitudes to the first (A1) amplitude. Numbers in the columns stand for the cell number. All data are mean \pm SEM (collected from 15-20 cells from at least five mice per condition/genotype). Significance of differences were tested by Student's t test for unpaired values; * $P < 0.05$, ** $P < 0.01$, *** $P < 0.001$ and "n.s." is not significant.

In summary, at the excitatory synapses, β Nrxns play important roles in both synaptic transmission and short-term plasticity. Deletion of one or more β Nrxn altered the amplitude and frequency in the basal synaptic transmission. On the other hand, the short-term plasticity is notably impaired in the neurons lacking β Nrxns. In order to further probe whether the loss of β Nrxn would also influence the inhibitory synaptic function, I explored the IPSC of WT and TKO as well. The evoked IPSC (eIPSC) was chosen, because this experimental approach could measure both the basal synaptic transmission and the synaptic plasticity. TKO, but not other β Nrxn KO variants, was investigated as a fast test to see whether deleting all three β Nrxns affects inhibitory synapses.

56

RESULTS

3.1.5 Basal synaptic transmission at inhibitory synapse

I probed the synaptic transmission with eIPSC in the somatosensory cortex of WT and β Nrxn TKO mice. In this experiment, the electrical stimulation electrode was placed approximately 100 μ m laterally from the recording position in the layer V. APV and CNQX were applied to block glutamatergic excitatory receptors of NMDA and AMPA. Stimuli ranging from 0.04 to 0.20 mA were applied through the stimulation electrode. The holding potential for eIPSC recording was -20 mV. Parameters of amplitude and kinetics were analyzed and compared between WT and TKO neurons.

After analyzing, data from 29 WT and 15 TKO neurons with good qualities were used in statistics. Under all stimulation strengths tested, no differences of amplitudes were detected between WT and TKO (Fig. 3.7 A). Traces of responses at half stimulus strength showed the same amplitude in WT and TKO (Fig. 3.7 B). Furthermore, quantified responses at half maximum stimulus strength showed that both the WT and β Nrxn TKO neurons yield similar amplitudes (WT: 406.7 ± 34 pA, n = 29 cells/8 mice; TKO: 395.6 ± 34 pA, n = 15 cells/5 mice; P = 0.837; Fig. 3.7 C). Therefore, in the activity-dependent inhibitory synaptic transmission, deletions of all β Nrxn genes do not influence the evoked amplitudes. Comparing with results of excitatory neurotransmission, this result suggested function of β Nrxn was limited at excitatory synapse.

Besides the amplitudes, the kinetics of the evoked inhibitory neural transmission was also analyzed. Decay time was measured at half stimulus strength. It was revealed that the decay times in WT and TKO of the eIPSC are constant (WT: 53.1 ± 2.1 ms, n = 29 cells/8 mice; TKO: 57.6 ± 4.6 ms, n = 15 cells/5 mice; P = 0.307 Fig. 3.7 B and D). This result suggested that the deletion of β Nrxns does not affect the kinetics of neurotransmission at inhibitory synapses in the somatosensory cortex.

57

RESULTS

Results above showed that in the action potential evoked inhibitory synaptic transmission, a deletion of β Nrxn influenced neither the eIPSC amplitudes nor the kinetics. These results differ from those at excitatory synapses where the amplitudes are increased in the β Nrxn KO neurons. The kinetics of neurotransmission, on the other hand, was not affected in both excitatory and inhibitory synapses.

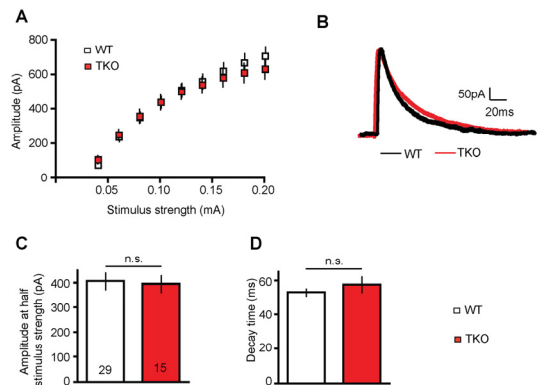


Figure 3.7 Synaptic transmission at inhibitory is not changed in the β Nrxn TKO. A) Responses to single stimulation of strength from 0.04 mA to 0.20 mA in the β Nrxn TKO. There is no difference detected in WT and TKO neurons. **B)** Averaged current traces taken at half maximum stimulus strength show the same amplitudes and decay times in WT (black), TKO (red). **C)** Quantification of amplitudes elicited at half maximum stimulus strength indicates that in the β Nrxn TKO (red), the amplitudes are the same as in the WT (white). **D)** Time constants of decay times are unaffected in the β Nrxn KOs. All data are mean \pm SEM (collected from 15 - 29 cells from at least three mice per condition/genotype). Significance of differences was tested by a Student's t test for unpaired values; "n.s." is not significant.

58

RESULTS

3.1.6 Short-term plasticity at inhibitory synapse

Since the deletion of β Nrxn impaired excitatory synaptic plasticity, I questioned whether it would influence the inhibitory synaptic plasticity. Usually, the application of two or more identical electrical shocks in a close succession would result in a frequency-dependent depression at inhibitory synapse (Davies et al., 1990). Therefore, I tested two protocols with one pair or a train of stimulations to find out whether the deletion would change the inhibitory synaptic depression.

In the experiment of one pair stimuli, different inter-stimulus intervals from 30 to 200 ms were applied. APV and CNQX in the bath solution served to block the NMDA and AMPA receptor currents, respectively. Thus only inhibitory signals were recorded. Neurons were measured with the voltage-clamp mode with holding potential of -20 mV.

Both the one pair stimuli experiment and the 20-Hz stimulation pulse train experiment revealed the same result: the deletion of all β Nrxns does not affect the short-term plasticity at the inhibitory synapses (Fig. 3.8). Representative traces of paired pulse experiments at an inter-stimulus interval of 75 ms show depressive patterns in WT and TKO neurons (Fig. 3.8 A). Quantitative statistics also indicates that there is no significant difference between WT and TKO at different frequencies (Fig. 3.8 B). Paired-pulse depression is observed in a wide range of different inter-stimulus intervals (75 to 200 ms) at inhibitory synapses in both genotypes (Fig. 3.8 B).

The unchanged inhibitory synaptic depression was further confirmed by the 20 Hz stimulus train experiment, in which 10 identical electrical stimuli were applied sequentially with an interval of 50 ms. The stimulus strength was at half maximum stimulus. Strong depression patterns are observed in both genotypes (Fig. 3.8 C). Quantified ratios between the second (A2), fifth (A5) and tenth (A10) amplitudes to the first (A1) amplitude were calculated and compared in Fig. 3.8

59

RESULTS

D. In both groups, the averaged values of A2/A1 are equal (Fig. 3.8 D), which is in accordance with the PPR results at 50 ms (Fig. 3.8 B) (A2/A1 values: WT: 0.95 ± 0.01 , n=25 cells; TKO: 1.00 ± 0.02 , n=15 cells; P = 0.077). Robust depression could be observed in the fifth response (A5/A1) and becomes even stronger in the tenth response (A10/A1) (A5/A1: WT: 0.79 ± 0.02 , n=25 cells; TKO: 0.80 ± 0.02 , n=15 cells; P = 0.769; A10/A1: 0.65 ± 0.02 , n=25 cells; TKO: 0.66 ± 0.02 , n=15 cells; P = 0.905; Fig. 3.8 D). Thus, the deletion of β Nrxn variants does not influence the short-term plasticity at inhibitory synapses.

As a result, at the inhibitory synapses, deletion of all β Nrxn does not influence either the basal neurotransmission, or the short-term synaptic plasticity. Taking together, studies at excitatory and inhibitory synapses revealed that β Nrxns is more likely to play a role at the excitatory synapses, rather than at the inhibitory ones. The changes of amplitude, frequency and short-term plasticity at excitatory synapse imply an alteration at both pre- and postsynaptic site in the β Nrxn deficient neurons.

Phenotypes observed in β Nrxn KO mutants further raise a question: is there any change of α Nrxn and Nlgn in the β Nrxn KO? Since the C-terminus of α Nrxns shares identical sequence with β Nrxns, and Nlgns physically and functionally interacts with β Nrxns, it is essential to check the expression of these two proteins in neurons lacking β Nrxns. If there were alternations of these proteins, it may shed light on the causes of the phenotypes that we observed in the β Nrxn KO mutants.

60

RESULTS

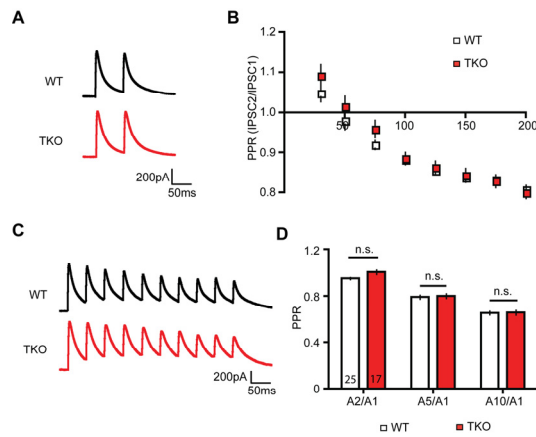


Figure 3.8 Short-term plasticity of inhibitory synapses in WT and β Nrxn TKO **A)** Averaged current traces representing mild paired-pulse depression at inter-stimulus interval of 75 ms in WT (black) and TKO (red). **B)** Quantified paired-pulse ratio analysis at different inter-stimulus intervals shows similar depression pattern in both genotypes (WT in white and TKO in red). **C)** Averaged current traces of the 20 Hz stimulus train reaction show a clear depression in WT (black) and TKO (red). **D)** Quantified ratios between the second (A2), fifth (A5) and tenth (A10) to the first (A1) amplitude in the WT (white) and TKO (red). The comparisons reveal no differences between different genotypes. All data are mean \pm SEM (collected from 15-29 cells from at least five mice per condition/genotype). Significance of differences was tested by a Student's *t*-test for unpaired values; "n.s." means not significant.

61

RESULTS

3.1.7 Expression of α Nrxn and Nlgn in the β Nrxn TKO

Proteins most closely related with β Nrxn are α Nrxn and Nlgn. The genes of α - and β nrxns locate at the same chromosome loci, but translate from two independent promoters. The same C-terminus of α - and β Nrxns are reported as essential parts for protein interactions. Nlgn is one of the most important postsynaptic binding partners of α - and β Nrxns. The interaction of Nlgn and Nrxn influences the balance between excitatory and inhibitory synapses (Scheiffele et al., 2000; Dean et al., 2003; Craig and Kang, 2007). Therefore, the expression of α Nrxn and Nlgn in the neurons lacking β Nrxn is highly suspected to change, and may give us a hint of the phenotypes observed in β Nrxn KO mutants.

Brain samples of WT and β Nrxn TKO were sent to Arrows Biomedical Deutschland GmbH for quantitative reverse transcription PCR (RT-qPCR) testing. This test was performed with two-step RT-qPCR. Firstly a reverse transcription (RT) reaction generated cDNA pool with non-specific oligo-dT primers. Then a qPCR step was made in separate tubes with optimized buffer and specific primers for α Nrxn and Nlgn. SYBR Green (Roche) that could bind to double-stranded DNA (dsDNA) was used as reporter for PCR product.

Three brain samples of each genotype, WT and β Nrxn TKO, were prepared for the RT-qPCR. The RNA from each sample were purified and then reversely transcribed into cDNA. In order to confirm that the efficiency of each RT reaction is equal, the content of house keeping gene (HKG) β -actin was tested with qPCR after RT reaction. Results showed that all samples contained the same amount of β -actin (Fig. 3.9 A). This indicates that RNA from all these six samples was equally transcribed into cDNA. Therefore the following qPCR of α Nrxn and Nlgn should reflect the real expression level of these genes in different genotypes.

62

RESULTS

Next, cDNA samples from RT reactions were applied in the qPCR as template. Specific primers were designed for Nrnx 1 α , Nrnx 2 α and Nrnx 3 α , as well as Nlgn 1, Nlgn 2 and Nlgn 3. After qPCR, the copy numbers of each gene were compared between WT and TKO (Fig. 3.9 B). The ratio between WT and TKO represent the relative expression level of these genes.

In absence of β Nrxn, neurons tended to express more α Nrxn and Nlgn (Fig. 3.9 B). In particular, the expression of Nrnx 2 α and Nrnx 3 α were up regulated to nearly two folds, while the expression of Nrnx 1 α did not alter (ratio of TKO / WT: Nrnx 1 α : 1.01 ± 0.07 ; Nrnx 2 α : 1.82 ± 0.11 ; Nrnx 3 α : 1.85 ± 0.11 ; n = 3 mice /genotype; Fig. 3.9 B). The strong up regulation of α Nrxn may result from a compensatory strategy in the neurons lacking β Nrxn. This could also be the reason for the milder phenotypes observed in β Nrxn mutants than in the α Nrxn mutants.

Genes of Nlgn were also up regulated. Specifically, expression of Nlgn 1 slightly increased, and expression of Nlgn 2 and 3 increased about two folds (ratio of TKO / WT: Nlgn 1: 1.15 ± 0.07 ; Nlgn 2: 1.93 ± 0.19 ; Nlgn 3: 1.75 ± 0.21 ; n = 3 mice /genotype; Fig. 3.9 B). All these Nlgn proteins were reported to locate at excitatory synapse, and Nlgn 2 additionally locate at inhibitory synapse (Varoqueaux et al., 2004). The electrophysiology studies in this project reviewed alternations at excitatory synapse in β Nrxn mutants, but not at inhibitory synapse. This indicates that the increased Nlgn 2 expression may either solely affect the excitatory synapse, or affect the inhibitory synaptic activity in other brain regions rather than in the somatosensory cortex.

63

RESULTS

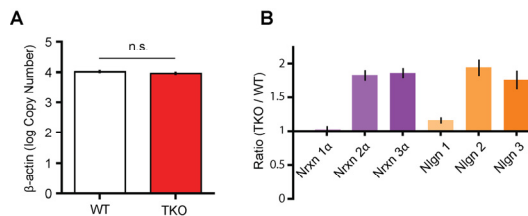


Figure 3.9 RT-qPCR of α Nrxn and Nlgn in WT and β Nrxn TKO mice brain. A) RT-qPCR results of HKG β -actin reveal the same amount of β -actin copy numbers in all the samples, suggesting an equal efficiency of RT reactions. Significance of differences was tested by a Student's *t*-test for unpaired values; "n.s." means not significant. **B)** Ratio between TKO and WT represent the relative expression level of target genes. In the TKO, Nrnx 1 α and Nlgn 1 are not or slightly affected, while Nrnx 2 α , Nrnx 3 α , Nlgn 2 and Nlgn 3 are up regulated to nearly two folds.

So far I used electrophysiological technics to investigate the synaptic transmission and plasticity of β Nrxn mutant, and identified functional changes at excitatory synapse. Expression of two proteins that closely related to β Nrxn was also tested with RT-qPCR. From that experiment, up regulation of different isoforms of α Nrxn and Nlgn were detected. These changes in α Nrxn and Nlgn expression may correlate with the changes observed in β Nrxn mutant.

The other factor that may affect β Nrxn is Nbea, since the trafficking of β Nrxn was changed in the Nbea KO neuron (unpublished data from C. Neupert). Both Nbea and Nrnx are related to ASD. Neurons lacking Nbea showed deficiency in dendritic spine formation and synaptic transmission (Madrihan et al., 2009; Niesmann et al., 2011). These facts lead to a question: does Nbea functionally related with β Nrxn? And what are the roles of Nbea in the neuron? In order to solve this question, I made Nbea clones as tools to probe the relation between Nbea and β Nrxn.

64

3.2 Cloning of Full-length Neurobeachin and domains

The *nbea* was found mutated in several autism patients (Castermans et al., 2003; Castermans et al., 2010; Volders et al., 2010). Previous study showed that Nbea was associated with Golgi membrane (Wang et al., 2000; Medrihan et al., 2009), and regulated formation of spinous synapses (Niesmann et al., 2011). Whether transfecting of Nbea cDNA would rescue Nbea null mutant phenotypes would provide evidence for the function of Nbea in synaptic formation and synaptic transmission. In addition, as Nbea is a multi-domain protein, it is important to know the role of domains in Nbea. In order to answer these questions, I made DNA constructs of GFP tagged full-length Nbea, as well as Nbea domains.

I modified a full-length Nbea vector from commercially obtained pEYFP-C1-Nbea plasmid (Imagenes), which contains Cytomegalovirus (CMV) promoter. However, this plasmid was difficult to analyze because it showed extremely high expression of Nbea in cell transfection and was difficult to analyze. Therefore, to reduce the Nbea expression level, I made an EGFP-Nbea construct with a low-copy number synapsin 1 (Syn) promoter (Kugler et al., 2003). Afterwards, I made Nbea related construct pSyn-EGFP-Nbea Δ AKAP, in which the AKAP motif of Nbea was deleted. In addition, GFP-tagged Nbea domains related plasmids were also constructed. Those domains included ARM, PH-BEACH, WD repeats, Lectin-like, and DUF1088.

3.2.1 FL-Nbea cloning

Nbea gene was cloned from the commercial pEYFP-C1-Nbea plasmid (Imagenes). The full-length Nbea gene in this plasmid is from *Homo sapiens*. In order to reduce the expression level, I exchanged the CMV promoter into a Syn promoter. This promoter is a neuron specific long-term transgene promoter (Kugler et al., 2003). As a consequence, Nbea could be expressed at a moderate level in neurons. The EYFP tag was also replaced with an enhanced Green Fluorescent

Protein (EGFP) tag, which is more convenient for the microscope system in the present study.

Since the pEYFP-C1-Nbea is a large vector with a size of more than 13 kb, most of common restriction sites do already exist. The absent restriction sites MluI and NotI were chosen to replace a fragment that contains both, promoter and fluorescent tag. The two sites were inserted at the borders of the CMV-EYFP fragment by applying Quikchange method (Agilent Technologies) in serial steps. Because pEYFP-C1-Nbea plasmid is larger than 10 kb, which is ineffective for Quikchange PCR reaction, the plasmid was firstly cut with BamHI at three sites to reduce its size to 6kb (Fig. 3.10 A). The 6kb DNA fragment was extracted from gel after PAGE using the QiaExII method (Qiagen) and re-ligated to obtain intermediate plasmids pEYFP-C1-Nbea(tr), where "tr" stands for "truncated" (Fig. 3.10 B).

After introducing MluI and NotI sites into the pEYFP-C1-Nbea(tr) vector (Fig. 3.10 C), sequence containing these two restriction sites, CMV promoter, and EYFP was transposed back into the 13kb vector by digesting and ligating at PvuI and SacII sites. Thus, the cutting sites of MluI and NotI were successfully inserted at the border of CMV and EYFP fragment in the pEYFP-C1-Nbea (Fig. 3.10 D). This plasmid was named as pEYFP-C1-Nbea(MN), where "M" stands for "MluI" and "N" stands for "NotI". This plasmid was amplified by *E.coli* in LB medium with proper concentration of ampicillin, and then purified with DNA maxipreps. The next step of cloning the FL-Nbea is to prepare the Syn promoter and EGFP together. This 1.5 kb fragment was amplified with PCR with pSyn-EGFP plasmid (from laboratory) as template. MluI and NotI restriction sites were added at the primers that the forward primer MM11-131 contains MluI site and the reverse primer MM11-132 contains NotI site (Fig. 3.10 E).

The critical step of cloning the pSyn-EGFP-Nbea is the replacement of CMV-EYFP with Syn-EGFP, since this step requires a ligation of 1.5 kb (Syn-EGFP) and 12 kb

RESULTS

(Nbea and vector backbone) fragments. These two fragments were purified from PAGE following MluI and NotI digestion. I tested several ligation conditions for these two fragments. Finally, this cloning worked only with modified ligation strategy of precisely calculated DNA amount of 50 ng Nbea vector and 250 ng Syn-EGFP and overnight ligation at 11°C. After ligation, the constructs were transformed in XL-100 *E. coli* by heat shock and amplified by overnight culture in LB. The ligation result was verified by restriction digestion with PvuI and NarI (Fig 3.10 F), as well as sequencing (GATC) to confirm the ligation result. This plasmid was named as pSyn-EGFP-Nbea.

This pSyn-EGFP-Nbea construct was further used in the cell culture experiments (Dr. Reppetto) and electrophysiological experiments (Dr. Brockhaus). Preliminary results show that exogenous EGFP-Nbea could rescue the Nbea KO phenotypes of decreased dendritic number, reduced mEPSC frequency, as well as altered mEPSC kinetics (unpublished). These results provide evidences that Nbea maintains normal morphology of spinous synapses, as well as functional excitatory synaptic transmission.

67

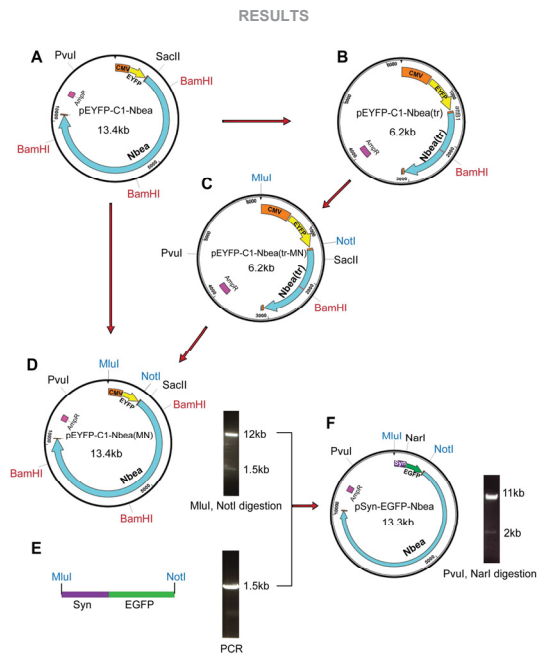


Figure 3.10 Process of full-length Nbea cloning A-B) Figure A shows the commercial vector with Nbea (cyan), CMV promoter (orange) and EGFP tag (yellow). This vector was cut with BamHI enzyme to form a smaller pEGFP-C1-Nbea (tr) plasmid (B) for Quikchange reaction. C) Restriction sites MluI and NotI were introduced into the pEYFP-C1-Nbea(tr) vector at the edges of CMV-EYFP sequence. D) A PvuI and SacI fragment containing newly introduced MluI and NotI sites in (C) replaces the corresponding fragment in the original vector in A. E) Syn promoter and EGFP was amplified with PCR, which shows a 1.5 kb band after PAGE. F) CMV-EYFP was replaced by SYN-EGFP, using MluI and NotI sites. The ligation proved by digestion with PvuI and NarI resulting bands of 2kb and 11kb.

68

RESULTS

3.2.2 Cloning of Nbea domain-related constructs

Previous studies suggest that Nbea null mutant neurons has reduced dendritic spine number and altered neural transmission characters (Niesmann et al., 2011). The transfection of pSyn-EGFP-Nbea into the Nbea KO neurons could rescue these phenotypes. However, Nbea is a large protein with nearly 3000 amino acids and multiple domains. It is not clear what is the function of each domain and how they cooperate. Cloning of each domain or domain combination might shed light on these questions.

Sequence alignment and computational modeling revealed that Nbea consists of mainly six important motif and domains, including AKAP motif, ARM, PH-BEACH, WD repeats, Lectin-like, and DUF1088 domains. They might involved in different cell functions or signaling pathways, including AKAP motif, ARM, PH-BEACH, WD repeats, Lectin-like, and DUF1088. In the following experiments, I made EGFP-Nbea Δ AKAP construct, in which the 19 amino acids long AKAP motif was deleted from the full-length Nbea gene. In addition, I cloned several related domain sequences into pSyn-EGFP.

Different strategies were applied in cloning Nbea domain related DNA constructs. Nbea Δ AKAP was modified from the FL-Nbea construct. The AKAP motif was deleted by Quikchange reaction. Other single domains or domain combinations were amplified from FL-Nbea with PCR. Restriction sites Sall and Xbal were added to the edges of domain sequence by PCR primers. Afterwards the DNA fragments from PCR were inserted into pSyn-EGFP plasmid via sticky-end ligation. Primers used in this study were designed with no frame shift and no amino acid alterations. All constructs were purified with mini-prep and sequenced (GATC). Those plasmids with no mutations were later amplified and purified with maxi-prep and stored at -20°C.

69

RESULTS

3.2.2.1 Cloning of Nbea Δ AKAP

Nbea was firstly identified as an A-kinase anchor protein (AKAP), since it encodes a 19-amino-acid AKAP motif with high affinity (K_d , 10nM) to the type II regulatory subunit of protein kinase A (Wang et al., 2000). AKAPs are thought to orient Protein Kinase A (PKA) towards selected substrates inside the soma (Wong and Scott, 2004). In addition, the endogenous Nbea was found to localize near the trans-Golgi network (Wang et al., 2000; Niesmann et al., 2011). Therefore, Nbea is supposed to recruit PKA to the membrane it associates. Here raise the question whether the deletion of AKAP motif would affect the function of Nbea. In order to study this question, I made the pSyn-EGFP-Nbea Δ AKAP plasmid, in which the sequence encoding the AKAP motif was removed with Quikchange reaction.

I firstly created a 7.4 kb plasmid with the Nbea sequence containing AKAP motif. It is because the size of FL-Nbea vector (13 kb) limits the success of Quikchange reaction. There are two EcoRI sites inside the pSyn-EGFP-Nbea, one of which is at the beginning of the EGFP sequence, and the other inside the Nbea gene (Fig. 3.11 A). The pSyn-EGFP-Nbea plasmid was digested with EcoRI. This digestion resulted in two bands of 8.9 and 4.4 kb (Fig. 3.11 A). The 4.4 kb band that contains AKAP motif was purified from PAGE and inserted into the pBlueScript vector (Stratagene). The resulting vector was named as pBlueScript-Nbea(EcoRI) (Fig. 3.11 B). This plasmid was then used as the template in the Quikchange reaction to remove the AKAP motif. Primers MM 12-45 and MM 12-46 were designed to bridge the gap of the AKAP sequence, and introduce a SpeI site at the deletion site without frame shift (Fig. 3.11 C). The Quikchange reaction result was verified with SpeI restriction enzyme digestion, which cut two sites, one at the AKAP deleting site, the other at the vector backbone. Positives of Quikchange reaction show two bands at 0.3 and 7kb (Fig. 3.11 C). This plasmid was named as pBS-NE Δ A, standing for "pBlueScript-Nbea(EcoRI) with AKAP deleted".

70

RESULTS

The next step of cloning the pSyn-EGFP-Nbea Δ AKAP was to replace the Nbea fragment between EcoRI sites with the Nbea Δ AKAP part in the pBS-NE Δ A vector. The Nbea Δ AKAP fragment on the pBS-NE Δ A plasmid and the pSyn-EGFP-Nbea was cut by EcoRI and purified from PAGE respectively. The 8.9 kb band from pSyn-EGFP-Nbea digestion, which contained the pSyn-EGFP-Nbea vector backbone and a truncated Nbea gene, was dephosphorylated, so that it would not self-ligate. These two fragments were ligated at 16 °C for overnight. The ligation result was verified with SpeI digestion, which showed 4 and 9.3 kb bands for positives (Fig. 3.11 D). Positives were further sequenced to confirm no unexpected mutation inside the vector. Thus, the pSyn-EGFP-Nbea Δ AKAP was successfully cloned.

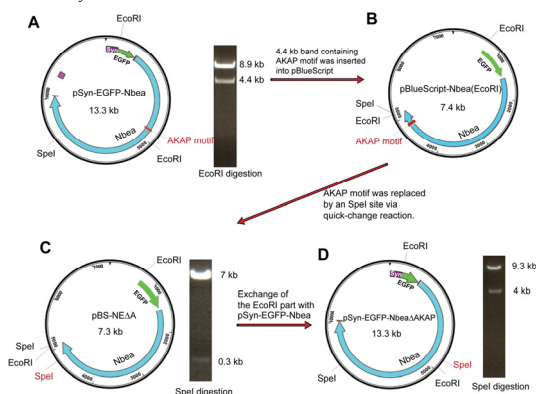


Figure 3.11 process of Nbea Δ AKAP cloning A) The vector pSyn-EGFP-Nbea was digested with the EcoRI enzyme and generated 4.4 and 8.9 kb bands. B) The 4.4 kb band that contained the AKAP motif was inserted into the pBlueScript vector as pBlueScript-Nbea(EcoRI). C) The AKAP motif was replaced by a SpeI restriction site. The new SpeI site is marked red. This plasmid was tested by SpeI digestion, which showed 0.3 and 7 kb bands. D) The AKAP motif deleted fragment was transferred back into the pSyn-EGFP-Nbea vector and generated the pSyn-EGFP-Nbea Δ AKAP vector. This vector was tested with SpeI digestion, which showed 4 and 9.3 kb bands for positive clones.

71

RESULTS

3.2.2.2 ARM domain cloning

ARM domain is characterized by a 40 amino acid motif composing three α -helices. It was firstly identified from *D. melanogaster* segment polarity protein Armadillo (Perfer et al., 1994). Tandem repeated copies fold together as a superhelix and form a platform-like structure, where many proteins can interact (Tewari et al., 2010). Therefore, ARM domain containing proteins are involved in several independent cellular processes, such as β -catenin in Wnt signaling (MacDonald et al., 2009), Importin α in protein transportation from cytoplasm to cell nucleus (Kohler et al., 1999), Kinesin-Associated Protein 3 (KAP3) in cargo movement along the microtubules (Manning and Snyder, 2000), and ARM containing protein 8 (ARMC8) in cytoskeletal regulation and degradation (Suzuki et al., 2008).

The DNA sequence of ARM domain in Nbea gene is approximately 2 kb long and translates to 652 amino acids. The main steps of ARM cloning were shown in figure 3.12. I cloned the ARM sequence from the pSyn-EGFP-Nbea plasmid with PCR. Primers MM12-46 and MM12-47 were designed to add Sall and XbaI sites at the borders of the domain coding sequence respectively, so that the DNA could be inserted by sticky ends ligation into the pSyn-EGFP vector (Figure 3.12, A and B). ARM sequence was amplified with PCR (Fig. 3.12 B). After purification from gel and Sall, XbaI digestion, the Sall-ARM-XbaI fragment was inserted into the pSyn-EGFP vector (Fig. 3.12 C). The newly formed pSyn-EGFP-ARM construct was verified with BspE1 and SacII digestion, which showed 2.3 and 4.9 kb bands for positive clones (Fig. 3.12 D). Finally, plasmid was sequenced to confirm no unexpected mutation. This plasmid will later be studied in the mammalian cell lines, as well as in neurons, to see whether the solely ARM domain from Nbea functions in the cell for cytoskeleton binding or protein transportation as its homologous proteins.

72

RESULTS

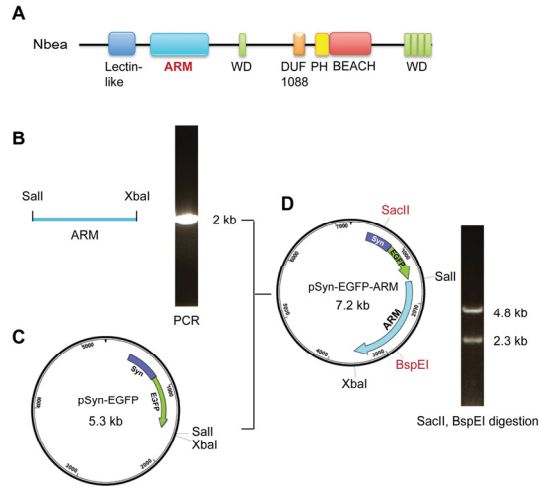


Figure 3.12 processes of ARM cloning A) Schematic diagram of Nbea domains. ARM domain is highlighted with red characters. B) ARM was amplified with PCR, and showed a 2 kb band in the electrophoresis gel. C) Plasmid pSyn-EGFP contains Sall and Xbal sites right after the EGFP tag. D) The newly formed pSyn-EGFP-ARM plasmid was tested with SacII and BspEI digestion, which showed 2.3 kb and 4.8 kb bands.

73

RESULTS

3.2.2.3 PH-BEACH domain cloning

In the Nbea protein, there are two closely connected domains, PH and BEACH domain (Fig. 3.13 A). BEACH domain is a module of about 300 amino acid residues. It is highly conserved in a large family of BEACH-containing proteins (~50-60% identity) (reviewed from De Lozanne, 2003). BEACH proteins are found in many species of the eukaryotes including Dictyostelium, Arabidosis, Drosophila, mouse and human. In human, there are nine BEACH-containing proteins. Alterations of these proteins affect lysosome size (LYST and NSMAF), apoptosis (NSMAF), autophagy (LYST, WDFY3, LRBA), granule size (LYST, NBEAL2, Nbea), and synapse formation (Nbea) (reviewed from Cullinane et al., 2013). In contrast, the PH domain is a weakly conserved pleckstrin-homology domain, which was identified from Nbea crystal structure analyses (Jogl et al., 2002). The structural study suggested strong interactions between the PH and BEACH domains. It is though unclear what is the function of the PH-BEACH domain combination in the Nbea. As a result, I cloned these two domains together as PH-BEACH domain.

The PH-BEACH coding sequence in Nbea is 1242 bp long. The same as in the ARM cloning, the PH-BEACH cloning used primers MM12-70 and MM12-71, which contain restriction site Sall and Xbal. After PCR and PAGE, the band at about 1300 bp was cut out and purified with gel purification kit (QiaGen) (Fig. 3.13 B). Then the PCR product and the pSyn-EGFP vector were digested with Sall and Xbal (Fig. 3.13 C). Afterwards, these two DNA fragments were ligated and amplified with *E.coli* in the LB media. The newly constructed pSyn-EGFP-PH-BEACH plasmid was confirmed by SacII and EcoRV digestion, which shows 1.4 and 5 kb bands in the positives (Fig. 3.13 D). The positive plasmids were also sequenced (GATC) to ensure that no mutation appears in the vector.

74

RESULTS

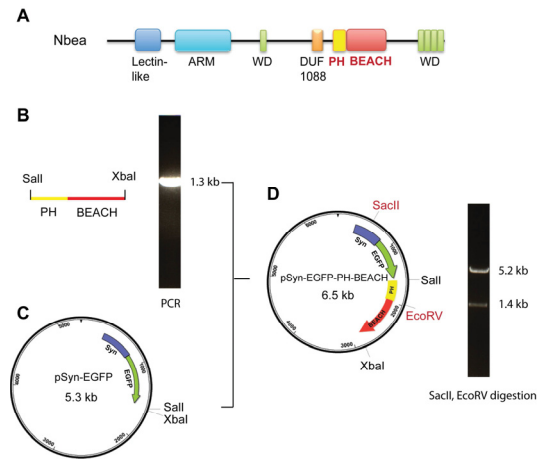


Figure 3.13 Processes of PH-BEACH cloning A) Schematic diagram of Nbea domains. PH-BEACH domain is highlighted with red characters. B) PH-BEACH was amplified with PCR, and showed a 1.3 kb band in the PAGE. C) Plasmid pSyn-EGFP contains Sall and Xbal sites right after the EGFP tag. D) The newly formed pSyn-EGFP-PH-BEACH plasmid was tested with SacI and EcoRV digestion, which showed 1.4 kb and 5.2 kb bands.

75

RESULTS

3.2.2.4 WD domain cloning

Another important domain in Nbea is the WD repeats. Each WD repeat contains a conserved core of approximately 40 amino acids that usually initiating with a glycine (G) and histidine (H), and ending with a tryptophan (W) and aspartic acid (D). Four or more repeats of this unit is defined as WD domain (Smith et al., 1999; Li and Roberts, 2001). Proteins containing this WD domain have critical roles in many essential biological functions such as signal transduction by G protein β subunit, cytoskeletal assembly by MAP, and vesicular trafficking by COP (reviewed from Li and Roberts, 2001).

The computational structure of Nbea revealed that there are five WD repeats in the Nbea protein. Four of them present at the C-terminal of the protein, namely WD 2 to 5 (Fig 3.14 A). The other one (WD 1) is in the middle region (Fig 3.15 A) of the Nbea sequence, but probably assembles closely with the other four WD repeats via protein folding. It is not clear, however, whether the four WD repeats at the C-terminal is able to form a functional domain, or the first one (WD 1) is also required. Therefore, two versions of WD domain cloning were made: a short version of the C-terminal WD repeats named "WD 2-5" (Fig. 3.14), and a long version of sequence from WD 1 to 5 named "WD-long" (Fig. 3.15). The WD-long sequence includes all the five WD repeats, as well as the DUF1088 domain and PH-BEACH domain between the first and the second WD repeats (Fig. 3.15).

Both WD 2-5 and WD-long was cloned from pSyn-EFGFP-Nbea plasmid. Restriction site Sall was added in the forward primers MM13-01 (for WD 2-5) and MM13-18 (for WD-Long), and Xbal was added in the reverse primer MM13-02 (for both constructs). The C-terminal WD 2-5 fragment is 672 bp long (Fig 3.14 B), and the WD-long fragment is 4848 bp (Fig. 3.15 B). These two fragments were amplified by PCR separately because different elongation times were required. Afterwards, bands with proper sizes were cut out from PAGE and purified by gel extraction kit (QiaGen). After digestion of purified PCR products

76

RESULTS

and pSyn-EGFP plasmid with Sall and XbaI restriction enzymes, WD 2-5 and WD-long were separately ligated to form the pSyn-EGFP-WD2-5 and pSyn-EGFP-WD-long plasmids (Fig. 3.14 D; Fig. 3.15 D). The newly formed pSyn-EGFP-WD2-5 was verified by EcoRV and SacII digestion, which shows 1.4 and 4.6 kb bands for the positive ligations (Fig. 3.14 D). In addition, the newly formed pSyn-EGFP-WD-long was verified by EcoRI and SpeI digestion, which shows 4.1 and 6.1 kb bands for the positives (Fig. 3.15 D). These clones were also sequenced to make sure that they are free of mutation.

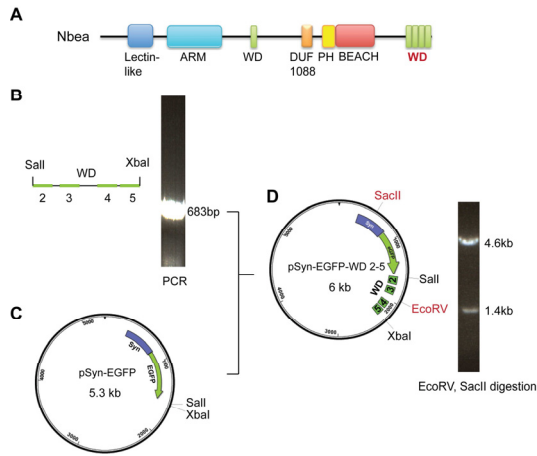


Figure 3.14 Processes of WD 2-5 cloning A) Schematic diagram of Nbea domains. The second to the fifth WD repeats domain is highlighted with red characters. B) WD 2-5 was amplified with PCR, and showed a 683 bp band in the electrophoresis gel. C) Plasmid pSyn-EGFP contains Sall and XbaI sites right after the EGFP tag. D) The newly formed pSyn-EGFP-WD2-5 plasmid was tested with SacII and EcoRV digestion, which showed 1.4 kb and 4.6 kb bands.

77

RESULTS

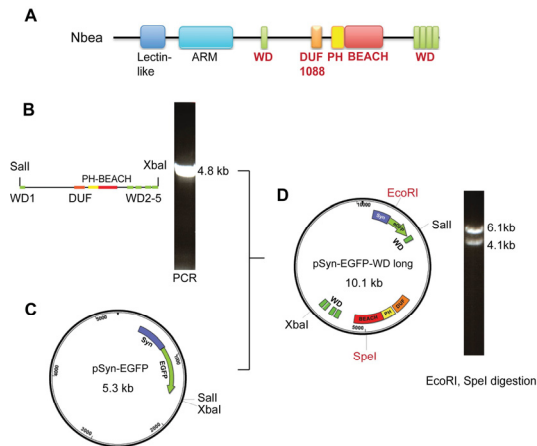


Figure 3.15 Processes of WD long cloning A) Schematic diagram of Nbea domains. The first to the fifth WD repeats domain, together with the DUF1088, PH and BEACH domains in between, are highlighted with red characters. B) WD long sequence was amplified with PCR, and showed a 4.8 kb band in the electrophoresis gel. C) Plasmid pSyn-EGFP contains Sall and XbaI sites right after the EGFP tag. D) The newly formed pSyn-EGFP-WD-long plasmid was tested with EcoRI and SpeI digestion, which showed 4.1 and 6.1 kb bands.

78

RESULTS

3.2.2.5 Lectin-like domain cloning

Lectin is a protein firstly identified from castor plant (*Ricinus communis*), and later found in many other species, including human. The main function of Lectin is to recognize specific extracellular glycoproteins. The N-terminal part of Nbea is predicted to form β -sheets that share striking similarity with legume lectin fold, and belongs to the concanavalin A-like lectin superfamily (Burgess et al., 2009). This raised the question why Nbea as an intracellular protein requires a Lectin-like domain that is used normally in extracellular glycoprotein binding? In order to investigate this question in detail, I cloned the Lectin-like domain into the pSyn-EGFP vector to generate a pSyn-EGFP-Lectin plasmid.

The Lectin-like domain was located close to the N-terminal of Nbea (Fig. 3.16 A). It was amplified from pSyn-EGFP-Nbea plasmid. Forward primer MM 12-68 was designed to contain Sall restriction site, and reverse primer MM 12-69 contains XbaI. The Lectin-like domain is 558 bp long (Fig. 3.16 B). After PCR, the band at about 600 bp was cut out, and then purified with gel extraction kit (QiaGen). After purification, the PCR product of Lectin-like domain was digested with Sall and XbaI restriction enzymes and then ligated into the pSyn-EGFP vector (Fig. 3.16 C). This newly formed plasmid was named as pSyn-EGFP-Lectin (Fig. 3.16 D). This plasmid was verified by BlnI and ClaI digestion, which shows 0.6 and 5.2 kb bands for the positives (Fig. 3.16 D). The positives were sequenced to avoid unexpected mutations.

79

RESULTS

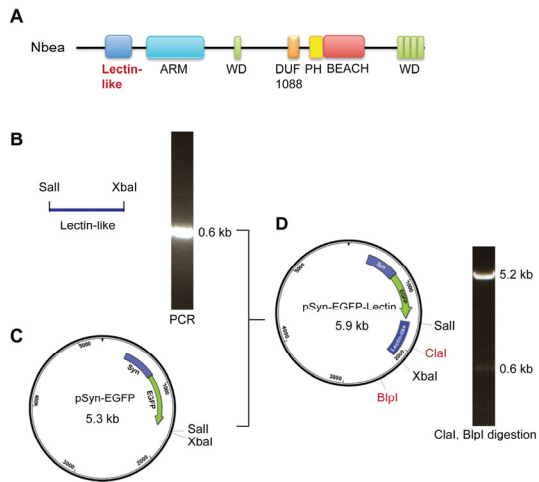


Figure 3.15 Processes of Lectin-like domain cloning A) Schematic diagram of Nbea domains. Lectin-like domain is close to the N-terminal of Nbea, and is highlighted with red characters. B) Lectin-like sequence was amplified with PCR, and showed a 0.6 kb band in the electrophoresis gel. C) Plasmid pSyn-EGFP contains Sall and XbaI sites right after the EGFP tag. D) The newly formed pSyn-EGFP-Lectin plasmid was tested with ClaI and BlnI digestion, which showed 0.6 and 5.3 kb bands.

80

RESULTS

3.2.2.6 DUF1088 domain cloning

The last but not the least domain of my interest in Nbea is the DUF1088 domain. It is short for domain of unknown function. It is a small domain consisted of 168 amino acids. However, it is yet unknown how this domain functions in Nbea protein, and whether it is essential for Nbea. Therefore, I made two constructs to answer these questions. One of the constructs is the pSyn-EGFP-DUF plasmid, which encodes a DUF1088 domain with EGFP tag (Fig. 3.16). The other construct is the pSyn-EGFP-Nbea Δ DUF, in which DUF domain was deleted from the full-length Nbea gene (Fig. 3.17).

DUF domain is located between the first WD repeats and the PH domain (Fig. 3.16 A). Cloning of DUF used primers MM 12-84 and MM 12-85. The forward primer was designed with Sall restriction site and the reverse primer with XbaI restriction site. After PCR, the band at about 0.5 kb was extracted from gel PAGE and purified with gel extraction kit (QiaGen) (Fig. 3.16 B). Afterwards, both the PCR product and the pSyn-EGFP plasmid (Fig. 3.16 C) were digested with Sall and XbaI, and then the insert and vector were ligated to form the pSyn-EGFP-DUF plasmid (Fig. 3.16 D). The ligation was tested with restriction enzymes MfeI and EcoRI, which showed 4.7 and 1.1 kb bands for the positives (Fig. 3.16 D). The positive clones were also sequenced to avoid unexpected mutations.

81

RESULTS

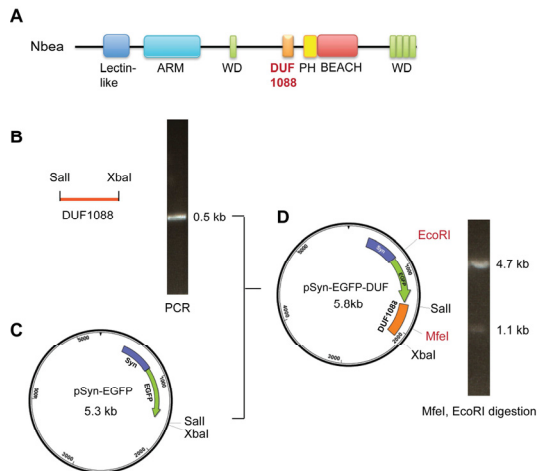


Figure 3.16 Processes of DUF1088 domain cloning A) Schematic diagram of Nbea domains. The DUF domain is between WD1 and PH domain. It is highlighted with red characters. B) DUF1088 sequence was amplified with PCR, and showed a 0.5 kb band in the electrophoresis gel. C) Plasmid pSyn-EGFP contains Sall and XbaI sites right after the EGFP tag. D) The newly formed pSyn-EGFP-DUF plasmid was tested with EcoRI and MfeI digestion, which showed 1.1 and 4.7 kb bands.

3.2.2.7 Nbea Δ DUF cloning

The strategy for DUF domain deletion is to cut out the DUF sequence from the full-length Nbea plasmid pSyn-EGFP-Nbea. Two ClaI restriction sites were introduced at the borders of DUF by Quikchange reactions.

Before the Quikchange reactions, I reduced the size of pSyn-EGFP-Nbea vector from 13.3 kb to 8.9 kb by digesting it at the two EcoRI sites inside Nbea gene and

82

RESULTS

EGFP sequence, and relegation (Fig. 3.17 A and B). The reason for this step is that large size of the vector reduce the possibility of success in Quikchange reactions. DUF sequence is on the newly ligated intermediate 9 kb vector named as pSNΔE, which is short for "pSyn-EGFP-Nbea deleting EcoRI part" (Fig. 3.17 B). Two Quikchange reactions were processed to add Clal at the 3'- and the 5'- site of DUF sequence successively. pSNΔE plasmid was used as template. Primers MM13-05 and MM13-06 were designed with no frame shift and no amino acid change in the gene. The resulting plasmid was used as template for the second Quikchange reaction to add Clal site at the edge of 5'-DUF. Primers MM 13-16 and MM 13-17 were used in the second Quikchange reaction. The plasmid from the second Quikchange reaction was named as pSNΔE+Clal-2 (Fig. 3.17 C). After that, there were two Clal sites at the borders of DUF sequence. Therefore, this plasmid was verified by Clal digestion, which shows 8.5 and 0.5 kb bands in the positives (Fig. 3.17 C). The positives were sent for sequencing. After sequencing, the correct pSNΔE+Clal-2 plasmid was digested with Clal. The upper band of 8.5 kb was purified from the PAGE and religated, so that the DUF gene was deleted from the pSNΔE+Clal-2 vector. This vector without DUF sequence was named as pSNΔEΔD, short for "pSNΔE plasmid with DUF deleted" (Fig. 3.17 D). The next step of generating pSyn-EGFP-NbeaΔDUF plasmid was to insert the deleted EcoRI part of Nbea back into the pSNΔEΔD vector. Both pSNΔEΔD and pSyn-EGFP-Nbea were digested with EcoRI. The EcoRI digested pSNΔEΔD fragment was then dephosphorylated, so that it will not ligate with itself. PAGE of EcoRI digested pSyn-EGFP-Nbea showed two bands (Fig. 3.17 A). The lower 4.4 kb band was purified and ligated with the EcoRI digested pSNΔEΔD fragment. After ligation, the newly formed pSyn-EGFP-NbeaΔDUF plasmid was verified with MluI and NotI digestion, which showed 7.9 and 4.9 kb bands in the positives (Fig. 3.17 E). The positives were also sequenced to ensure that the cloning process introduced no frame shift or mutation. Thus, the DUF1088 domain deleted Nbea gene ((Fig. 3.17 F) was successfully constructed. This construct will further be used in the functional studies of Nbea.

83

RESULTS

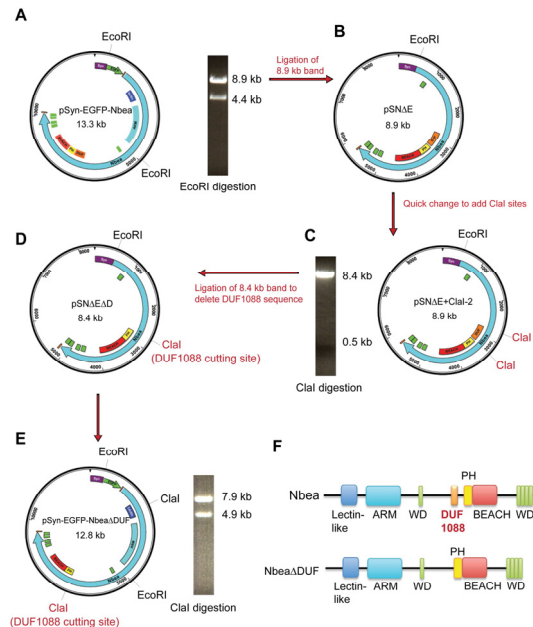


Figure 3.17 Processes of NbeaΔDUF cloning **A)** The pSyn-EGFP-Nbea plasmid was digested with EcoRI, which shows 8.9 and 4.4 kb bands. **B)** The 8.9 kb band from (A) was purified and ligated as vector pSNΔE, which is short for pSyn-EGFP-NbeaΔEcoRI part. **C)** Two Clal sites were introduced at the edges of DUF 1088 domain by quick change. Digestion of pSNΔE+Clal-2 showed 0.5 and 8.4 kb bands. The 0.5 kb band is the DUF 1088 domain. **D)** The 8.4 kb band from (C) was ligated into the pSNΔEΔD plasmid. **E)** The EcoRI part of 4.4 kb band from (A) was inserted into the pSNΔEΔD plasmid to form the pSyn-EGFP-NbeaΔDUF construct. Clal was used to test the ligation result. The positives show 4.9 and 7.9 kb bands **F)** Schematic diagram of Nbea and NbeaΔDUF. The DUF domain is highlighted with red characters.

84

RESULTS

I successfully cloned the Syn promoted EGFP-Nbea, as well as several Nbea related constructs. The FL-Nbea and Nbea Δ AKAP were studied in our group in neuronal cell culture and showed ability in rescuing Nbea KO phenotypes (unpublished data from Dr. Brockhaus and Dr. Repetto). The Nbea domain constructs will further be used in functional investigations in the WT and Nbea KO neurons.

85

4. Discussion

This study involves two ASD related genes, *β Nrxn* and *nbea*. Among them, *β Nrxn* was previously investigated with exogenous expression and *in vitro* experiments, and was proposed to play important roles in the ASD trans-synaptic protein network. The main gap in *β Nrxn* is the lack of KO study. On the other hand, Nbea KO was investigated intensively and showed profound phenotypes in synapse formation and neurotransmission. However, the exact role of this multi-domain protein has not yet been determined. In this project, the stable *β Nrxn* KO mouse lines were investigated for the first time. Results show that *β Nrxns* are required for the basal synaptic transmission and maintaining the short-term plasticity at excitatory synapses. Deletion of *β Nrxn* does not affect the function of inhibitory synapses, as well as the physical properties like body weight. In addition, the full-length Nbea and some domain constructs that may involve in the regulating the trafficking of Nrxn are cloned.

4.1 Comparison of *β Nrxn* KO and *α Nrxn* KO

β Nrxn and *α Nrxn* are closely related. Even though they are transcribed from two independent promoters, they share an identical C-terminus, which contains an extracellular LNS domain, and an intracellular PDZ binding motif (Missler et al., 1998 b; Biederer and Sudhof, 2000). The LNS domain in *β Nrxn* is able to interact with several postsynaptic SynCAMs, such as Nlgn, Cbln-GluR2 complex, GABA_A receptor, and LRRTM (Ichtchenko et al., 1995; Zhang et al., 2005; de Wit et al., 2009; Zhang et al., 2010). In addition, recombinant experiments suggest that *β Nrxn* regulates postsynaptic development and balance between excitatory and inhibitory synapses via its postsynaptic binding partners (Dean et al., 2003; Graf et al., 2004; Mondin et al., 2011). All these results point to an essential role of *β Nrxn* in the neuron development, and imply that *β Nrxn* KO mouse models will have a more dramatic effect than that have shown in *α Nrxn* KO. Surprisingly,

86

DISCUSSION

different from the α Nrxn KO mice, which have severe or lethal phenotypes, even the TKO of β Nrxn are vital and fertilizable.

Synaptic transmission of α Nrxn variants has been studied via electrophysiology in acute brain slices and cultured neurons. Different brain regions are involved, including brain stem (Missler et al., 2003; Zhang et al., 2005; Dudanova et al., 2006), hippocampus (Etherton et al., 2009), somatosensory cortex (Born et al., 2014) and cultured cortical neuron (Missler et al., 2003). In this study, β Nrxn mutants were studied in the primary somatosensory region in the acute cortex slice. This region was chosen because firstly, β Nrxn KOs were as vital as WT and did not show brain stem-related abnormal respiration rate as in α Nrxn KO mutants (Missler et al., 2003). Secondly, no obvious physical changes like in body weight were observed in β Nrxn KO variants. In addition, cortex is a premium region with well-developed synapses and is suitable for electrophysiological investigations of many different conditions.

In α Nrxn KO mutants, a decreased frequency in the spontaneous excitatory synaptic transmission was observed in different brain regions (Missler et al., 2003; Etherton et al., 2009; Born et al., 2014). In particular, deletion of all α Nrxns caused a large decrease of about 60% in the frequency of mEPSC. Other parameters of excitatory synaptic transmission, like amplitude and kinetics, were not affected by the deletion of α Nrxns (Missler et al., 2003; Zhang et al., 2005). These observations are independent of a particular brain region (Missler et al., 2003; Born et al., 2014). These studies together reflect a fundamental dysfunction of α Nrxn KO in spontaneous neurotransmitter release.

In β Nrxn KO neurons, a decreased mEPSC frequency was also observed (Fig 3.3). In all three variants of β Nrxn KO, namely 2SKO, 1/3DKO and TKO, the frequency decreased to the same extent of about 70%. This decreased frequency is in the same tendency as the observation in α Nrxn KO mutants (Missler et al., 2003; Etherton et al., 2009). However, this alteration was not as gross as in α Nrxn KO.

87

DISCUSSION

The milder phenotype in β Nrxn KO than that in α Nrxn KO could be one reason that even TKO mice still survive, while already a DKO of α Nrxn cannot.

Besides decreased frequency in spontaneous transmission, altered excitatory synaptic plasticity was also detected in both α Nrxn KO and β Nrxn KO. A slightly impaired synaptic plasticity was reported from C1 region of hippocampus in Nrxn 1 α KO neurons (Etherton et al., 2009) and somatosensory cortex in Nrxn 2 α KO (Born et al., 2014). These results indicated that α Nrxns, at least Nrxn 1 and 2 α , mediates the synaptic plasticity. Similar as in α Nrxn KO, β Nrxn KO mutants in this study revealed impaired short-term plasticity as well (Fig 3.5 & Fig. 3.6). Substantial impairment was observed in neurons lacking Nrxn 2 β . The short-term facilitation in the WT neurons was almost abolished or even turned to depression in the 2SKO neurons. When all β Nrxns were deleted, neurons showed similar impairment of synaptic plasticity as in 2SKO. However, this phenotype in neurons lacking Nrxn 1 and 3 β was much milder. These results suggest that among those three β Nrxns, the 2 β isoform is probably the key component in regulating the short-term plasticity at excitatory synapses.

Besides these similar phenotypes of vesicle release and synaptic plasticity, there are also differences between α Nrxn KO and β Nrxn KO mutant. One major difference lies in the parameter of amplitude. In contrast to α Nrxn mutants, which show no alteration in amplitude, β Nrxn KO neurons presented increased amplitudes in both spontaneous and evoked excitatory neurotransmission. In mEPSC experiment, all three β Nrxn KO variants showed a 25% increase of amplitude (Fig. 3.3 C). The increased amplitude was also found in action potential evoked neurotransmission (Fig. 3.4). In that experiment, larger amplitudes in β Nrxn KO were detected at a variety of stimulus strengths. These double approaches verified that the increased amplitudes observed were independent of a particular type of synaptic transmission. Therefore, a general change in the function of synapse may contribute to this phenotype in β Nrxn KO neurons. In addition, degrees of increased amplitude were the same in different

88

DISCUSSION

KO variants. This suggested that the number of deleted β Nrxn did not affect the extent of change. Therefore, each individual β Nrxn isoform is required in regulating the amplitudes at excitatory synapses. Taking together, different from α Nrxn, β Nrxn play a unique role in modulating the amplitude at excitatory synapses.

The other difference between α Nrxn and β Nrxn lies in their function at inhibitory synapse. At inhibitory synapses that lacking all three β Nrxn, neither neurotransmission nor synaptic plasticity was changed (Fig. 3.7 & Fig. 3.8). In the action potential evoked neurotransmission at various stimulus strengths, WT and TKO presented identical amplitudes. Short-term plasticity probed with stimuli at different frequencies was also constant in WT and β Nrxn TKO. α Nrxn KO variants, however, showed alterations in both basal neurotransmission and synaptic plasticity. First of all, evoked amplitudes were nearly diminished in TKO of α Nrxn (Missler et al., 2003). Furthermore, PPR of the α Nrxn TKO neurons were notably decreased when stimulating with a 20-Hz train of pulses (Missler et al., 2003). These results imply that β Nrxns mainly function at the excitatory synapses, while α Nrxns are probably involved in both excitatory and inhibitory synaptic function.

In brief, comparisons of α - and β Nrxn variants indicate that their roles in regulating synaptic transmission and plasticity are partially overlapped, partially unique. At excitatory synapse, α - and β Nrxn participate in regulating the synaptic transmission and plasticity. Altered frequency of spontaneous vesicle release in both α Nrxn and β Nrxn KO implies their essential role in synaptic vesicle release. In addition, both of these proteins are required to maintain the short-term facilitation at excitatory synapse. The unique role of β Nrxn is in regulating amplitude in both spontaneous and evoked excitatory synaptic transmission. The unique function of α Nrxn lies in the inhibitory synapse, where α Nrxn plays a fundamental role in both basal synaptic transmission and plasticity, while an influence of β Nrxn is not obvious.

89

DISCUSSION

Table 4.1 Comparison of α Nrxn KO and β Nrxn KO electrophysiology

Synapse	Parameters	α Nrxn KO	β Nrxn KO
Excitatory synapse	mEPSC	Frequency	Decrease 30-60%
		Amplitude	No change
	Evoked amplitude	Decrease 10-60%	Increase 30%
	Short-term plasticity	Impaired	Impaired
Inhibitory synapse	Evoked amplitude	Decrease 85%	No change
	Short-term plasticity	Severe impairment	No change
References		Missler et al., 2003; Etherton et al., 2009; Born et al., 2014.	From this project

4.2 Underlying explanations for the β Nrxn mutant phenotypes

My observed phenotypes of β Nrxn KO were present at excitatory synapse. One of the major changes was increased amplitude in neurons lacking one or more β Nrxns. This increment was detected in both spontaneous and evoked excitatory neurotransmission (Fig. 3.3; Fig. 3.4; Table 4.1). Changed amplitude usually implies alteration in number of released vesicles, quantal size, or postsynaptic receptor density and sensitivity (Liu and Tsien, 1995; Lisman et al., 2007). Number of released vesicles was probably not changed in the β Nrxn KO. It is because changed number of released vesicle would result in a multiplied difference, while the difference of amplitudes between WT and β Nrxn KO mutants were about 25%. Change in quantal size is also not likely to relate with the increased amplitude in β Nrxn KO. As a presynaptic cell adhesion molecule, Nrxns is not supposed to involve in neurotransmitter loading or sorting.

90

DISCUSSION

The third possibility, changed postsynaptic receptor density and sensitivity, may be the reason for the increased amplitude. At the excitatory postsynaptic membrane, there are mainly two types of ionotropic receptors, AMPA receptor and NMDA receptor. They are both activated by glutamate binding, but differ at excitation potentials and speed of response. AMPA receptor could activate at resting potential (-65 mV), while NMDA receptor excites at membrane potential at 30 mV (Cattabeni et al., 2004; Purves et al., 2011). Normal time constants of AMPA receptor are rise time within 2 ms, and decay time within 10ms. However, a single NMDA receptor requires more than 2 ms to open the ion channel, and it stays opening for 10-100 ms (Cattabeni et al., 2004; Purves et al., 2011). In this study, experimental measurements for mEPSC and eEPSC were set at -70 mV and the pipette solution included Mg^{2+} , an NMDA receptor blocker. The rise times of mEPSC were about 1.7 ms, and decay times at about 6.0 ms (Fig. 3.3 E and F). The time constants were in agreement with the AMPA receptor, but not NMDA receptor. Therefore, AMPA receptor is probably the main receptor related to the increased amplitudes in the β Nrxn mutants. Together with the fact of enlarged amplitude, an increase in the number of postsynaptic AMPA receptor could be an underlying reason.

The hypothesis of increased postsynaptic AMPA receptor corresponds with previous experiments (Aoto et al., 2013; unpublished data from Dr. Born). Aoto et al. (2013) revealed decreased AMPA amplitude when exogenous β Nrxn was expressed in the WT neuron (Aoto et al., 2013). It was supposed to have an enhanced AMPA receptor endocytosis at the synapse when β Nrxn was overexpressed (Aoto et al., 2013). This result implies that when β Nrxn is deleted, there would be more AMPA receptors at the postsynaptic membrane. Furthermore, preliminary results from Dr. Born showed a decreased NMDA/AMPA ratio in the 2SKO of β Nrxn (Unpublished data from Dr. Born). The decreased ratio may be due to more AMPA receptors than NMDA receptors at synapses lacking β Nrxn. Taking together, these facts all indicate that there may

91

DISCUSSION

be more postsynaptic AMPA receptors in β Nrxn deficient neurons. Therefore, β Nrxn is probably involved in regulating postsynaptic AMPA receptor.

Moreover, previous investigations of α Nrxn KO mutants proved that postsynaptic NMDA receptor, but not AMPA receptor, were affected when all three α Nrxns were deleted (Kattenstroth et al., 2004). Therefore, these data imply that α - and β Nrxn both play a role in regulating postsynaptic receptors at excitatory synapse, among which the α Nrxn mainly regulates NMDA receptor, and β Nrxn regulates AMPA receptor (Fig. 4.1).

Frequency of spontaneous vesicle release was another parameter that changed in both α - and β Nrxn mutants (Missler et al., 2003; Fig. 3.3 B). Frequency reflects the possibility of spontaneous vesicle release at resting potential. Altered frequency usually implies a presynaptic change, such as activity of Ca^{2+} channels at active zone, vesicle release machinery, or number of synapses. The frequency of mEPSC was found to decrease in both α Nrxn KO (Missler et al., 2003) and β Nrxn KO (Fig. 3.3 B). Changes in α Nrxn mutants were resulted from a coupling of α Nrxn and Ca^{2+} channels during the process of vesicle exocytosis (Missler et al., 2003; Zhang et al., 2005; Dudanova et al., 2006). It was identified that α Nrxn selectively affected the activation of N- and P/Q-type Ca^{2+} channels (Zhang et al., 2005). How exactly does α Nrxn link with these Ca^{2+} channels is yet not clear. One possibility is through CASK or yet undefined PDZ proteins. N- and P/Q type Ca^{2+} channels both contain CASK binding site at the C-terminal of the sequence (Catterall and Few, 2008). CASK, as a potential interacting partner to the PDZ binding motif of Nrxns (Mukherjee et al., 2008), may bridge α Nrxns to Ca^{2+} channels (Fig. 4.1). This model of coupling applies to both α Nrxn and β Nrxn, as they share the identical intracellular PDZ binding motif that may recruit CASK or other PDZ proteins (Zhang et al., 2005; Spafford and Zamponi, 2003; Catterall and Few, 2008).

92

DISCUSSION

A correlation of Nrnx to Ca^{2+} channels could also explain the impaired short-term plasticity observed in α - and β Nrxn mutants (Missler et al., 2003; Fig. 3.5; Fig. 3.6). Short-term facilitation detected at excitatory synapse of WT was almost diminished in α Nrxn TKO (Missler et al., 2003) and β Nrxn KO mutants (Fig. 3.5; Fig. 3.6). There are mainly two Ca^{2+} -dependent mechanisms proposed for synaptic facilitation. Firstly, saturation of local Ca^{2+} buffers, e.g. calbindin-D28k, results in an increased local Ca^{2+} concentration (Blatow et al., 2003). Secondly, residual Ca^{2+} binds to a Ca^{2+} sensor (CaS) and increases or prevents the Ca^{2+} channel activity, which occurs in a time scale of milliseconds (Catterall and Few, 2008; Catterall et al., 2013). Among those Ca^{2+} channels, the P/Q-type Ca^{2+} channel is a major contributor to short-term plasticity. Binding of Ca^{2+} with CaS proteins like calmodulin (CaM), Ca^{2+} binding protein-1 (CaBP1), or visinin-like protein-2 (VILIP-2) mediates the facilitation or inactivation of P/Q-type Ca^{2+} , and further regulates the synaptic plasticity (Catterall and Few, 2008; Catterall et al., 2013). In accordance with this model, activity of N- and P/Q-type Ca^{2+} channels were found largely affected by the α Nrxn null mutant, and the short-term facilitation was nearly diminished (Missler et al., 2003; Zhang et al., 2005). Depending on the identical intracellular PDZ binding motif in α - and β Nrxn, those Ca^{2+} channels may also be affected in the β Nrxn KO. Therefore, the impaired short-term plasticity observed in β Nrxn ZSKO and TKO is probably due to a coupling of β Nrxn and Ca^{2+} channels. Further investigations of a relation between β Nrxn and Ca^{2+} channels may shed light on their roles and the molecular basis of synaptic plasticity.

93

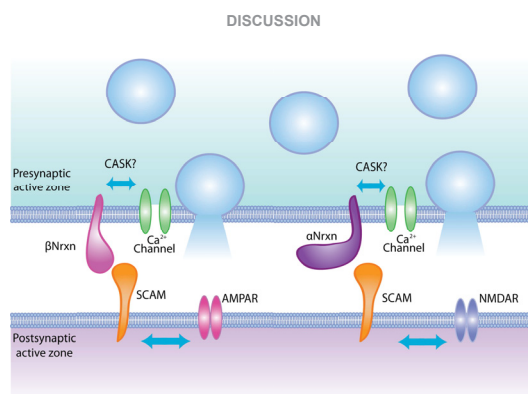


Figure 4.1 Model of how presynaptic Nrnx proteins may regulate the excitatory synaptic active zone. At presynaptic site, α - and β Nrxn may couple with Ca^{2+} channels via CASK or other undefined PDZ proteins. This coupling further mediates presynaptic vesicle release. At postsynaptic site, α - and β Nrxn may regulate NMDA receptor (NMDAR) and AMPA receptor (AMPA), respectively. Different synaptic cell adhesion molecules (SCAM) may bridge α - and β Nrxn to receptors.

4.3 Roles of Nbea at synapse

There are several connections between Nbea and Nrnx. First of all, both of them are mainly expressed in the brain, and are reported as ASD related genes (Wang et al., 2000; Castermans et al., 2003; Püschel and Betz, 1995; Feng et al., 2006; Vaags et al., 2012). Secondly, several independent studies revealed that they both participate in the excitatory and inhibitory synaptic function (Giannone et al., 2013; Sun et al., 2012; Missler et al., 2003; Su et al., 2004; Medrihan et al., 2009; Niesmann et al., 2011). Furthermore, our preliminary experimental data show that trafficking of Nrnx in axons is altered in Nbea KO neurons (unpublished data from C. Neupert). Besides these connections, there are big differences between these proteins. Firstly, these two proteins are located differently in the neuron:

94

DISCUSSION

Nbea is an intracellular scaffold protein, while Nrnx is a presynaptic transmembrane protein. Secondly, deletion of Nbea severely impairs the formation of dendritic spines (Medrihan et al., 2009; Niesmann et al., 2011), while deletion of Nrnx shows no obvious impairment in axonal path finding and synapses formation (Dudanova et al., 2007). Further study of Nbea, as well as its correlation with Nrnx and other proteins may shed light on their molecular mechanisms in neural function, as well as the underlying causes of ASD.

There are both functional and morphological defects observed in the neurons lacking Nbea. The major functional defect of Nbea mutants lies in the impaired neurotransmission (Su et al., 2004; Medrihan et al., 2009; Niesmann et al., 2011). The morphological change is mainly the decreased dendritic spine formation (Niesmann et al., 2011). Transfection of pSyn-EGFP-Nbea generated in this study into Nbea KO neurons could successfully rescue both of these phenotypes (unpublished data from Dr. Brockhaus and Dr. Repetto). This suggests Nbea is an essential factor in maintaining normal synaptic transmission and formation.

Decreased frequency in spontaneous synaptic transmission was reported from different brain regions of Nbea deficient mice, including brainstem (Medrihan et al., 2009), neuromuscular junction (Su et al., 2004), neocortex and cultured hippocampal neuron (Niesmann et al., 2011). Decreased frequency in spontaneous neurotransmission could result from several changes, such as a decreased synaptic number, reduced vesicles at active zone, or altered vesicle release machinery (Liu and Tsien, 1995; Lisman et al., 2007). Even though the number of spinous synapse is reduced in Nbea KO, the exact numbers of both excitatory and inhibitory synapses were not changed (Niesmann et al., 2011). Instead, the excitatory synapse, which is usually present at the spinous synapse (Kandel et al., 2012), shifts towards the dendritic shaft in the Nbea KO (Niesmann et al., 2011). This indicates that the reduced frequency detected in the Nbea deficient neuron may be not from a change in synaptic number. In addition, the number of vesicles that accumulate near the presynaptic active

95

DISCUSSION

zone in Nbea deficient neurons is constant with WT (Su et al., 2004; Niesmann et al., 2011). This suggests that the vesicles available for synaptic transmission are not changed in the Nbea KO neuron. Therefore, the vesicle number is probably not the factor that related to the reduced spontaneous neurotransmission. Whether the last possibility of altered vesicle release machinery could responsible for that phenotype? There is yet no direct proof to this question. However, several vesicle-related proteins, like SV2 and Mint-1, are found down regulated in mutant neurons (Medrihan et al., 2009). Moreover, evidences are accumulating for roles of Nbea in remodeling the actin cytoskeleton dependent synaptic organization (Niesmann et al., 2011; Nair et al., 2013). These facts imply that the proteins involved in the vesicle release machinery may be not properly arranged at the presynaptic terminal. Therefore, the abnormal organization of presynaptic terminal and vesicle release machinery is likely the reason to the altered spontaneous neurotransmission in the Nbea deficient neurons. Succeed in rescuing of the neurotransmission and dendritic spine formation with pSyn-EGFP-Nbea that was cloned in this study emphasizes the importance of Nbea in the organization of presynaptic terminal. Moreover, those Nbea domain-related clones would be powerful tools in investigating the exact cellular role and molecular determinants of Nbea.

4.4 Potential functions of Nbea domains

Besides the Nbea full-length construct, I also cloned several Nbea domain related constructs as tools for further investigation. So far, one of them, Nbea Δ AKAP, was transfected into Nbea KO neuron to study the synaptic formation. Interestingly, my Nbea construct lacking AKAP motif (pSyn-EGFP-Nbea Δ AKAP) could only partially rescue the impaired synaptic formation deficiency observed in the Nbea KO neuron (unpublished data from Dr. Repetto). The AKAP motif in Nbea contains 19 amino acids, and has high affinity to PKA (Wang et al., 2000). The role of AKAP proteins is supposed to tether PKA to specific subcellular sites, thereby focusing its activity to relevant substrates (Beene and Scott, 2007). Nbea

96

DISCUSSION

potentially interact with different proteins via domains like PH-BEACH and ARM. Therefore, it may provide a platform to recruit selective proteins for phosphorylation. The PH-BEACH and ARM constructs made in this study could be used in biochemistry studies to identify interacting partners with Nbea.

So far, there are two proteins reported as Nbea interacting partners, SAP102 and GlyR (del Pino et al., 2011; Lauks et al., 2012). SAP102 is a component of the PSD at excitatory synapses (Chen et al., 2012; del Pino et al., 2011), while GlyR is a neurotransmitter receptor at inhibitory synapses (Lauks et al., 2012). Both of these proteins interact with only the C-terminal part of Nbea (Lauks et al., 2012; del Pino et al., 2011). Depending on the sequence information from those reports, WD-40 repeats, DUF1088, and PH-BEACH were the domains required for the interaction between Nbea and SAP102 / GlyR (del Pino et al., 2011; Lauks et al., 2012). These interactions were tested *in vitro*, but provided hints of the intracellular location and binding partners of Nbea.

Another important question is how Nbea regulates actin organization and further the dendritic spine formation. Especially, which domain in Nbea may be involved in this function? Some hints suppose a potential relevance of the WD-40 repeats in Nbea and actin remodeling at dendritic spines. In Nbea deficient neurons, excitatory synapses tend to terminate at dendritic shaft rather than spine head (Niesmann et al., 2011). This supposes a failure in dendritic spine elongation (Hotulainen and Hoogenraad, 2011). A mature excitatory dendritic spine is mushroom-shaped, consisting of a narrow spine neck and an enlarged head (Hotulainen and Hoogenraad, 2011). This spine morphology is conferred by actin filament polymerization and branching (Penzes and Rafalovich, 2013). Formation of spine neck requires mostly linear actin filaments, and spine head requires branched ones (Hotulainen and Hoogenraad, 2011; Penzes and Rafalovich, 2013). Investigations of actin dynamics indicate that in mammalian cells, Coronin is one of the main factors regulating linear actin formation (Rybakin and Clemen, 2005; Utrecht and Bear, 2006). Coronin prevents actin

97

DISCUSSION

branching through suppressing inherent actin nucleation of the Arp2/3 complex (Rybakin and Clemen, 2005). Coronin belongs to WD-40 repeats domain containing proteins. The WD-40 repeats is exactly the domain binding to actin (Utrecht and Bear, 2006). Nbea also contains WD-40 repeats domain. Moreover, the shift of synaptic terminals to dendritic shafts in Nbea KO implies an impairment of linear actin filament formation. On the other hand, number of asymmetric synapses in Nbea KO is unaltered (Niesmann et al., 2011; Medrihan et al., 2009). This supposes the spine head, which is mainly composed with branched actin filaments, is not severely influenced. Taking together, WD-40 repeats in Nbea may play a role in dendritic spine growth via binding with actin. This binding may suppress actin branching through preventing other regulators, like Arp2/3, bind to actin. Investigations with the WD-40 constructs created in this study could exam the involvement of this domain in dendritic spine formation.

In conclusion, the first glance of β Nrxn KO mice revealed that lacking of β Nrxn affects basal synaptic transmission and impairs the synaptic plasticity at excitatory synapse. These impairments may result form increased postsynaptic AMPA receptor number and altered presynaptic Ca^{2+} channel activity. The other ASD related protein, Nbea, alters trafficking of Nrxn and independently regulates the neurotransmission as well as spinous synapse formation. Molecular mechanisms of how Nbea regulates the synapse formation and Nrxn trafficking could be further studied with the Nbea and domain related constructs. Identifying the cellular function of Nrxn and Nbea may explain the underlying pathogenesis of ASD.

98

5. Summery

One of the most challenging tasks for a better understanding of signal transmission in the normal and diseased central nervous system is to unravel the molecular basics of function on the cellular and synaptic levels. The β -isoform of Neurexins (Nrxns) has been shown as an essential protein that involved in inducing synaptic differentiation. In order to assay the contribution of β Nrxn in neurotransmission, I have explored for the first time the electrophysiological changes in β Nrxn KO mouse models. Quantitative analysis revealed a 30% decrease in the mEPSC frequency at excitatory synapses. The amplitude in both spontaneous and action potential evoked neurotransmission was increased about 25%. Number of deleted β Nrxns did not affect the extent of changes, suggesting a requirement of all three β Nrxns in maintaining a normal basal transmission. Paired-pause facilitations were almost diminished in 2SKO and TKO, but not in 1/3DKO. This indicated Nrxn 2 β is probably the key component in modulating excitatory synaptic plasticity in the somatosensory cortex. Inhibitory transmission in the neocortex of all β Nrxn models remained unaltered.

Moreover, the brain-enriched multi-domain protein Neurobeachin (Nbea) has been shown to influence Nrxn trafficking in neuron. Mice lacking Nbea have been investigated, and presented lethal phenotypes and impaired neurotransmission. However, the underlying determinants of this large protein are not clear. Clones of Nbea and domain-related plasmids were made as tools to study the role of Nbea in synaptic functions. Rescue experiments with full-length Nbea confirmed the importance of Nbea in modulating dendritic spine formation and synaptic transmission. Furthermore, the partial rescue with Nbea Δ AKAP suggested the PKA binding motif is essential in Nbea function.

Altogether, I firstly identified the role of β Nrxn in basal synaptic transmission and synaptic plasticity at excitatory synapses. Furthermore, Nbea and domains were cloned to study the molecular determinants. Both of these proteins may act as modulators to alter molecular composition at different subpopulations of synapses and thus contribute to neural disorder disease like autism.

99

References

- Abrahams, B.S., and Geschwind, D.H. (2008). Advances in autism genetics: on the threshold of a new neurobiology. *Nature reviews Genetics* 9, 341-355.
- Aoto, J., Martinelli, D.C., Malenka, R.C., Tabuchi, K., and Sudhof, T.C. (2013). Presynaptic Neurexin-3 Alternative Splicing trans-Synaptically Controls Postsynaptic AMPA Receptor Trafficking. *Cell* 154, 75-88.
- Arac, D., Boucard, A.A., Ozkan, E., Strop, P., Newell, E., Sudhof, T.C., and Brunger, A.T. (2007). Structures of neuroligin-1 and the neuroligin-1/neurexin-1 beta complex reveal specific protein-protein and protein-Ca2+ interactions. *Neuron* 56, 992-1003.
- Aronoff, R., and Petersen, C.C. (2008). Layer, column and cell-type specific genetic manipulation in mouse barrel cortex. *Frontiers in neuroscience* 2, 64-71.
- Bailey, A., Lecouteur, A., Gottesman, I., Bolton, P., Simonoff, E., Yuzda, E., and Rutter, M. (1995). Autism as a Strongly Genetic Disorder - Evidence from a British Twin Study. *Psychological medicine* 25, 63-77.
- Bang, M.L., and Owczarek, S. (2013). A matter of balance: role of neurexin and neuroligin at the synapse. *Neurochemical research* 38, 1174-1189.
- Banovic, D., Khorramshahi, O., Oswald, D., Wichmann, C., Riedt, T., Fouquet, W., Tian, R., Sigrist, S.J., and Aberle, H. (2010). Drosophila neuroligin 1 promotes growth and postsynaptic differentiation at glutamatergic neuromuscular junctions. *Neuron* 66, 724-738.
- Baumgartner, S., Littleton, J.T., Broadie, K., Bhat, M.A., Harbecke, R., Lengyel, J.A., Chiquet-Ehrismann, R., Prokop, A., and Bellen, H.J. (1996). A Drosophila neurexin is required for septate junction and blood-nerve barrier formation and function. *Cell* 87, 1059-1068.
- Beene, D.L., and Scott, J.D. (2007). A-kinase anchoring proteins take shape. *Current opinion in cell biology* 19, 192-198.
- Biederer, T., and Sudhof, T.C. (2000). Mints as adaptors. Direct binding to neurexins and recruitment of munc18. *The Journal of biological chemistry* 275, 39803-39806.
- Blatow, M., Caputi, A., Burnashev, N., Monyer, H., and Rozov, A. (2003). Ca2+ buffer saturation underlies paired pulse facilitation in calbindin-D28k-containing terminals. *Neuron* 38, 79-88.
- Boucard, A.A., Chubykin, A.A., Comoletti, D., Taylor, P., and Sudhof, T.C. (2005). A splice code for trans-synaptic cell adhesion mediated by binding of neuroligin 1 to alpha- and beta-neurexins. *Neuron* 48, 229-236.
- Boucard, A.A., Ko, J., and Sudhof, T.C. (2012). High affinity neurexin binding to cell adhesion G-protein-coupled receptor C1RL1/latrophilin-1 produces an intercellular adhesion complex. *The Journal of biological chemistry* 287, 9399-9413.
- Born, G., Grayton, H.M., Langhorst, H., Dudanova, I., Rohlmann, A., Woodward, B.W., Collier, D.A., Fernandes, C., and Missler, M. (2014). Genetic targeting of NRXN2 in mice unveils role in social behaviors and excitatory cortical synapse function. *Translational Psychiatry* (Submitted).

REFERENCES

- Burgess, A., Mornon, J.P., de Saint-Basile, G., and Callebaut, I. (2009). A concanavalin A-like lectin domain in the CHS1/LYST protein, shared by members of the BEACH family. *Bioinformatics* 25, 1219-1222.
- Calahorra, F., and Ruiz-Rubio, M. (2013). Human alpha- and beta-NRXN1 isoforms rescue behavioral impairments of *Caenorhabditis elegans* neurexin-deficient mutants. *Genes, brain, and behavior* 12, 453-464.
- Cattabeni, F., Gardoni, F., and Di Luca, M. (2004). Molecular biology of postsynaptic structures. *Oxford university press* 2, 165-181.
- Carter, A.S., Black, D.O., Tewani, S., Connolly, C.E., Kadlec, M.B., and Tager-Flusberg, H. (2007). Sex differences in toddlers with autism spectrum disorders. *J Autism Dev Disord* 37, 86-97.
- Castermans, D., Volders, K., Crepel, A., Backx, L., De Vos, R., Freson, K., Meulemans, S., Vermeesch, J.R., Schrander-Stumpel, C.T.R.M., De Rijk, P., et al. (2010). SCAMP5, NBEA and AMISYN: three candidate genes for autism involved in secretion of large dense-core vesicles. *Human molecular genetics* 19, 1368-1378.
- Castermans, D., Wilquet, V., Parthoens, E., Huysmans, C., Steyaert, J., Swinnen, L., Fryns, J.P., Van de Ven, W., and Devriendt, K. (2003). The neurobeachin gene is disrupted by a translocation in a patient with idiopathic autism. *J Med Genet* 40, 352-356.
- Catterall, W.A., and Few, A.P. (2008). Calcium channel regulation and presynaptic plasticity. *Neuron* 59, 882-901.
- Catterall, W.A., Leal, K., and Nanou, E. (2013). Calcium channels and short-term synaptic plasticity. *The Journal of biological chemistry* 288, 10742-10749.
- Chen, B.S., Gray, J.A., Sanz-Clemente, A., Wei, Z., Thomas, E.V., Nicoll, R.A., and Roche, K.W. (2012a). SAP102 mediates synaptic clearance of NMDA receptors. *Cell reports* 2, 1120-1128.
- Chen, K., Gracheva, E.O., Yu, S.C., Sheng, Q., Richmond, J., and Featherstone, D.E. (2010). Neurexin in embryonic *Drosophila* neuromuscular junctions. *PLoS one* 5, e11115.
- Chen, Y.C., Lin, Y.Q., Banerjee, S., Venken, K., Li, J., Ismat, A., Chen, K., Duraine, L., Bellen, H.J., and Bhat, M.A. (2012b). *Drosophila* neuroligin 2 is required presynaptically and postsynaptically for proper synaptic differentiation and synaptic transmission. *The Journal of neuroscience : the official journal of the Society for Neuroscience* 32, 16018-16030.
- Chubykin, A.A., Atasoy, D., Etherton, M.R., Brose, N., Kavalali, E.T., Gibson, J.R., and Sudhof, T.C. (2007). Activity-dependent validation of excitatory versus inhibitory synapses by neuroligin-1 versus neuroligin-2. *Neuron* 54, 919-931.
- Cingolani, L.A., and Goda, Y. (2008). Actin in action: the interplay between the actin cytoskeleton and synaptic efficacy. *Nature Reviews Neuroscience* 9, 344-356.
- Craig, A.M., and Kang, Y. (2007). Neurexin-neuroligin signaling in synapse development. *Current opinion in neurobiology* 17, 43-52.
- Cullinane, A.R., Schaffer, A.A., and Huizing, M. (2013). The BEACH is hot: a LYST of emerging roles for BEACH-domain containing proteins in human disease. *Traffic* 14, 749-766.
- De Camilli, P., Haucke, V., Takei, K., Mugnaini, E. (2001). The structure of synapses. Synapses. Johns Hopkins University Press, Baltimore.
- De Lozanne, A. (2003). The role of BEACH proteins in Dictyostelium. *Traffic* 4, 6-12.

REFERENCES

- de Souza, N., Vallier, L.G., Fares, H., and Greenwald, I. (2007). SEL-2, the *C.elegans* neurobeachin/LRBA homolog, is a negative regulator of lin-12/Notch activity and affects endosomal traffic in polarized epithelial cells. *Development* 134, 691-702.
- de Wit, J., Sylwestrak, E., O'Sullivan, M.L., Otto, S., Tiglio, K., Savas, J.N., Yates, J.R., 3rd, Comoletti, D., Taylor, P., and Ghosh, A. (2009). LRRTM2 interacts with Neurexin1 and regulates excitatory synapse formation. *Neuron* 64, 799-806.
- Dean, C., Scholl, F.G., Choib, J., DeMaria, S., Berger, J., Isacoff, E., and Scheiffele, P. (2003). Neurexin mediates the assembly of presynaptic terminals. *Nature neuroscience* 6, 708-716.
- del Pino, I., Paarmann, I., Karas, M., Kilimann, M.W., and Betz, H. (2011). The trafficking proteins Vacuolar Protein Sorting 35 and Neurobeachin interact with the glycine receptor beta-subunit. *Biochemical and biophysical research communications* 412, 435-440.
- Dell'Acqua, M.L., Smith, K.E., Gorski, J.A., Horne, E.A., Gibson, E.S., and Gomez, L.L. (2006). Regulation of neuronal PKA signaling through AKAP targeting dynamics. *Eur J Cell Biol* 85, 627-633.
- Dudanova, I., Sedej, S., Ahmad, M., Masius, H., Sargsyan, V., Zhang, W.Q., Riedel, D., Angenstein, F., Schild, D., Rupnik, M., et al. (2006). Important contribution of alpha-neurexins to Ca²⁺-triggered exocytosis of secretory granules. *Journal of Neuroscience* 26, 10599-10613.
- Dudanova, I., Tabuchi, K., Rohmann, A., Sudhof, T.C., and Missler, M. (2007). Deletion of alpha-neurexins does not cause a major impairment of axonal pathfinding or synapse formation. *J Comp Neurol* 502, 261-274.
- Elia, L.P., Yamamoto, M., Zang, K.L., and Reichardt, L.F. (2006). p120 Catenin regulates dendritic spine and synapse development through Rho-family GTPases and cadherins. *Neuron* 51, 43-56.
- Etherton, M.R., Blaiss, C.A., Powell, C.M., and Sudhof, T.C. (2009). Mouse neurexin-1alpha deletion causes correlated electrophysiological and behavioral changes consistent with cognitive impairments. *Proceedings of the National Academy of Sciences of the United States of America* 106, 17998-18003.
- Fairless, R., Masius, H., Rohmann, A., Heupel, K., Ahmad, M., Reissner, C., Dresbach, T., and Missler, M. (2008). Polarized Targeting of Neurexins to Synapses Is Regulated by their C-Terminal Sequences. *Journal of Neuroscience* 28, 12969-12981.
- Feldman, D.E. (2009). Synaptic mechanisms for plasticity in neocortex. *Annual review of neuroscience* 32, 33-55.
- Feng, J., Schroer, R., Yan, J., Song, W., Yang, C., Bockholt, A., Cook, E.H., Jr., Skinner, C., Schwartz, C.E., and Sommer, S.S. (2006). High frequency of neurexin 1beta signal peptide structural variants in patients with autism. *Neuroscience letters* 409, 10-13.
- Gauthier, J., Siddiqui, T.J., Huashan, P., Yokomaku, D., Hamdan, F.F., Champagne, N., Lapointe, M., Spiegelman, D., Noreau, A., Lafrenie, R.G., et al. (2011). Truncating mutations in NRXN2 and NRXN1 in autism spectrum disorders and schizophrenia. *Hum. Genet.* 130, 563-573.
- Geschwind, D.H. (2011). Genetics of autism spectrum disorders. *Trends in cognitive sciences* 15, 409-416.

REFERENCES

- Giannone, G., Mondin, M., Grillo-Bosch, D., Tessier, B., Saint-Michel, E., Czondor, K., Sainlos, M., Choquet, D., and Thoumine, O. (2013). Neurexin-1beta binding to neuroligin-1 triggers the preferential recruitment of PSD-95 versus gephyrin through tyrosine phosphorylation of neuroligin-1. *Cell reports* 3, 1996-2007.
- Giarelli, E., Wiggins, L.D., Rice, C.E., Levy, S.E., Kirby, R.S., Pinto-Martin, J., and Mandell, D. (2010). Sex differences in the evaluation and diagnosis of autism spectrum disorders among children. *Disability and health journal* 3, 107-116.
- Gilbert, D.J., Engel, H., Wang, X.L., Grzeschik, K.H., Copeland, N.G., Jenkins, N.A., and Kilmann, M.W. (1999). The neurobeachin gene (Nbea) identifies a new region of homology between mouse central Chromosome 3 and human Chromosome 13q13. *Mammalian Genome* 10, 1030-1031.
- Gillberg, C., and Wing, L. (1999). Autism: not an extremely rare disorder. *Acta psychiatrica Scandinavica* 99, 399-406.
- Gjorlund, M.D., Nielsen, J., Pankratova, S., Li, S., Korshunova, I., Bock, E., and Berezin, V. (2012). Neuroligin-1 induces neurite outgrowth through interaction with neurexin-1beta and activation of fibroblast growth factor receptor-1. *FASEB journal : official publication of the Federation of American Societies for Experimental Biology* 26, 4174-4186.
- Gorny, X., Mikhaylova, M., Seeger, C., Reddy, P.P., Reissner, C., Schott, B.H., Danielson, U.H., Kreutz, M.R., and Seidenbecher, C. (2012). AKAP79/150 interacts with the neuronal calcium-binding protein caldendrin. *Journal of neurochemistry* 122, 714-726.
- Graf, E.R., Zhang, X., Jin, S.X., Linhoff, M.W., and Craig, A.M. (2004). Neurexins induce differentiation of GABA and glutamate postsynaptic specializations via neuroligins. *Cell* 119, 1013-1026.
- Grice, D.E., and Buxbaum, J.D. (2006). The genetics of autism spectrum disorders. *Neuromol Med* 8, 451-460.
- Haklai-Topper, L., Soutschek, J., Sabanay, H., Scheel, J., Hobert, O., and Peles, E. (2011). The neurexin superfamily of *Caenorhabditis elegans*. *Gene expression patterns : GEP* 11, 144-150.
- Hallmayer, J., Cleveland, S., Torres, A., Phillips, J., Cohen, B., Torigoe, T., Miller, J., Fedele, A., Collins, J., Smith, K., Lotspeich, L., Croen, L.A., Ozonoff, S., Lajonchere, C., Grether, J.K., and Risch, N. (2011). Genetic Heritability and Shared Environmental Factors Among Twin Pairs With Autism. *Arch Gen Psychiat* 68, 1095-1102.
- Ho, V.M., Lee, J.A., and Martin, K.C. (2011). The cell biology of synaptic plasticity. *Science* 334, 623-628.
- Hotulainen, P., and Hoogenraad, C.C. (2010). Actin in dendritic spines: connecting dynamics to function. *Journal of Cell Biology* 189, 619-629.
- Humphries, C.L., Balcer, H.I., D'Agostino, J.L., Winsor, B., Drubin, D.G., Barnes, G., Andrews, B.J., and Goode, B.L. (2002). Direct regulation of Arp2/3 complex activity and function by the actin binding protein coronin. *Journal of Cell Biology* 159, 993-1004.
- Ichtchenko, K., Hata, Y., Nguyen, T., Ullrich, B., Missler, M., Moomaw, C., and Sudhof, T.C. (1995). Neuroligin-1 - a Splice Site-Specific Ligand for Beta-Neurexins. *Cell* 81, 435-443.
- Joo, J.Y., Lee, S.J., Uemura, T., Yoshida, T., Yasumura, M., Watanabe, M., and Mishina, M. (2011). Cerebellin precursor protein (Cbln) subtypes in the forebrain bind to

REFERENCES

- specific neurexin variants and induce presynaptic differentiation. *Neuroscience research* 71, E216-E216.
- Jungling, K., Eulenburg, V., Moore, R., Kemler, R., Lessmann, V., and Gottmann, K. (2006). N-cadherin transsynaptically regulates short-term plasticity at glutamatergic synapses in embryonic stem cell-derived neurons. *Journal of Neuroscience* 26, 6968-6978.
- Kandel, E.R., Schwartz, J.H., Jessell, T.M., Siegelbaum, S.A., and Hudspeth, A.J. (2012) *Principles of Neural Science*, 5th edition. McGraw-Hill Professional.
- Kaplan, J., De Domenico, I., and Ward, D.M. (2008). Chediak-Higashi syndrome. *Current opinion in hematology* 15, 22-29.
- Kattenstroth, G., Tantalaki, E., Sudhof, T.C., Gottmann, K., and Missler, M. (2004). Postsynaptic N-methyl-D-aspartate receptor function requires alpha-neurexins. *Proceedings of the National Academy of Sciences of the United States of America* 101, 2607-2612.
- Kohler, M., Speck, C., Christiansen, M., Bischoff, F.R., Prehn, S., Haller, H., Gorlich, D., and Hartmann, E. (1999). Evidence for distinct substrate specificities of importin alpha family members in nuclear protein import. *Molecular and cellular biology* 19, 7782-7791.
- Kugler, S., Kilic, E., and Bahr, M. (2003). Human synapsin 1 gene promoter confers highly neuron-specific long-term transgene expression from an adenoviral vector in the adult rat brain depending on the transduced area. *Gene therapy* 10, 337-347.
- Lauks, J., Klemmer, P., Farzana, F., Karupothula, R., Zalm, R., Cooke, N.E., Li, K.W., Smit, A.B., Toonen, R., and Verhage, M. (2012). Synapse associated protein 102 (SAP102) binds the C-terminal part of the scaffolding protein neurobeachin. *PLoS one* 7, e39420.
- Li, D., and Roberts, R. (2001). WD-repeat proteins: structure characteristics, biological function, and their involvement in human diseases. *Cellular and molecular life sciences : CMLS* 58, 2085-2097.
- Li, Z., and Sheng, M. (2003). Some assembly required: the development of neuronal synapses. *Nature reviews Molecular cell biology* 4, 833-841.
- Lisman, J.E., Raghavachari, S., and Tsien, R.W. (2007). The sequence of events that underlie quantal transmission at central glutamatergic synapses. *Nature reviews Neuroscience* 8, 597-609.
- Liu, G.S., and Tsien, R.W. (1995). Properties of Synaptic Transmission at Single Hippocampal Synaptic Boutons. *Nature* 375, 404-408.
- Lord, C., Risi, S., Lambrecht, L., Cook, E.H., Leventhal, B.L., DiLavore, P.C., Pickles, A., and Rutter, M. (2000). The Autism Diagnostic Observation Schedule-Generic: A standard measure of social and communication deficits associated with the spectrum of autism. *J Autism Dev Disord* 30, 205-223.
- Lortter, V. (1996). Epidemiology of autistic conditions in young children. *Social Psychiatry* 1, 124-137.
- Lujan, R., Maylie, J., and Adelman, J.P. (2009). New sites of action for GIRK and SK channels. *Nature reviews Neuroscience* 10, 475-480.
- Lyckman, A.W., Horng, S., Leamey, C.A., Tropea, D., Watakabe, A., Van Wart, A., McCurry, C., Yamamori, T., and Sur, M. (2008). Gene expression patterns in visual cortex during the critical period: Synaptic stabilization and reversal by visual

REFERENCES

- deprivation. *Proceedings of the National Academy of Sciences of the United States of America* 105, 9409-9414.
- MacDonald, B.T., Tamai, K., and He, X. (2009). Wnt/beta-catenin signaling: components, mechanisms, and diseases. *Developmental cell* 17, 9-26.
- Malenka, R.C., and Bear, M.F. (2004). LTP and LTD: An embarrassment of riches. *Neuron* 44, 5-21.
- Malyala, A., Kelly, M.J., and Ronnekleiv, O.K. (2005). Estrogen modulation of hypothalamic neurons: Activation of multiple signaling pathways and gene expression changes. *Steroids* 70, 397-406.
- Manning, B.D., and Snyder, M. (2000). Drivers and passengers wanted! the role of kinesin-associated proteins. *Trends in cell biology* 10, 281-289.
- Mariani, M., Baldessari, D., Francisconi, S., Viggiano, L., Rocchi, M., Zappavigna, V., Malgaretti, N., and Consalez, G.G. (1999). Two murine and human homologs of mab-21, a cell fate determination gene involved in *Caenorhabditis elegans* neural development. *Human molecular genetics* 8, 2397-2406.
- Martin, S.J., Grimwood, P.D., and Morris, R.G.M. (2000). Synaptic plasticity and memory: An evaluation of the hypothesis. *Annual review of neuroscience* 23, 649-711.
- McCleskey, E.W. (2007). Neuroscience: a local route to pain relief. *Nature* 449, 545-546.
- Medrihan, L., Rohlmann, A., Fairless, R., Andrae, J., Doring, M., Missler, M., Zhang, W., and Kilmann, M.W. (2009). Neurobeachin, a protein implicated in membrane protein traffic and autism, is required for the formation and functioning of central synapses. *The Journal of physiology* 587, 5095-5106.
- Missler, M. (2003). Synaptic cell adhesion goes functional. *Trends in neurosciences* 26, 176-178.
- Missler, M., Fernandez-Chacon, R., and Sudhof, T.C. (1998a). The making of neurexins. *Journal of neurochemistry* 71, 1339-1347.
- Missler, M., Hammer, R.E., and Sudhof, T.C. (1998b). Neurexophilin binding to alpha-neurexins - A single LNS domain functions as an independently folding ligand-binding unit. *Journal of Biological Chemistry* 273, 34716-34723.
- Missler, M., and Sudhof, T.C. (1998). Neurexins: three genes and 1001 products. *Trends Genet* 14, 20-26.
- Missler, M., Sudhof, T.C., and Biederer, T. (2012). Synaptic cell adhesion. *Cold Spring Harbor perspectives in biology* 4, a005694.
- Missler, M., Zhang, W.Q., Rohlmann, A., Kattenstroth, G., Hammer, R.E., Gottmann, K., and Sudhof, T.C. (2003). alpha-neurexins couple Ca²⁺ channels to synaptic vesicle exocytosis. *Nature* 423, 939-948.
- Mukherjee, K., Sharma, M., Urlaub, H., Bourenkov, G.P., Jahn, R., Sudhof, T.C., and Wahl, M.C. (2008). CASK Functions as a Mg²⁺-independent neurexin kinase. *Cell* 133, 328-339.
- Mondin, M., Labrousse, V., Hosy, E., Heine, M., Tessier, B., Levet, F., Poujol, C., Blanchet, C., Choquet, D., and Thoumine, O. (2011). Neurexin-neuroigin adhesions capture surface-diffusing AMPA receptors through PSD-95 scaffolds. *The Journal of neuroscience : the official journal of the Society for Neuroscience* 31, 13500-13515.

REFERENCES

- Moy, S.S., Nadler, J.J., Magnuson, T.R., and Crawley, J.N. (2006). Mouse models of autism spectrum disorders: The challenge for behavioral genetics. *Am J Med Genet C* 142C, 40-51.
- Nam, C.I., and Chen, L. (2005). Postsynaptic assembly induced by neurexin-neuroigin interaction and neurotransmitter. *Proceedings of the National Academy of Sciences of the United States of America* 102, 6137-6142.
- Nair, R., Lauks, J., Jung, S., Cooke, N.E., de Wit, H., Brose, N., Kilmann, M.W., Verhage, M., and Rhee, J. (2013). Neurobeachin regulates neurotransmitter receptor trafficking to synapses. *The Journal of cell biology* 200, 61-80.
- Niesmann, K., Breuer, D., Brockhaus, J., Born, G., Wolff, I., Reissner, C., Kilmann, M.W., Rohlmann, A., and Missler, M. (2011). Dendritic spine formation and synaptic function require neurobeachin. *Nature communications* 2, 557.
- Pettem, K.L., Yokomaku, D., Luo, L., Linhoff, M.W., Prasad, T., Connor, S.A., Siddiqui, T.J., Kawabe, H., Chen, F., Zhang, L., *et al* (2013). The Specific alpha-Neurexin Interactor Calsyntenin-3 Promotes Excitatory and Inhibitory Synapse Development. *Neuron* 80, 113-128.
- Penzes, P., and Rafalovich, I. (2012). Regulation of the actin cytoskeleton in dendritic spines. *Advances in experimental medicine and biology* 970, 81-95.
- Puschel, A.W., and Betz, H. (1995). Neurexins are differentially expressed in the embryonic nervous system of mice. *The Journal of neuroscience : the official journal of the Society for Neuroscience* 15, 2849-2856.
- Purves, D., Augustine, G.J., Fitzpatrick, D., Katz, L.C., LaMantia, A-S., McNamara, J.O., and Williams, S.M. (2011) *Neuroscience*, 2nd edition. Sinauer Associates.
- Racz, B., and Weinberg, R.J. (2008). Organization of the Arp2/3 complex in hippocampal spines. *The Journal of neuroscience : the official journal of the Society for Neuroscience* 28, 5654-5659.
- Reissner, C., Klose, M., Fairless, R., and Missler, M. (2008). Mutational analysis of the neurexin/neuroigin complex reveals essential and regulatory components. *Proceedings of the National Academy of Sciences of the United States of America* 105, 15124-15129.
- Reissner, C., and Missler, M. (2011). Unveiled alpha-Neurexins Take Center Stage. *Structure* 19, 749-750.
- Reissner, C., Runkel, F., and Missler, M. (2013). Neurexins. *Genome Biol* 14.
- Rissone, A., Monopoli, M., Beltrame, M., Bussolino, F., Cotelli, F., and Arese, M. (2007). Comparative genome analysis of the neurexin gene family in *Danio rerio*: insights into their functions and evolution. *Molecular biology and evolution* 24, 236-252.
- Ronald, A., and Hoekstra, R.A. (2011). Autism Spectrum Disorders and Autistic Traits: A Decade of New Twin Studies. *Am J Med Genet B* 156B, 255-274.
- Rudenko, G., Nguyen, T., Chelliah, Y., Sudhof, T.C., and Deisenhofer, J. (1999). The structure of the ligand-binding domain of neurexin I beta: Regulation of LNS domain function by alternative splicing. *Cell* 99, 93-101.
- Rybakin, V., and Clemen, C.S. (2005). Coronin proteins as multifunctional regulators of the cytoskeleton and membrane trafficking. *Bioessays* 27, 625-632.
- Savelyeva, L., Sagulenko, E., Schmitt, J.G., and Schwab, M. (2006). The neurobeachin gene spans the common fragile site FRA13A. *Hum Genet* 118, 551-558.

REFERENCES

- Scheiffele, P., Fan, J., Choih, J., Fetter, R., and Serafini, T. (2000a). Neuroligin expressed in nonneuronal cells triggers presynaptic development in contacting axons. *Cell* *101*, 657-669.
- Scheiffele, P., Fan, J.H., Choih, J., Fetter, R., and Serafini, T. (2000b). Neuroligin expressed in nonneuronal cells triggers presynaptic development in contacting axons. *Cell* *101*, 657-669.
- Shastry, B.S. (2003). Molecular genetics of autism spectrum disorders. *J Hum Genet* *48*, 495-501.
- Sheng, M., and Kim, E. (2000). The Shank family of scaffold proteins. *J Cell Sci* *113 (Pt 11)*, 1851-1856.
- Sheng, M., and Kim, M.J. (2002). Postsynaptic signaling and plasticity mechanisms. *Science* *298*, 776-780.
- Shinoda, Y., Sadakata, T., and Furuichi, T. (2013). Animal Models of Autism Spectrum Disorder (ASD): A Synaptic-Level Approach to Autistic-Like Behavior in Mice. *Exp Anim Tokyo* *62*, 71-78.
- Sippy, T., Cruz-Martin, A., Jeromin, A., and Schweizer, F.E. (2003). Acute changes in short-term plasticity at synapses with elevated levels of neuronal calcium sensor-1. *Nature neuroscience* *6*, 1031-1038.
- Smith, M., Woodroffe, A., Smith, R., Holguin, S., Martinez, J., Filipek, P.A., Modahl, C., Moore, B., Bocian, M.E., Mays, L., *et al.* (2002). Molecular genetic delineation of a deletion of chromosome 13q12 -> q13 in a patient with autism and auditory processing deficits. *Cytogenet Genome Res* *98*, 233-239.
- Smith, T.F., Gaitatzes, C., Saxena, K., and Neer, E.J. (1999). The WD repeat: a common architecture for diverse functions. *Trends in biochemical sciences* *24*, 181-185.
- Sons, M.S., Busche, N., Strenzke, N., Moser, T., Ernsberger, U., Mooren, F.C., Zhang, W., Ahmad, M., Steffens, H., Schomburg, E.D., *et al.* (2006). alpha-Neurexins are required for efficient transmitter release and synaptic homeostasis at the mouse neuromuscular junction. *Neuroscience* *138*, 433-446.
- Spafford, J.D., and Zamponi, G.W. (2003). Functional interactions between presynaptic calcium channels and the neurotransmitter release machinery. *Current opinion in neurobiology* *13*, 308-314.
- Su, Y., Balice-Gordon, R.J., Hess, D.M., Landsman, D.S., Minarcik, J., Golden, J., Hurwitz, I., Lieberhaber, S.A., and Cooke, N.E. (2004). Neurobeachin is essential for neuromuscular synaptic transmission. *The Journal of neuroscience : the official journal of the Society for Neuroscience* *24*, 3627-3636.
- Sudhof, T.C. (2001). alpha-Latrotoxin and its receptors: Neurexins and C1r1/latrophilins. *Annual review of neuroscience* *24*, 933-962.
- Sudhof, T.C. (2013). Neurotransmitter release: the last millisecond in the life of a synaptic vesicle. *Neuron* *80*, 675-690.
- Sudhof, T.C., and Rothman, J.E. (2009). Membrane fusion: grappling with SNARE and SM proteins. *Science* *323*, 474-477.
- Sun, M., and Xie, W. (2012). Cell adhesion molecules in Drosophila synapse development and function. *Science China Life sciences* *55*, 20-26.
- Suzuki, T., Ueda, A., Kobayashi, N., Yang, J., Tomaru, K., Yamamoto, M., Takeno, M., and Ishigatsubo, Y. (2008). Proteasome-dependent degradation of alpha-catenin is regulated by interaction with ARMC8 alpha. *Biochemistry journal* *411*, 581-591.

107

REFERENCES

- Szatmari, P., Paterson, A.D., Zwaigenbaum, L., Roberts, W., Brian, J., Liu, X.Q., Vincent, J.B., Skaug, J.L., Thompson, A.P., Senman, L., *et al.* (2007). Mapping autism risk loci using genetic linkage and chromosomal rearrangements. *Nat Genet* *39*, 319-328.
- Tabuchi, K., and Sudhof, T.C. (2002). Structure and evolution of neurexin genes: insight into the mechanism of alternative splicing. *Genomics* *79*, 849-859.
- Taniguchi, H., Gollan, L., Scholl, F.G., Mahadomrongkul, V., Dobler, E., Limthong, N., Peck, M., Aoki, C., and Scheiffele, P. (2007). Silencing of neuroligin function by postsynaptic neurexins. *The Journal of neuroscience : the official journal of the Society for Neuroscience* *27*, 2815-2824.
- Tewari, R., Bailes, E., Bunting, K.A., and Coates, J.C. (2010). Armadillo-repeat protein functions: questions for little creatures. *Trends in cell biology* *20*, 470-481.
- Tsang, W.H., Shek, K.F., Lee, T.Y., and Chow, K.L. (2009). An evolutionarily conserved nested gene pair - Mab21 and Lrba/Nbea in metazoan. *Genomics* *94*, 177-187.
- Uemura, T., Lee, S.J., Yasumura, M., Takeuchi, T., Yoshida, T., Ra, M., Taguchi, R., Sakimura, K., and Mishina, M. (2010). Trans-Synaptic Interaction of GluR delta 2 and Neurexin through Cbln1 Mediates Synapse Formation in the Cerebellum. *Cell* *141*, 1068-1079.
- Utrecht, A.C., and Bear, J.E. (2006). Coronins: the return of the crown. *Trends in cell biology* *16*, 421-426.
- Ushkaryov, Y.A., Petrenko, A.G., Geppert, M., and Sudhof, T.C. (1992). Neurexins: synaptic cell surface proteins related to the alpha-latrotoxin receptor and laminin. *Science* *257*, 50-56.
- Vaags, A.K., Lionel, A.C., Sato, D., Goodenberger, M., Stein, Q.P., Curran, S., Ogilvie, C., Ahn, J.W., Drmic, I., Senman, L., *et al.* (2012). Rare deletions at the neurexin 3 locus in autism spectrum disorder. *American journal of human genetics* *90*, 133-141.
- van Spronsen, M., and Hoogenraad, C.C. (2010). Synapse pathology in psychiatric and neurologic disease. *Current neurology and neuroscience reports* *10*, 207-214.
- Varoqueaux, F., Jamain, S., and Brose, N. (2004). Neuroligin 2 is exclusively localized to inhibitory synapses. *Eur J Cell Biol* *83*, 449-456.
- Voineskos, A.N., Lett, T.A., Lerch, J.P., Tiwari, A.K., Ameis, S.H., Rajji, T.K., Muller, D.J., Mulsant, B.H., and Kennedy, J.L. (2011). Neurexin-1 and frontal lobe white matter: an overlapping intermediate phenotype for schizophrenia and autism spectrum disorders. *PLoS one* *6*, e20982.
- Volders, K., Nuytens, K., and Creemers, J.W.M. (2011). The Autism Candidate Gene Neurobeachin Encodes a Scaffolding Protein Implicated in Membrane Trafficking and Signaling. *Curr Mol Med* *11*, 204-217.
- Volders, K., Scholz, S., Slabbaert, J.R., Nagel, A.C., Verstreken, P., Creemers, J.W.M., Callaerts, P., and Schwarzel, M. (2012). Drosophila rugose Is a Functional Homolog of Mammalian Neurobeachin and Affects Synaptic Architecture, Brain Morphology, and Associative Learning. *Journal of Neuroscience* *32*, 15193-15204.
- Wang, X.L., Herberg, F.W., Laue, M.M., Wullner, C., Hu, B., Petrasch-Parwez, E., and Kilmann, M.W. (2000). Neurobeachin: A protein kinase A-anchoring, beige/Chediak-Higashi protein homolog implicated in neuronal membrane traffic. *Journal of Neuroscience* *20*, 8551-8555.
- Werling, D.M., and Geschwind, D.H. (2013). Sex differences in autism spectrum disorders. *Current opinion in neurology* *26*, 146-153.

108

REFERENCES

- Wong, W., and Scott, J.D. (2004). AKAP signalling complexes: focal points in space and time. *Nature reviews Molecular cell biology* 5, 959-970.
- Wright, G.J., and Washbourne, P. (2011). Neurexins, neuroligins and LRRTMs: synaptic adhesion getting fishy. *Journal of neurochemistry* 117, 765-778.
- Zhang, C., Atasoy, D., Arac, D., Yang, X., Fucillo, M.V., Robison, A.J., Ko, J., Brunger, A.T., and Sudhof, T.C. (2010). Neurexins physically and functionally interact with GABA(A) receptors. *Neuron* 66, 403-416.
- Zhang, W.Q., Rohlmann, A., Sargsyan, V., Aramuni, G., Hammer, R.E., Sudhof, T.C., and Missler, M. (2005). Extracellular domains of alpha-neurexins participate in regulating synaptic transmission by selectively affecting N- and P/Q-type Ca²⁺ channels. *Journal of Neuroscience* 25, 4330-4342.
- Zeng, X., Sun, M., Liu, L., Chen, F., Wei, L., and Xie, W. (2007). Neurexin-1 is required for synapse formation and larvae associative learning in *Drosophila*. *FEBS letters* 581, 2509-2516.
- Zucker, R.S., and Regehr, W.G. (2002). Short-term synaptic plasticity. *Annual review of physiology* 64, 355-405.

REFERENCES

Acknowledgements

At the end of my thesis, it is my greatest honor to express my sincere thanks to all those who helped me in many ways during this exciting and challenging journey through my PhD studies.

I would like to take this opportunity to express my deepest gratitude to my supervisor Prof. Dr. Markus Missler for his great support, consistent coach and continuous encouragement throughout my study. He is always available to answer my questions whenever I knock his door. His devotion to science has inspired me a lot and will continue to guide me in my future career.

I do appreciate Dr. Carsten Reissner's untiring help in my entire PhD period. He assisted nearly every stage of my research, and was always there to answer my endless questions. Without his support, I would never have accomplished this thesis.

I especially thank Dr. Gesche Born, Dr. Johannes Brockhaus and Dr. Shaopeng Wang for introducing the patch-clamp technology, as well as numerous experimental procedures and practical experiences to me.

I also want to warmly thank Prof. Dr. Andreas Püschel for the constructive discussion during my CEDAD progress reports and thesis committee meetings.

Many warm thanks to Prof. Christian Klämbt and PD Dr. Sven Bogdan, as well as their lab members, for their assistance when I teaching the experimental course in their laboratory.

It was a great pleasure and honor to work with my friendly and helpful colleagues. Kai Kerkhoff carried out the routine mouse husbandry and genotyping. Ilka Wolff did great job in cell cultures and laboratory management. Miriam Schreitmüller, Enno-F. Löffler, Christian Neupert, Johanna Stahn, Anja Blanqué, Dr. Astrid Rohlmann, Dorothee Breuer, Daniela Aschhoff, Dr. Daniele Repetto created such a good working atmosphere for the whole team, thank all of you for sharing with me the helpful practical tips, and for the help that you have ever given to me.

Thank Prof. Dr. Martin K. Wild and Sylvia Krüger for their support in administrative matters from the joint graduate school CEDAD-IMPRS. Thanks to the financial support from CEDAD program.

Thank all my dear friends and fellow students, for they always being supportive and great company full of laughter and joy.

There is no word I can use to describe my appreciation to my family. I want to thank my parents, Qing Guo and Liling Cui, for their unconditional love and support. They always encourage me to chase my interest and curiosity. Finally I would like to thank my boyfriend Dr. Xiaoke Mu, whose patience, understanding, intelligence and sense of humor were a great help for me.

Curriculum Vitae